

QCD factorization of exclusive processes beyond leading twist: $\gamma_T^* \rightarrow \rho_T$ impact factor with twist three accuracy

I. V. Anikin,¹ D.Yu. Ivanov,² B. Pire,³ L. Szymanowski,⁴ and S. Wallon⁵

¹*Bogoliubov Laboratory of Theoretical Physics, JINR, 141980 Dubna, Russia*

²*Sobolev Institute of Mathematics, 630090 Novosibirsk, Russia*

³*CPHT, École Polytechnique, CNRS, 91128 Palaiseau Cedex, France*

⁴*Soltan Institute for Nuclear Studies, PL-00-681 Warsaw, Poland*

⁵*LPT, Université Paris-Sud, CNRS, 91405, Orsay, France &*

UPMC Univ. Paris 06, faculté de physique, 4 place Jussieu, 75252 Paris Cedex 05, France

We describe a consistent approach to factorization of scattering amplitudes for exclusive processes beyond the leading twist approximation. The method involves the Taylor expansion of the scattering amplitude in the momentum space around the dominant light-cone direction and thus naturally introduces an appropriate set of non-perturbative correlators which encode effects not only of the lowest but also of the higher Fock states of the produced particle. The reduction of original set of correlators to a set of independent ones is achieved with the help of equations of motion and invariance of the scattering amplitude under rotation on the light cone. We compare the proposed method with the covariant method formulated in the coordinate space, based on the operator product expansion. We prove the equivalence of two proposed parametrizations of the ρ_T distribution amplitudes. As a concrete application, we compute the expressions of the impact factor for the transition of virtual photon to transversally polarised ρ -meson up to the twist 3 accuracy within these two quite different methods and show that they are identical.

PACS numbers: 12.38.Bx, 13.60.Le

I. INTRODUCTION

The study of exclusive reactions in the generalized Bjorken regime has been the scene of significant progresses in the recent years, thanks to the factorization properties of the leading twist amplitudes [1] for deeply virtual Compton scattering and deep exclusive meson production. It however turned out that transversally polarized ρ -meson production did not enter the leading twist controllable case [2] but only the twist 3 more intricate part of the amplitude [3, 4, 5]. This is due to the fact that the leading twist distribution amplitude (DA) of a transversally polarized vector meson is chiral-odd, and hence decouples from hard amplitudes at the twist two level, even when another chiral-odd quantity is involved [2] unless in reactions with more than two final hadrons [6]. An understanding of the quark-gluon structure of a transversally polarized vector meson is however an important task of hadronic physics if one cares about studying confinement dynamics. This quark gluon structure may be described by distribution amplitudes which have been discussed in great detail [7, 8]. On the experimental side, a continuous effort has been devoted to the exploration of ρ -meson photo and electro-production, from moderate to very large energy [9, 10]. The kinematical analysis of the final π -meson pair allows then to separate the different helicity amplitudes, hence to measure the transversally polarized ρ -meson production amplitude. Although non-dominant for deep electroproduction, this amplitude is by no means negligible at moderately large Q^2 and needs to be understood in terms of QCD. Up to now, experimental information comes from electroproduction on a proton or nucleus. Future progress may come from real or virtual photon-photon collisions, which may be accessible either at electron-positron colliders or in ultraperipheral collisions at hadronic colliders, as recently discussed [11, 12].

In the literature there are two approaches to the factorization of the scattering amplitudes in exclusive processes at leading and higher twists. The first approach [4, 13], being the generalization of the Ellis-Furmanski-Petronzio (EFP) method [14] to the exclusive processes, deals with the factorization in the momentum space around the dominant light-cone direction. We shall call it the Light-Cone Collinear Factorization (LCCF). On the other hand, there exists a covariant approach in coordinate space successfully applied in [7] for a systematic description of distribution amplitudes of hadrons carrying different twists. This approach will be called the Covariant Collinear Factorization approach (CCF). Although being quite different and using different distribution amplitudes, both approaches can be applied to the description of the same processes. This fact calls for verification whether these two descriptions are equivalent and lead to the same physical consequences. This

can be clarified by establishing a precise vocabulary between objects appearing in the two approaches and by comparing physical results obtained with the help of the two methods.

The first aim of our paper is to prove that LCCF and CCF are equivalent methods for the description of exclusive processes. For that we derive the dictionary between DAs appearing in the LCCF method and in the CCF one. We perform our analysis within LCCF method in momentum space and use the invariance of the scattering amplitude under rotation of the light-cone vector n^μ , which we call n -independence condition. This method leads to a definitions of relevant soft correlators which are generally not independent ones. The reduction of their number to a minimal set of independent correlators is obtained with the use of equation of motions and of the n -independence condition. We obtain the same number of independent correlators in both LCCF and in CCF approaches and establish explicit relations between them.

As a concrete application, the second aim of our paper is to calculate within both methods the impact factor $\gamma^* \rightarrow \rho_T$, which is the building block of the description of the $\gamma^* p \rightarrow \rho p$ and $\gamma^* \gamma^* \rightarrow \rho \rho$ processes at large s , up to twist 3 accuracy and to verify that we get a full consistency between the two results.

The paper is organized as follows. In Section II we discuss the general framework of the LCCF method. In Subsection II A, we recall basics on factorization within the LCCF method. In Subsection II B, we present the parametrization of the matrix elements relevant to ρ -meson production. In Subsection II C we derive the constraint on these matrix elements coming from the QCD equations of motion. In Subsection II D we derive additional constraints based on the n -independence condition and we then perform the reduction to a minimal set of distribution amplitudes. This results in the dictionary given in subsection II E. In Section III, we compute the $\gamma^* \rightarrow \rho_T$ impact factor. After recalling the necessary definitions and kinematics in Subsection III A, we firstly perform the calculation in the LCCF framework in Subsection III B, then in the CCF framework in Subsection III C. We compare the two approaches in subsection III D. Section IV presents our conclusions. A few appendices present the calculational details needed to complete the proofs. Partial results of this paper have been briefly presented in [15, 16].

II. FACTORIZATION OF EXCLUSIVE PROCESSES IN THE LIGHT-CONE COLLINEAR APPROACH

A. Factorization beyond leading twist

Let us start with the most general form of the exclusive amplitude for the hard process $A \rightarrow \rho B$ (where A and B denotes initial and final states in kinematics where a hard scale allows a partonic interpretation) which we are interested in, written in the momentum representation and in axial gauge, as

$$\mathcal{A} = \int d^4\ell \text{tr} \left[H(\ell) \Phi(\ell) \right] + \int d^4\ell_1 d^4\ell_2 \text{tr} \left[H_\mu(\ell_1, \ell_2) \Phi^\mu(\ell_1, \ell_2) \right] + \dots, \quad (1)$$

where H and H_μ are the coefficient functions with two parton legs and three parton legs, respectively, as illustrated in Fig.1 on the example of $\gamma^* \rightarrow \rho$ impact factor, which is defined in full length in Sec.III. In

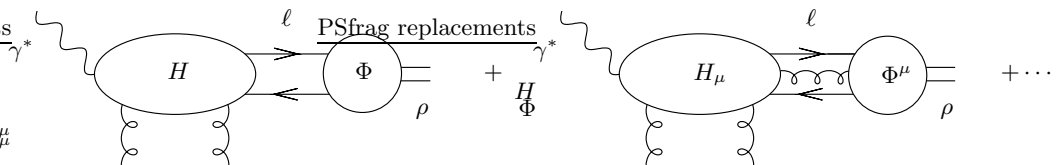


Figure 1: 2- and 3-parton correlators attached to a hard scattering amplitude in the example of the $\gamma^* \rightarrow \rho$ impact factor, where vertical lines are hard t -channel gluons in the color singlet state.

(1), the soft parts are given by the Fourier-transformed two or three partons correlators which are matrix elements of non-local operators. We consider the leading asymptotics of $1/Q$ expansion, separately for the cases of longitudinally (twist 2) and transversely polarized (twist 3) meson production. The amplitude (1) is not factorized yet because the hard and soft parts are related by the four-dimensional integration in the momentum space and by the summation over the Dirac indices.

To factorize the amplitude, we first choose the dominant direction around which we intend to decompose our relevant momenta and we Taylor expand the hard part. Let p and n be the conventionally called “plus” and

“minus” light-cone vectors, respectively, normalized as $p \cdot n = 1$. We carry out an expansion of ℓ in the basis defined by the p and n light-cone vectors:

$$\ell_{i\mu} = y_i p_\mu + (\ell_i \cdot p) n_\mu + \ell_{i\mu}^\perp, \quad y_i = \ell_i \cdot n, \quad (2)$$

and make the following replacement of the integration measure in (1):

$$d^4\ell_i \rightarrow d^4\ell_i dy_i \delta(y_i - \ell \cdot n). \quad (3)$$

Afterwards, the hard part coefficient function $H(\ell)$ has to be decomposed around the dominant “plus” direction:

$$H(\ell) = H(yp) + \frac{\partial H(\ell)}{\partial \ell_\alpha} \Big|_{\ell=yp} (\ell - y p)_\alpha + \dots \quad (4)$$

where $(\ell - y p)_\alpha \approx \ell_\alpha^\perp$ up to twist 3. One can see that the above-mentioned steps (2)-(4) do not yet allow us to factorize collinearly the amplitude in the momentum space since the ℓ^\perp dependence of the hard part is an excursion out of the collinear framework. To obtain a factorized amplitude, one performs an integration by parts to replace ℓ_α^\perp by ∂_α^\perp acting on the soft correlator. This leads to new operators \mathcal{O}^\perp which contain transverse derivatives, such as $\bar{\psi} \partial^\perp \psi$, and thus to the necessity of considering additional DAs $\Phi^\perp(l)$. This procedure accomplishes the factorization of the amplitude in momentum space. Factorization in the Dirac space can be achieved by the Fierz decomposition. For example, in the case of two fermions, one should project out the Dirac matrix $\psi_\alpha(0) \bar{\psi}_\beta(z)$ which appears in the soft part of the amplitude on the relevant Γ matrices. Thus, after all

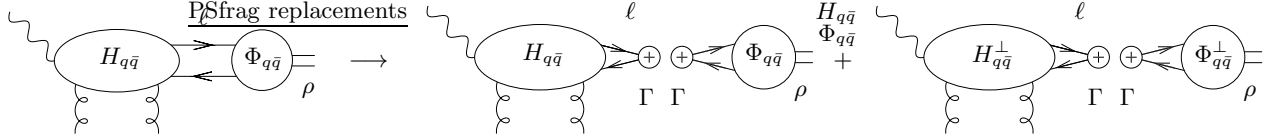


Figure 2: Factorization of 2-parton contributions in the example of the $\gamma^* \rightarrow \rho$ impact factor.

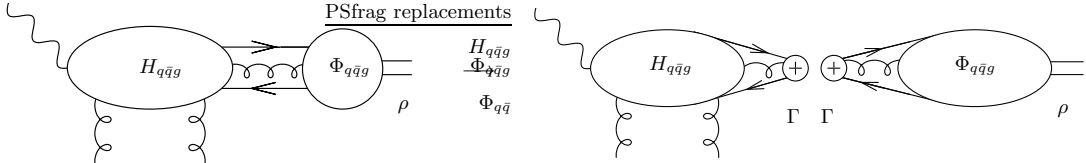


Figure 3: Factorization of 3-parton contributions in the example of the $\gamma^* \rightarrow \rho$ impact factor.

these stages, the amplitude takes the simple factorized form¹,

$$\mathcal{A} = \int_0^1 dy \text{tr} [H_{q\bar{q}}(y) \Gamma] \Phi_{q\bar{q}}^\Gamma(y) + \int_0^1 dy \text{tr} [H_{q\bar{q}}^\perp(y) \Gamma] \Phi_{q\bar{q}\mu}^{\perp\Gamma}(y) + \int_0^1 dy_1 dy_2 \text{tr} [H_{q\bar{q}g}^\mu(y_1, y_2) \Gamma] \Phi_{q\bar{q}g\mu}^\Gamma(y_1, y_2), \quad (5)$$

in which the two first terms in the r.h.s correspond to the two parton contribution and the last one to the three body contribution. This is illustrated symbolically in the example of the $\gamma^* \rightarrow \rho$ impact factor in Fig.2 for 2-parton contributions and in Fig.3 for 3-parton contributions.

Alternatively, combining the two last terms together in order to emphasize the fact they both originate from the Taylor expansion based on the covariant derivative, this factorization can be written as

$$\mathcal{A} = \int_0^1 dy \text{tr} [H(y) \Gamma] \Phi^\Gamma(y) + \int_0^1 dy_1 dy_2 \text{tr} [H^\mu(y_1, y_2) \Gamma] \Phi_\mu^\Gamma(y_1, y_2). \quad (6)$$

¹ Despite the fact that these formulae are given here up to twist 3, the method can be extended to higher twist contributions.

For definiteness², let us focus on the ρ -meson production case where the soft parts of the amplitude read

$$\begin{aligned}\Phi^\Gamma(y) &= \int_{-\infty}^{+\infty} \frac{d\lambda}{2\pi} e^{-i\lambda y} \langle \rho(p) | \bar{\psi}(\lambda n) \Gamma \psi(0) | 0 \rangle \\ \Phi_\rho^\Gamma(y_1, y_2) &= \int_{-\infty}^{+\infty} \frac{d\lambda_1 d\lambda_2}{4\pi^2} e^{-i\lambda_1 y_1 - i(y_2 - y_1)\lambda_2} \langle \rho(p) | \bar{\psi}(\lambda_1 n) \Gamma i \overset{\leftrightarrow}{D}_\rho^T(\lambda_2 n) \psi(0) | 0 \rangle.\end{aligned}\quad (7)$$

where

$$i \vec{D}_\mu = i \overset{\rightarrow}{\partial}_\mu + g A_\mu. \quad (8)$$

Eq.(7) supplemented by the appropriate choice of the Fierz matrices defines the set of non-perturbative correlators relevant for the description of the ρ -meson, which we will now discuss.

B. Parametrizations of vacuum-to- ρ -meson matrix elements up to twist 3

In this section, we introduce the parametrizations of the vacuum-to- ρ -meson matrix elements needed when calculating the process of exclusive ρ -production. As a concrete example, we shall below calculate the $\gamma_T^* \rightarrow \rho_T$ impact factor. Since we will follow two different approaches for our calculations, it is instructive to present two ways for parametrizing the corresponding matrix elements.

1. LCCF parametrization

We insist on the fact that in LCCF approach, the coordinates z_i in the parametrizations have to be proportional to the light-cone vector n . This is in contrast to the CCF approach where z lies on the light cone but does not correspond to any fixed light-cone direction. The transverse polarization of the ρ -meson is defined by the conditions (at twist 3, $p_\rho \sim p$)

$$e_T \cdot n = e_T \cdot p = 0, \quad (9)$$

i.e. e_T has only a \perp component, while e_L has no \perp component. Now, we introduce the parametrizations of the vacuum-to- ρ -meson matrix elements needed for the calculation, for example, of the $\gamma_T^* \rightarrow \rho_T$ impact factor. Keeping all the terms up to the twist-3 order with the axial (light-like) gauge, $n \cdot A = 0$, the matrix elements of quark-antiquark non-local operators can be written in terms of the light-cone basis vectors as (here, $z = \lambda n$)

$$\langle \rho(p_\rho) | \bar{\psi}(z) \gamma_\mu \psi(0) | 0 \rangle \stackrel{\mathcal{F}_1}{=} m_\rho f_\rho [\varphi_1(y) (e^* \cdot n) p_\mu + \varphi_3(y) e_{T\mu}^*], \quad (10)$$

$$\langle \rho(p_\rho) | \bar{\psi}(z) \gamma_5 \gamma_\mu \psi(0) | 0 \rangle \stackrel{\mathcal{F}_1}{=} m_\rho f_\rho i \varphi_A(y) \varepsilon_{\mu\alpha\beta\delta} e_T^{*\alpha} p^\beta n^\delta, \quad (11)$$

where the corresponding flavour matrix has been omitted³, and where we use $\varepsilon^{0123} = -\varepsilon_{0123} = 1$ and $\gamma_5 = i \gamma^0 \gamma^1 \gamma^2 \gamma^3$. For the sake of conciseness, we denote $\stackrel{\mathcal{F}_1}{=}$ the Fourier transformation with measure

$$\int_0^1 dy \exp [iy p \cdot z], \quad (12)$$

where $z = \lambda n$. The momentum fraction y ($\bar{y} \equiv 1 - y$) corresponds to the quark (antiquark). Note that the decomposition over the γ -matrix basis has been taken in the form:

$$- \langle \psi \bar{\psi} \rangle = \frac{1}{4} \langle \bar{\psi} \gamma_\mu \psi \rangle \gamma^\mu + \frac{1}{4} \langle \bar{\psi} \gamma_5 \gamma_\mu \psi \rangle \gamma^\mu \gamma_5 + \dots, \quad (13)$$

² In the following, the notations $|\rho\rangle$ or $|V\rangle$ will be used when the specific nature of the vector meson does not matter.

³ The normalization in (10,11) thus corresponds to a meson which would be a one flavour quark-antiquark state $|V\rangle = |f \bar{f}\rangle$, with for example $\langle V(p) | \bar{\psi}_f(z) \gamma_\mu \psi_f(0) | 0 \rangle \stackrel{\mathcal{F}_1}{=} m_V f_V [\dots]$.

in such a way that the minus sign in front of the axial term is absorbed into the axial correlators. The matrix elements of the quark–antiquark operators with transverse derivatives are parametrized according to

$$\langle \rho(p_\rho) | \bar{\psi}(z) \gamma_\mu i \overleftrightarrow{\partial}_\alpha^T \psi(0) | 0 \rangle \stackrel{\mathcal{F}_1}{=} m_\rho f_\rho \varphi_1^T(y) p_\mu e_{T\alpha}^*, \quad (14)$$

$$\langle \rho(p_\rho) | \bar{\psi}(z) \gamma_5 \gamma_\mu i \overleftrightarrow{\partial}_\alpha^T \psi(0) | 0 \rangle \stackrel{\mathcal{F}_1}{=} m_\rho f_\rho i \varphi_A^T(y) p_\mu \varepsilon_{\alpha\lambda\beta\delta} e_T^{*\lambda} p^\beta n^\delta, \quad (15)$$

where we introduced $\overleftrightarrow{\partial}_\rho = \frac{1}{2}(\overrightarrow{\partial}_\rho - \overleftarrow{\partial}_\rho)$ which is the standard antisymmetric derivative. The DAs φ_1 , φ_3 , φ_A satisfy the normalization conditions

$$\int_0^1 dy \varphi_1(y) = 1, \int_0^1 dy \varphi_3(y) = 1 \quad \text{and} \quad \int_0^1 dy (y - \bar{y}) \varphi_A(y) = \frac{1}{2}. \quad (16)$$

In the same way, the matrix elements of quark–gluon non-local operators can be parametrized as

$$\begin{aligned} \langle \rho(p_\rho) | \bar{\psi}(z_1) \gamma_\mu g A_\alpha^T(z_2) \psi(0) | 0 \rangle &\stackrel{\mathcal{F}_2}{=} m_\rho f_{3\rho}^V B(y_1, y_2; y_g) p_\mu e_{T\alpha}^*, \\ \langle \rho(p_\rho) | \bar{\psi}(z_1) \gamma_5 \gamma_\mu g A_\alpha^T(z_2) \psi(0) | 0 \rangle &\stackrel{\mathcal{F}_2}{=} m_\rho f_{3\rho}^A i D(y_1, y_2; y_g) p_\mu \varepsilon_{\alpha\lambda\beta\delta} e_T^{*\lambda} p^\beta n^\delta, \end{aligned} \quad (17)$$

where the momentum fractions y_1 , \bar{y}_2 and y_g correspond to the quark, antiquark and gluon, respectively. The symbol $\stackrel{\mathcal{F}_2}{=}$ now stands for (here, $z_i = \lambda_i n$)

$$\int_0^1 dy_1 dy_2 dy_g \delta(y_2 - y_1 - y_g) \exp [iy_1 p \cdot z_1 + iy_g p \cdot z_2]. \quad (18)$$

In the *r.h.s.* of (17), it is useful to perform the integration over the gluon fraction y_g (which then equals $y_2 - y_1$). Afterwards, the parametrizations (17) take the forms:

$$\langle \rho(p_\rho) | \bar{\psi}(z_1) \gamma_\mu g A_\alpha^T(z_2) \psi(0) | 0 \rangle \stackrel{\mathcal{F}_2}{=} m_\rho f_{3\rho}^V B(y_1, y_2) p_\mu e_{T\alpha}^*, \quad (19)$$

$$\langle \rho(p_\rho) | \bar{\psi}(z_1) \gamma_5 \gamma_\mu g A_\alpha^T(z_2) \psi(0) | 0 \rangle \stackrel{\mathcal{F}_2}{=} m_\rho f_{3\rho}^A i D(y_1, y_2) p_\mu \varepsilon_{\alpha\lambda\beta\delta} e_T^{*\lambda} p^\beta n^\delta, \quad (20)$$

with the symbol $\stackrel{\mathcal{F}_2}{=}$ implying

$$\int_0^1 dy_1 \int_0^1 dy_2 \exp [iy_1 p \cdot z_1 + i(y_2 - y_1) p \cdot z_2]. \quad (21)$$

Note that the positivity of the gluon light-cone momentum fraction imposes that quark–gluon parameterizing functions have the form

$$B(y_1, y_2) \stackrel{\text{def}}{=} \mathcal{B}(y_1, y_2; y_2 - y_1) \theta(y_1 \leq y_2 \leq 1), \quad D(y_1, y_2) \stackrel{\text{def}}{=} \mathcal{D}(y_1, y_2; y_2 - y_1) \theta(y_1 \leq y_2 \leq 1). \quad (22)$$

As we already mentioned by writing Eq.(6), it is also natural to introduce the following objects:

$$\begin{aligned} \langle \rho(p_\rho) | \bar{\psi}(z_1) \gamma_\mu i \overleftrightarrow{D}_\alpha^T(z_2) \psi(0) | 0 \rangle &\stackrel{\mathcal{F}_2}{=} m_\rho f_\rho \tilde{B}(y_1, y_2) p_\mu e_{T\alpha}^*, \\ \langle \rho(p_\rho) | \bar{\psi}(z_1) \gamma_5 \gamma_\mu i \overleftrightarrow{D}_\alpha^T(z_2) \psi(0) | 0 \rangle &\stackrel{\mathcal{F}_2}{=} m_\rho f_\rho i \tilde{D}(y_1, y_2) p_\mu \varepsilon_{\alpha\lambda\beta\delta} e_T^{*\lambda} p^\beta n^\delta, \end{aligned} \quad (23)$$

where these parameterizing functions are now equal to

$$\begin{aligned} \tilde{B}(y_1, y_2) &= \frac{1}{2} \left(\varphi_1^T(y_1) + \varphi_1^T(y_2) \right) \delta(y_1 - y_2) + \zeta_3^V B(y_1, y_2), \\ \tilde{D}(y_1, y_2) &= \frac{1}{2} \left(\varphi_A^T(y_1) + \varphi_A^T(y_2) \right) \delta(y_1 - y_2) + \zeta_3^A D(y_1, y_2), \end{aligned} \quad (24)$$

with the dimensionless coupling constants

$$\zeta_3^V = \frac{f_{3\rho}^V}{f_\rho} \quad \text{and} \quad \zeta_3^A = \frac{f_{3\rho}^A}{f_\rho}. \quad (25)$$

Note that the function φ_1 corresponds to the twist-2, and functions B and D to the genuine (dynamical) twist-3, while functions φ_3 , φ_A , φ_1^T , φ_A^T (or alternatively \tilde{B} and \tilde{D}) contain both parts: kinematical (à la Wandzura-Wilczek, noted WW) twist-3 and genuine (dynamical) twist-3.

In (10)–(11), the functions φ_1 , φ_3 , φ_A , φ_1^T and φ_A^T parameterizing the two-particle correlators obey the following symmetry properties:

$$\varphi_1(y) = \varphi_1(1-y), \varphi_3(y) = \varphi_3(1-y), \varphi_A(y) = -\varphi_A(1-y), \varphi_1^T(y) = -\varphi_1^T(1-y), \varphi_A^T(y) = \varphi_A^T(1-y). \quad (26)$$

These symmetry properties result from G -conjugation (or C -conjugation for neutral mesons). At the same time, the symmetry properties of the functions parameterizing the quark-gluon correlators are:

$$\mathcal{B}(y_1, y_2; y_g) = -\mathcal{B}(1-y_2, 1-y_1; y_g), \quad \mathcal{D}(y_1, y_2; y_g) = \mathcal{D}(1-y_2, 1-y_1; y_g). \quad (27)$$

Notice that, in the case of three-particle functions, G -conjugation involves the replacement: $y_1 \leftrightarrow \bar{y}_2$, while the gluon fraction y_g remains invariant under G -conjugation.

2. CCF parametrization

We recall and rewrite (doing standard fields transformations) the original CCF parametrizations of the ρ DAs [7], adapting them to our case when vector meson is produced in the final state. The formula for the axial-vector correlator reads

$$\langle \rho(p_\rho) | \bar{\psi}(z) [z, 0] \gamma_\mu \gamma_5 \psi(0) | 0 \rangle = \frac{1}{4} f_\rho m_\rho \varepsilon_\mu^{e_T^* p z} \int_0^1 dy e^{iy(p \cdot z)} g_\perp^{(a)}(y), \quad (28)$$

where we denote⁴

$$\varepsilon_\mu^{e_T^* p z} = \varepsilon_\mu^{\alpha\beta\gamma} e_{T\alpha}^* p_\beta z_\gamma, \quad (29)$$

and where

$$[z_1, z_2] = P \exp \left[ig \int_0^1 dt (z_1 - z_2)_\mu A^\mu(t z_1 + (1-t) z_2) \right] \quad (30)$$

is the Wilson line, defined in accordance with the convention (8). The transverse vector e_T is orthogonal to the light-cone vectors p and z . Neglecting mass effects, i.e. up to twist 3 level, it is decomposed as follows

$$e_{T\mu} = e_\mu - p_\mu \frac{e \cdot z}{p \cdot z} - z_\mu \frac{e \cdot p}{p \cdot z}, \quad (31)$$

where e is the meson polarization vector. Since as we will discuss later n can be arbitrary, and since the concrete definition of n influences the definition of transverse polarization, it is useful to remove the dependence on e_T in correlation functions. For that, we use Eq.(31) and rewrite the original CCF parametrization in terms of the full meson polarization vector e . This is already done for the axial-vector correlator (28) since due to the properties of fully antisymmetric tensor $\epsilon_{\mu\nu\alpha\beta}$ one can use in the r.h.s. of (28) the full meson polarization vector e instead of e_T .

⁴ Note that, as already emphasized, our sign convention for the antisymmetric tensor is $\epsilon^{0123} = 1$, opposite to the one used in Ref.[7]. The corresponding sign change is taken here into account.

The definition of 2-parton vector correlator of a ρ -meson can be written in the form

$$\langle \rho(p_\rho) | \bar{\psi}(z) [z, 0] \gamma_\mu \psi(0) | 0 \rangle = f_\rho m_\rho \int_0^1 dy e^{iy(p \cdot z)} \left[p_\mu \frac{e^* \cdot z}{p \cdot z} \phi_{\parallel}(y) + e_{T\mu}^* g_{\perp}^{(v)}(y) - z_\mu \frac{m^2}{2} \frac{e^* \cdot z}{(p \cdot z)^2} g_3(y) \right]. \quad (32)$$

All distribution amplitudes describing two particle correlators are normalized to unity

$$\int_0^1 dy \left\{ \phi_{\parallel}, g_{\perp}^{(a)}, g_{\perp}^{(v)}, g_3 \right\} (y) = 1. \quad (33)$$

Using relations (31, 33) and integration by parts one can rewrite the vector correlator (32) in the form

$$\langle \rho(p_\rho) | \bar{\psi}(z) [z, 0] \gamma_\mu \psi(0) | 0 \rangle = f_\rho m_\rho \int_0^1 dy e^{iy(p \cdot z)} \left[-i p_\mu (e^* \cdot z) h(y) + e_\mu^* g_{\perp}^{(v)}(y) + i z_\mu \frac{m^2}{2} \frac{e^* \cdot z}{p \cdot z} \bar{h}(y) \right], \quad (34)$$

where we introduce the auxiliary functions

$$h(y) = \int_0^y dv \left(\phi_{\parallel}(v) - g_{\perp}^{(v)}(v) \right), \quad (35)$$

$$\bar{h}(y) = \int_0^y dv \left(g_3(v) - g_{\perp}^{(v)}(v) \right). \quad (36)$$

Note that the r.h.s of (34) now only involves the full polarization vector e , as was noted above for the axial correlator. The last term in the r.h.s. of (34) contributes to the physical amplitude starting from the twist 4 level only, therefore we will neglect it in the following.

For quark–antiquark–gluon correlators (up to twist 3 level) the parametrizations of Ref.[7] have the forms⁵

$$\langle \rho(p_\rho) | \bar{\psi}(z) [z, t z] \gamma_\alpha g G_{\mu\nu}(t z) [t z, 0] \psi(0) | 0 \rangle = -ip_\alpha [p_\mu e_{\perp\nu}^* - p_\nu e_{\perp\mu}^*] m_\rho f_{3\rho}^V \int D\alpha V(\alpha_1, \alpha_2) e^{i(p \cdot z)(\alpha_1 + t \alpha_g)}, \quad (37)$$

$$\langle \rho(p_\rho) | \bar{\psi}(z) [z, t z] \gamma_\alpha \gamma_5 g \tilde{G}_{\mu\nu}(t z) [t z, 0] \psi(0) | 0 \rangle = -p_\alpha [p_\mu e_{\perp\nu}^* - p_\nu e_{\perp\mu}^*] m_\rho f_{3\rho}^A \int D\alpha A(\alpha_1, \alpha_2) e^{i(p \cdot z)(\alpha_1 + t \alpha_g)}, \quad (38)$$

where $\alpha_1, \alpha_2, \alpha_g$ correspond to momentum fractions of quark, antiquark and gluon respectively inside the ρ -meson,

$$\int D\alpha = \int_0^1 d\alpha_1 \int_0^1 d\alpha_2 \int_0^1 d\alpha_g \delta(1 - \alpha_1 - \alpha_2 - \alpha_g) \quad (39)$$

and $\tilde{G}_{\mu\nu} = -\frac{1}{2} \epsilon_{\mu\nu\alpha\beta} G^{\alpha\beta}$. These three partons DAs are normalized as follows

$$\int D\alpha (\alpha_1 - \alpha_2) V(\alpha_1, \alpha_2) = 1, \quad \int D\alpha A(\alpha_1, \alpha_2) = 1. \quad (40)$$

In what follows we will work in the axial gauge $A \cdot n = 0, n^2 = 0$. In this gauge the gluon field can be expressed in terms of field strength as follows

$$A_\alpha(y) = \int_0^\infty d\sigma e^{-\epsilon\sigma} n^\beta G_{\alpha\beta}(y + \sigma n) \quad (41)$$

⁵ Note that in those definition f_ρ , $f_{3\rho}^V$ and $f_{3\rho}^A$ have dimension of mass. This is agreement with Ref.[8] but differ from Ref.[7] in which $f_{3\rho}^V$ and $f_{3\rho}^A$ have dimension of mass square.

which implies that the $(\bar{q} A q)$ correlators involving the gluon field A reads

$$\langle \rho(p_\rho) | \bar{\psi}(z) \gamma_\mu g A_\alpha(tz) \psi(0) | 0 \rangle = -p_\mu e_{T\alpha}^* m_\rho f_{3\rho}^V \int \frac{D\alpha}{\alpha_g} e^{i(p \cdot z)(\alpha_1 + t\alpha_g)} V(\alpha_1, \alpha_2), \quad (42)$$

$$\langle \rho(p_\rho) | \bar{\psi}(z) \gamma_\mu \gamma_5 g A_\alpha(tz) \psi(0) | 0 \rangle = -ip_\mu \frac{\varepsilon_\alpha^{zp e_T^*}}{(p \cdot z)} m_\rho f_{3\rho}^A \int \frac{D\alpha}{\alpha_g} e^{i(p \cdot z)(\alpha_1 + t\alpha_g)} A(\alpha_1, \alpha_2). \quad (43)$$

C. Equations of motion

The correlators introduced above are not independent, since they are constrained by the QCD equations of motion for the field operators entering them (see, for example, [4]). In the simplest case of fermionic fields, they follow from the vanishing of matrix elements $\langle (i\hat{D}(0)\psi(0))_\alpha \bar{\psi}_\beta(z) \rangle = 0$ and $\langle \psi_\alpha(0) i(\hat{D}(z)\bar{\psi}(z))_\beta \rangle = 0$ due to the Dirac equation, then projected on different Fierz structure.

Let us start with the QCD equation of motion written for the fermion field $\psi(0)$:

$$\langle i \vec{\not{D}}(0) \psi(0) \bar{\psi}(z) \rangle = 0, \quad (44)$$

where $\langle \dots \rangle$ denote arbitrary hadron states which we here specify as $\langle \rho | \dots | 0 \rangle$. Also, we stress that, in (44), the fermion fields ψ and $\bar{\psi}$ should be understood as fields with free Dirac indices. Then, we first focus on the quark–antiquark part of (44) which can be written as

$$\int d^4z e^{-ipy \cdot z - i\bar{y}p \cdot x} \left\{ \langle i \vec{\not{\partial}}_L^x \psi(x) \bar{\psi}(z) \rangle + \langle i \vec{\not{\partial}}_T^x \psi(x) \bar{\psi}(z) \rangle \right\} \Big|_{x=0}. \quad (45)$$

Here, we separate out the longitudinal derivatives from the transverse ones. Working with the longitudinal derivative contribution, we get

$$i\gamma_\rho \int d^4z e^{-ipy \cdot z - i\bar{y}p \cdot x} \frac{\partial^L}{\partial x_\rho} \langle \psi(x) \bar{\psi}(z) \rangle \Big|_{x=0} = \bar{y} \not{p} \int d^4z e^{-ipy \cdot z - i\bar{y}p \cdot x} \langle \psi(x) \bar{\psi}(z) \rangle \Big|_{x=0}, \quad (46)$$

where an integration by parts has been used. Let us now decompose $\langle \psi(x) \bar{\psi}(z) \rangle$ over the γ -basis (the Fierz decomposition):

$$-\langle \psi(x) \bar{\psi}(z) \rangle = \frac{1}{4} \langle \bar{\psi}(z) \gamma_\alpha \psi(x) \rangle \gamma^\alpha + \frac{1}{4} \langle \bar{\psi}(z) \gamma_5 \gamma_\alpha \psi(x) \rangle \gamma^\alpha \gamma_5. \quad (47)$$

With (47), after the use of the parametrization of the relevant correlators, one gets for the longitudinal derivative contribution (see, (46)):

$$\frac{\bar{y}}{4} \not{p} \not{\epsilon}^T \varphi_3(y) + i \frac{\bar{y}}{4} \not{p} \not{\epsilon}^T \gamma_5 \varphi_A(y) = -\frac{i}{4} \sigma_{p e^T} \left\{ \bar{y} \varphi_3(y) + \bar{y} \varphi_A(y) \right\}, \quad (48)$$

where again we introduced the short-hand notations:

$$\sigma_{p e^T} = \sigma_{\alpha\beta} p^\alpha e_T^* \epsilon^\beta, \quad a_{T\rho} = \varepsilon_{\rho e_T^* p n}. \quad (49)$$

We thus have for the longitudinal derivative contribution:

$$\int d^4z e^{-ipy \cdot z - i\bar{y}p \cdot x} \langle i \vec{\not{\partial}}_L \psi(x) \bar{\psi}(z) \rangle \Big|_{x=0} = -\frac{i}{4} \sigma_{p e^T} m_\rho f_\rho \left\{ \bar{y} \varphi_3(y) + \bar{y} \varphi_A(y) \right\}. \quad (50)$$

While, the correlators with the transverse derivatives in (45) can directly be expressed via the corresponding parameterizing functions with the help of (14) and (15):

$$\int d^4z e^{-ipy \cdot z - i\bar{y}p \cdot x} \langle i \vec{\not{\partial}}_T \psi(x) \bar{\psi}(z) \rangle \Big|_{x=0} = -\frac{i}{4} \sigma_{p e_T^*} m_\rho f_\rho \left\{ \varphi_1^T(y) + \varphi_A^T(y) \right\}. \quad (51)$$

Therefore, within the WW approximation (where all genuine twist 3 are disappeared) the equations of motion takes the following simple form:

$$\varphi_+^T(y) = -\bar{y} \varphi_+^{WW}(y), \quad (52)$$

where the plus (minus)-combination is defined as

$$\varphi_{\pm}(y) = \varphi^{\text{"vector"}}(y) \pm \varphi^{\text{"axial"}}(y). \quad (53)$$

Let us now take into account the quark–gluon correlators. Using (17), one can obtain that

$$-\gamma_{\rho} \langle A^{T\rho}(0) \psi(0) \bar{\psi}(z) \rangle = \frac{1}{4} \gamma_{\rho} \left\{ \langle \bar{\psi}(z) \gamma_{\alpha} A^{T\rho}(0) \psi(0) \rangle \gamma_{\alpha} + \langle \bar{\psi}(z) \gamma_5 \gamma_{\alpha} A^{T\rho}(0) \psi(0) \rangle \gamma_{\alpha} \gamma_5 \right\}, \quad (54)$$

where

$$\begin{aligned} \langle \bar{\psi}(z) \gamma_{\alpha} g A_{\rho}^T(0) \psi(0) \rangle &= m_{\rho} f_{3\rho}^V p_{\alpha} e_{T\rho}^* \int_0^1 dy_1 dy_2 e^{iy_1 p \cdot z} B(y_1, y_2), \\ \langle \bar{\psi}(z) \gamma_5 \gamma_{\alpha} g A_{\rho}^T(0) \psi(0) \rangle &= m_{\rho} f_{3\rho}^A i p_{\alpha} a_{T\rho} \int_0^1 dy_1 dy_2 e^{iy_1 p \cdot z} D(y_1, y_2). \end{aligned} \quad (55)$$

Thus, combining the quark–antiquark and quark–gluon correlators, one derives the following relation:

$$\int_0^1 dx \left(\tilde{B}(y, x) + \tilde{D}(y, x) \right) = -\bar{y} \varphi_+(y), \quad (56)$$

where one used the notations (24).

In a similar way, we can derive the relation associated with the C -conjugated equation:

$$\langle \psi(0) \bar{\psi}(z) i \not{D}(0) \rangle = 0. \quad (57)$$

which reads

$$\int_0^1 dx \left(\tilde{B}(x, y) - \tilde{D}(x, y) \right) = y \varphi_-(y). \quad (58)$$

Combining the relations (56) and (58) with the use of (24) and (53), we obtain

$$\begin{aligned} \bar{y}_1 \varphi_3(y_1) + \bar{y}_1 \varphi_A(y_1) + \varphi_1^T(y_1) + \varphi_A^T(y_1) \\ = - \int_0^1 dy_2 [\zeta_3^V B(y_1, y_2) + \zeta_3^A D(y_1, y_2)] \end{aligned} \quad (59)$$

and

$$\begin{aligned} y_1 \varphi_3(y_1) - y_1 \varphi_A(y_1) - \varphi_1^T(y_1) + \varphi_A^T(y_1) \\ = - \int_0^1 dy_2 [-\zeta_3^V B(y_2, y_1) + \zeta_3^A D(y_2, y_1)]. \end{aligned} \quad (60)$$

Note that Eq.(60) can be obtained by the replacement $y_1 \rightarrow \bar{y}_1$ in (59) and the use of symmetry properties (26, 27).

D. Additional set of equations

1. Light-cone factorization direction arbitrariness

Contrarily to the light-cone vector p related to the out-going meson momentum, the second light-cone vector n (with $p \cdot n = 1$), required for the parametrization of the needed correlators introduced in section II B 1 is arbitrary. The physical observables do not depend on the specific choice of n , thus the scattering amplitudes should be n -independent. For any specific process, there is a natural choice for n , which one may denote as n_0 . For instance, in forward $e - p$ collision, the proton momentum defines n_0 . More generally, one may expand an arbitrary choice of n as [4, 14]

$$n_\mu = \alpha p_\mu + \beta n_{0\mu} + n_\mu^\perp, \quad (61)$$

with the two constraints

$$p \cdot n = 1 \quad \text{and} \quad n^2 = 0, \quad (62)$$

which fixes the coefficients $\beta = 1$ and $\alpha = -n_\perp^2/2$. The light-cone vector n is thus parametrized by its transverse components n_\perp .

Let us now analyse the various source of n -dependence. First, it enters the definition of the non-local correlators introduced in Sec.II B 1 through the light-like separation $z = \lambda n$. These correlators are defined in the axial light-like gauge $n \cdot A = 0$, which allows to get rid of Wilson lines. Second, it determines the notion of transverse polarization of the ρ . Last, n enters the Sudakov decomposition (2) which defines the transverse parton momentum involved in the collinear factorization. Note that this notion of parton transverse momentum should not be confused with the notion of transverse momenta of external particles (e.g. in the case of $\gamma^* \rightarrow \rho$ impact factor to be discussed in Sec.III, entering in $\gamma^* N(p_2) \rightarrow \rho(p) N$ process, the t -channel gluons have a transverse momentum determined within another Sudakov basis defined by the external light-cone momenta $p_1 = p$ and incoming nucleon momentum p_2).

This n -independence principle leads to additional non-trivial constraints between the non-perturbative correlators entering the factorized amplitude. It was crucial for the understanding of inclusive structure functions properties at the twist three level [14] and its relevance for some exclusive processes was pointed out in [4]. We show now that this condition expressed at the level of the *full amplitude* of any process can be reduced to a set of conditions involving only the soft correlators. The obtained equations are process independent and do not assume a priori any Wandzura-Wilczek approximation. The strategy for deriving these equations relies on the power of the Ward identities to relate firstly amplitudes with different number of legs and secondly higher order coefficients in the Taylor expansion (4) to lower order ones.

In the case of processes involving ρ_T production up to twist 3 level, we will now derive the equations

$$\frac{d}{dy_1} \varphi_1^T(y_1) + \varphi_1(y_1) - \varphi_3(y_1) + \zeta_3^V \int_0^1 \frac{dy_2}{y_2 - y_1} (B(y_1, y_2) + B(y_2, y_1)) = 0, \quad (63)$$

$$\frac{d}{dy_1} \varphi_A^T(y_1) - \varphi_A(y_1) + \zeta_3^A \int_0^1 \frac{dy_2}{y_2 - y_1} (D(y_1, y_2) + D(y_2, y_1)) = 0. \quad (64)$$

The n -independence of \mathcal{A} for an arbitrary fixed polarization vector e is expressed by the condition

$$\frac{d}{dn_\perp^\mu} \mathcal{A} = 0, \quad (65)$$

which we write in the form

$$\frac{d}{dn_\perp^\mu} \mathcal{A} = \frac{\partial n^\alpha}{\partial n_\perp^\mu} \frac{\partial \mathcal{A}}{\partial n^\alpha} + \frac{\partial(e^* \cdot n)}{\partial n_\perp^\mu} \frac{\partial \mathcal{A}}{\partial(e^* \cdot n)} = [-n_\perp^\mu p^\alpha + g_{\perp\mu}^\alpha] \frac{\partial}{\partial n^\alpha} \mathcal{A} + e_{\perp\mu}^* \frac{\partial \mathcal{A}}{\partial(e^* \cdot n)}. \quad (66)$$

Let us emphasize the fact that although n fixes the gauge, the hard part does not depend on this gauge fixing vector, as we will show below after the technical derivation of Eqs.(63, 64). It means that the variation of n only affects the n -dependence related to the definition of transverse momentum ℓ_\perp and of transverse ρ polarization.

We also note that the appearance of the total derivative in Eqs.(65, 66) may be interpreted as a (vector) analog of the renormalization group (RG) invariance equation when the dependency on the renormalization parameter coming from various sources cancel. One can view this as a RG-like flow in the space of light-cone directions of contributions to the amplitude where the polarization vector plays the role of a beta function.

The scattering amplitude \mathcal{A} receives contributions from the vector correlators, which result into \mathcal{A}^{vector} , and from the axial vector correlators, which lead to \mathcal{A}^{axial} part of \mathcal{A} . Due to different parity properties of the vector and the axial-vector correlators, the condition (66) means effectively two separate conditions:

$$\frac{d}{dn_\perp^\mu} \mathcal{A}^{vector} = 0 \quad (67)$$

and

$$\frac{d}{dn_\perp^\mu} \mathcal{A}^{axial} = 0. \quad (68)$$

The dependence of \mathcal{A} on the vector n_\perp is obtained through the dependence of \mathcal{A} on the full vector n . This dependence on n is different in \mathcal{A}^{axial} and in \mathcal{A}^{vector} parts.

The dependence of \mathcal{A}^{axial} on the vector n enters only through the expression $\varepsilon^{p n \beta \gamma}$ involving the contraction with the momentum p and in which the indices β and γ are contracted with some other vectors. Thus the condition (68) is equivalent to

$$\frac{\partial n^\alpha}{\partial n_\perp^\mu} \frac{\partial}{\partial n^\alpha} \mathcal{A}^{axial} = [-n_\perp^\mu p^\alpha + g_\perp^{\alpha\mu}] \frac{\partial}{\partial n^\alpha} \mathcal{A}^{axial} = \frac{\partial}{\partial n_\perp^\mu} \mathcal{A}^{axial} = 0 \quad (69)$$

where we took into account the peculiar dependence of \mathcal{A}^{axial} on n discussed above. This will lead at the level of DAs to the equation (64).

In the vector part, the dependence with respect to n is identified by rewriting the polarization vector for transversally polarized ρ with the help of the identity

$$e_T^\mu = e^\mu - p^\mu e \cdot n, \quad (70)$$

since $e \cdot p = 0$. Thus the dependence of \mathcal{A}^{vector} on the vector n enters only through the scalar product $e^* \cdot n$, and Eq.(67) can be written as

$$\frac{d}{dn_\perp^\mu} \mathcal{A}^{vector} = e_T^{*\mu} \frac{\partial}{\partial (e^* \cdot n)} \mathcal{A}^{vector} = 0 \quad (71)$$

which results in

$$\frac{\partial}{\partial (e^* \cdot n)} \mathcal{A}^{vector} = 0 \quad (72)$$

from which follows Eq.(63).

We will now derive equations (63, 64) using as a tool the explicit example of the $\gamma^* \rightarrow \rho$ impact factor. We want here to insist on the fact that the proof is independent of the specific process under consideration, and only rely on general arguments based on Ward identities. For the $\gamma^* \rightarrow \rho$ impact factor, which will be computed in details in section III, one needs to consider 2-parton contributions both without transverse derivative (illustrated by diagrams of Fig.4) and with transverse derivative (see Fig.5), as well as 3-parton contributions (see Figs.6, 7, 8). Note that these drawing implicitly assume that the two right-hand side spinor lines are closed on the the two possible Fierz structures \not{p} or $\not{p}\gamma^5$ involved in the correlators of ρ -meson DAs.

In the color space, each of those diagrams can be projected in two parts, characterized by the two Casimir invariants C_F and N_c . The equations (63, 64) are obtained by considering the consequence of the n -independence on the contribution to the C_F color structure. The n -independence condition applied to the N_c structure is automatically satisfied and does not lead to new constraints, as we show in Appendix A.

We start with the derivation of Eq.(63), which corresponds to the vector correlator contributions with C_F invariant. The 3-parton ($q\bar{q}g$) contribution and the 2-parton contribution involving Φ^\perp to \mathcal{A} can be reduced to the convolution of the leading order hard 2-parton contributions with linear combination of correlators, thanks to the use of the Ward identity.

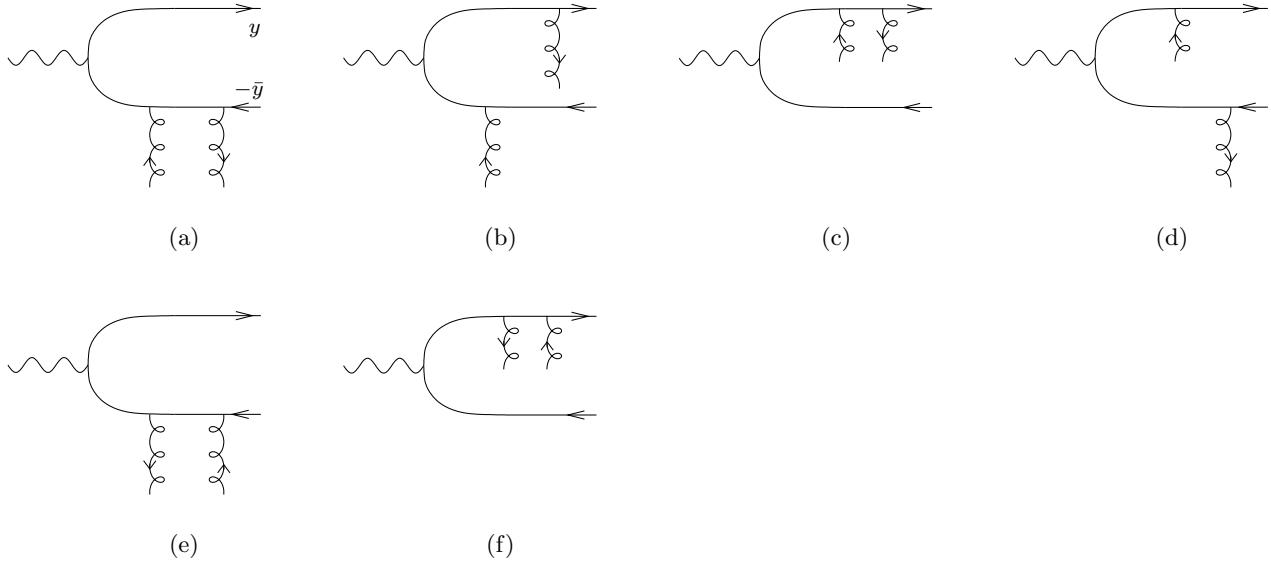


Figure 4: The 6 hard diagrams attached to the 2-parton correlators, which contribute to the $\gamma^* \rightarrow \rho$ impact factor, with momentum flux of external line, along p_1 direction. These drawing implicitly assume that the two right-hand side spinor lines are closed on the the two possible Fierz structures \not{p} or $\not{p}\gamma^5$.

In the case of the 3-parton vector correlator (19), due to (70) the dependency on n enters linearly and only through the scalar product $e^* \cdot n$. Thus, the action on the amplitude of the derivative d/dn_\perp involved in (72) can be extracted by the replacement $e_\alpha^* \rightarrow -p_\alpha$, which means in practice that the Feynman rule (using conventions of Ref.[17] for computing the T matrix element) $g t^a \gamma^\alpha e_\alpha^*$ entering the coupling of the gluon inside the hard part should be replaced by $-g t^a \gamma^\alpha p_\alpha$. Then, using the Ward identity for the hard part, it reads

$$(y_1 - y_2) \text{tr} [H_{q\bar{q}g}^\rho(y_1, y_2) p_\rho \not{p}] = \text{tr} [H_{q\bar{q}}(y_1) \not{p}] - \text{tr} [H_{q\bar{q}}(y_2) \not{p}] ,$$

which can be seen graphically as

$$p_\mu \left[\begin{array}{c} \text{Diagram of a particle with mass } \mu \text{ and momentum } y_1 \\ \text{coupled to a particle with mass } 1-y_2 \text{ and momentum } y_2 - y_1 \end{array} \right] = \frac{1}{y_1 - y_2} \left[\begin{array}{c} \text{Diagram of a particle with mass } y_1 \text{ and momentum } y_1 \\ \text{coupled to a particle with mass } 1-y_1 \text{ and momentum } 1-y_1 \end{array} \right] - \left[\begin{array}{c} \text{Diagram of a particle with mass } y_2 \text{ and momentum } y_2 \\ \text{coupled to a particle with mass } 1-y_2 \text{ and momentum } 1-y_2 \end{array} \right] \quad (73)$$

as we will show below with more details, and will give the last term of r.h.s of Eq.(63). The proof can be settled easily relying on a graphical rule in order to use the collinear Ward identity. Indeed within the conventions of [17], the collinear Ward identity can be symbolically written as

$$p_\mu \frac{y_1 p}{y_1 p + \gamma^\mu y_2 p} = \frac{1}{y_2 - y_1} \left[\frac{(y_2 - y_1) p}{y_2 p} - \frac{(y_2 - y_1) p}{y_1 p} \right] \quad (74)$$

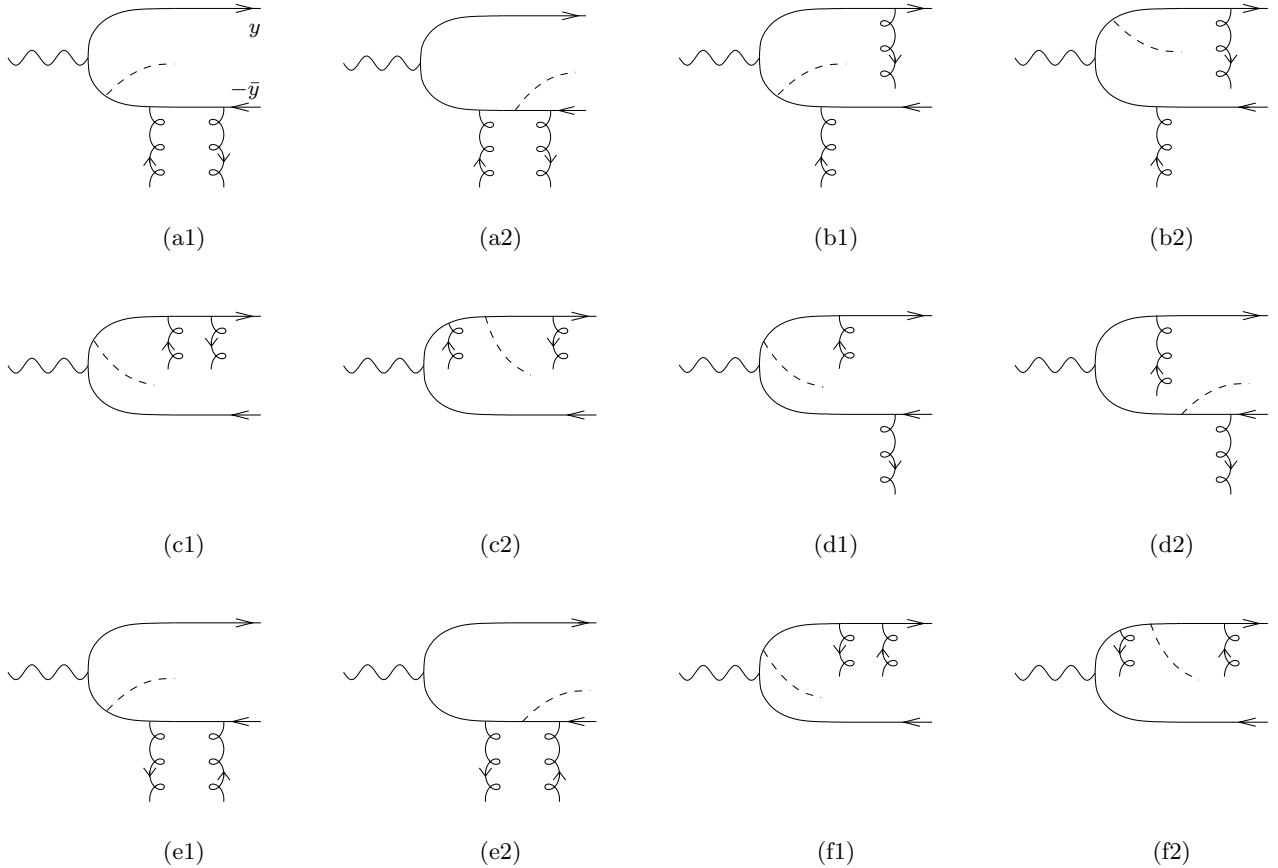


Figure 5: The 12 contributions arising from the first derivative of the 6 hard diagrams attached to the 2-parton correlators, which contribute to the $\gamma^* \rightarrow \rho$ impact factor, with momentum flux of external line, along p_1 direction.

where each fermionic line is a propagator. The wavy lines with double arrows are there in order to fulfill momentum conservation, since the *incoming* momentum is $y_1 p$ while the *outgoing* momentum is $y_2 p$.

Let us consider the 3-parton "Abelian" diagrams, illustrated in Fig.6. Applying the Ward identity (74) to

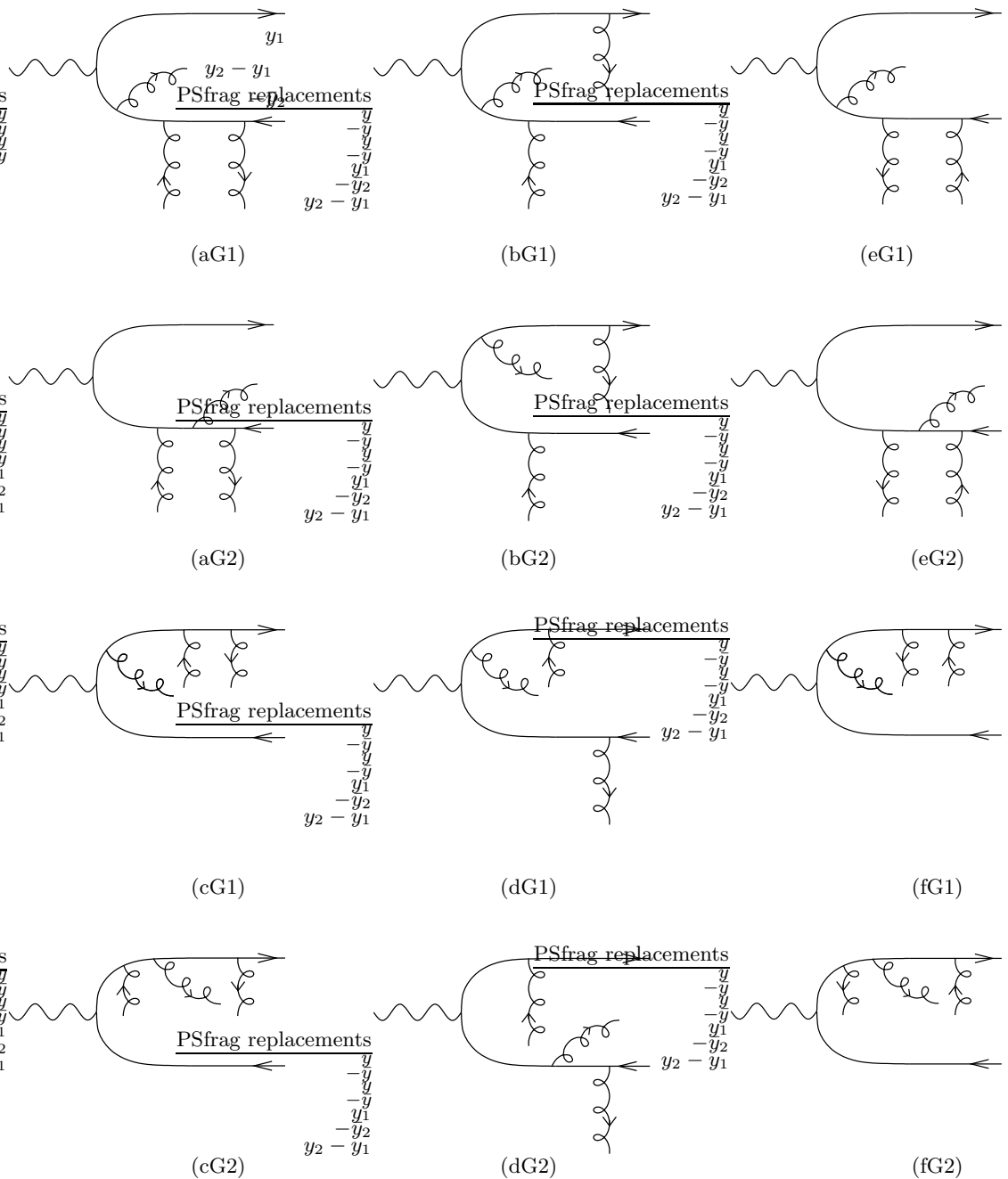


Figure 6: The 12 "Abelian" (i.e. without triple gluon vertex) type contributions from the hard scattering amplitude attached to the 3-parton correlators for the $\gamma^* \rightarrow \rho$ impact factor, with momentum flux of external line, along p_1 direction.

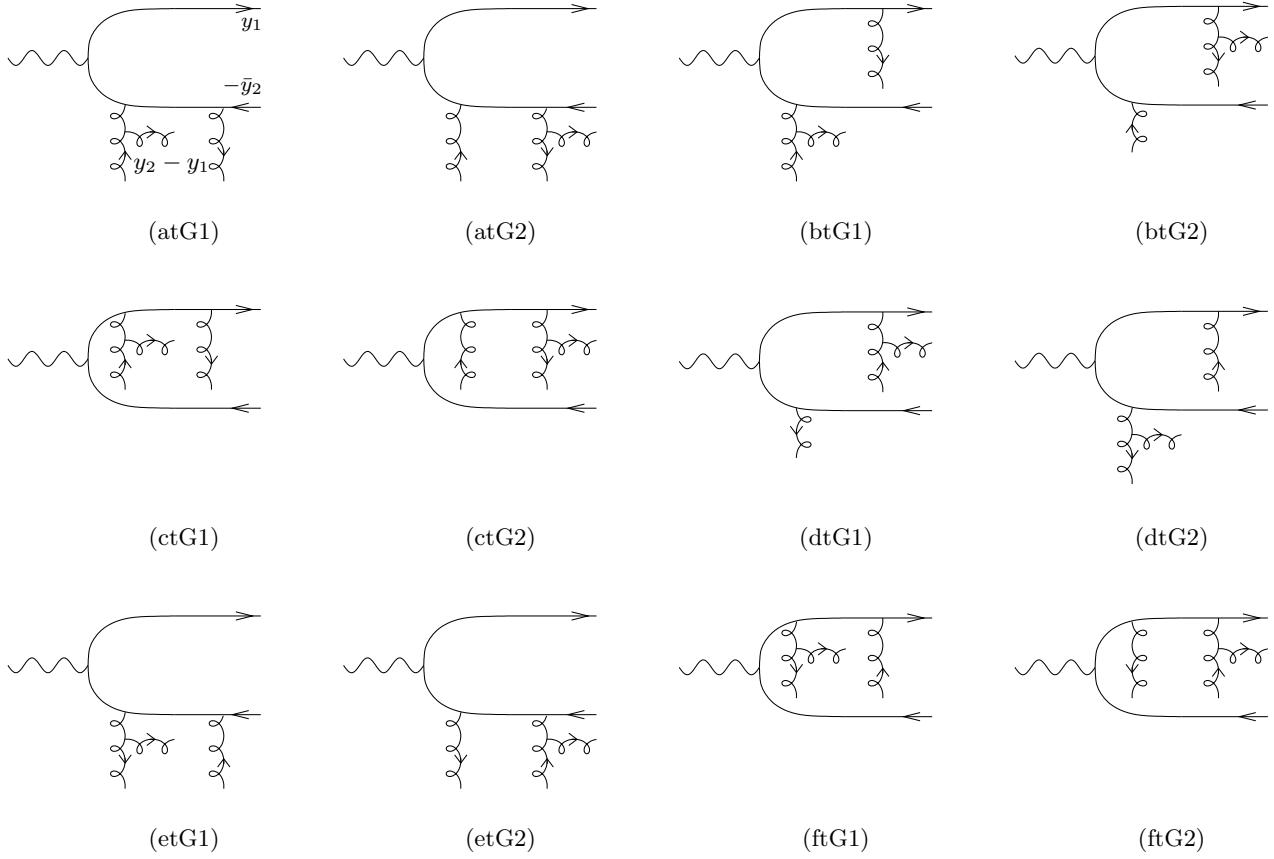


Figure 7: The 12 "non-Abelian" -(with one triple gluon vertex) contributions from the hard scattering amplitude attached to the 3-parton correlators, for the $\gamma^* \rightarrow \rho$ impact factor, with momentum flux of external line, along p_1 direction.

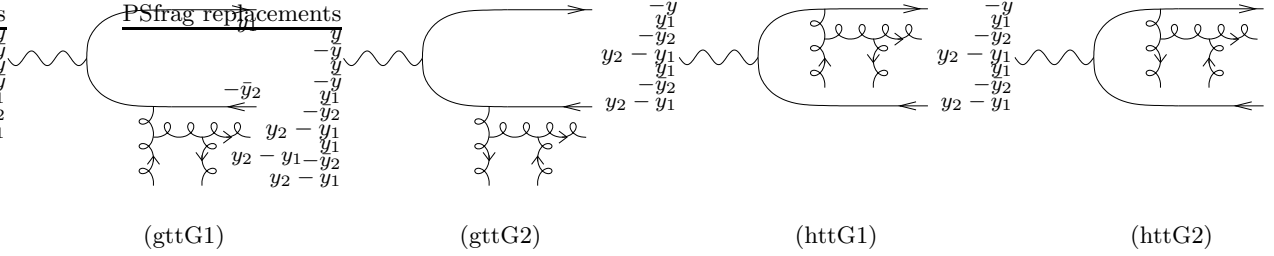


Figure 8: The 4 "non-Abelian" -(with two triple gluon vertices) contributions from the hard scattering amplitude attached to the 3-parton correlators, for the $\gamma^* \rightarrow \rho$ impact factor, with momentum flux of external line, along p_1 direction.

graphs (aG1) and (aG2) gives

$$\begin{aligned}
 & - (y_2 - y_1) p_\mu \left[\begin{array}{c} \text{Diagram (aG1)} \\ + \\ \text{Diagram (aG2)} \end{array} \right] \\
 = & \quad \text{Diagram (aG1)} - \text{Diagram (aG2)} \\
 + & \quad \text{Diagram (aG3)} - \text{Diagram (aG4)} \\
 = & \quad \text{Diagram (aG5)} - \text{Diagram (aG6)}, \tag{75}
 \end{aligned}$$

where the indicated momentum fractions correspond to flow along the momentum p_1 of the ρ -meson. The last line of Eq.(75) has been obtained after cancellation of the first and fourth term in the second equality, and the two remaining diagrams have been relabelled (in the first term of the last line, one does $y_2 - 1 \rightarrow y_1 - 1$ for the outgoing antiquark, and in the second term, one does $y_1 \rightarrow y_2$ for the outgoing quark), as far as the external lines are concerned, after using the fact that this does not change its internal structure.

The same identity applies for each couple of graphs (bG1, bG2), (cG1, cG2), (dG1, dG2), (eG1, eG2) and

(fG1, fG2). This leads to the following identity

$$\begin{aligned}
& - \int_0^1 dy_1 \int_0^1 dy_2 B(y_1, y_2) \\
& \times p_\mu \left[\begin{array}{c} \text{Diagram 1} \\ + \text{Diagram 2} \\ + \text{Diagram 3} \\ + \text{Diagram 4} \\ + \text{Diagram 5} \\ + \text{Diagram 6} \\ + \text{Diagram 7} \\ + \text{Diagram 8} \end{array} \right] \\
& = \int_0^1 dy_1 \int_0^1 dy_2 \frac{B(y_1, y_2)}{y_2 - y_1} \\
& \times \left\{ \left[\begin{array}{c} \text{Diagram 1} \\ + \text{Diagram 2} \\ + \text{Diagram 3} \\ + \text{Diagram 4} \\ + \text{Diagram 5} \\ + \text{Diagram 6} \end{array} \right] - (y_1 \leftrightarrow y_2) \right\} \\
& = \int_0^1 dy_1 \int_0^1 \frac{dy_2}{y_2 - y_1} [B(y_1, y_2) + B(y_2, y_1)] \\
& \times \left[\begin{array}{c} \text{Diagram 1} \\ + \text{Diagram 2} \\ + \text{Diagram 3} \\ + \text{Diagram 4} \\ + \text{Diagram 5} \\ + \text{Diagram 6} \end{array} \right] \quad (76)
\end{aligned}$$

where the last line is obtained after performing the change of variable $y_1 \leftrightarrow y_2$ in the second term. Note that the hard part given by diagrams inside Eq.(76) is convoluted with the last term of Eq.(63).

A similar treatment of 2-parton correlators with transverse derivative whose contributions can be viewed as 3-parton processes with vanishing gluon momentum leads to

$$\begin{aligned}
& - \int_0^1 dy_1 \int_0^1 dy_2 \delta(y_1 - y_2) \varphi_1^T(y_1) \\
& \times p_\mu \left[\begin{array}{c} \text{Diagram 1} \\ + \text{Diagram 2} \\ + \text{Diagram 3} \\ + \text{Diagram 4} \\ + \text{Diagram 5} \\ + \text{Diagram 6} \\ + \text{Diagram 7} \\ + \text{Diagram 8} \end{array} \right] \\
& = \int_0^1 dy_1 \int_0^1 dy_2 \delta(y_1 - y_2) \frac{\varphi_1^T(y_1)}{y_2 - y_1} \\
& \times \left\{ \left[\begin{array}{c} \text{Diagram 1} \\ + \text{Diagram 2} \\ + \text{Diagram 3} \\ + \text{Diagram 4} \\ + \text{Diagram 5} \\ + \text{Diagram 6} \end{array} \right] - (y_1 \leftrightarrow y_2) \right\}
\end{aligned}$$

$$\begin{aligned}
&= \int_0^1 dy_1 \frac{d}{dy_1} \varphi_1^T(y_1) \\
&\times \left[\text{Diagram 1} + \text{Diagram 2} + \text{Diagram 3} + \text{Diagram 4} + \text{Diagram 5} + \text{Diagram 6} \right], \quad (77)
\end{aligned}$$

where the last line is obtained after integration by part. This leads to the convolution of the first term of the l.h.s of Eq.(63) with the $[\dots]$ part in (77).

The second term, with φ_1 , of the l.h.s of Eq.(63) originates from the 2-parton vector correlator and corresponds to the contribution for the longitudinally polarized ρ with $e_L \sim p$. The third term with φ_3 corresponds to the contribution of the same correlator for the polarization vector of ρ_T written as in Eq.(70). To get Eq.(63), we used the fact that each individual term obtained above when expressing the n -independence condition involve the *same* 2-parton hard part, convoluted with the Eq.(63) through an integration over y_1 . The arguments used above, based on the collinear Ward identity, are clearly independent of the detailed structure of this resulting 2-parton hard part. Therefore, we deduce from this that Eq.(63) itself should be satisfied.

A similar treatment for axial correlators leads to Eq.(64). To prove this, we start from Eq.(69) and we note that the parametrizations of matrix elements of correlators with axial-vector currents (15, 17, 20) involve the quantity

$$p^\mu \varepsilon^\alpha e_T^* p^n \quad (78)$$

in which the index α is contracted with the matrix γ^α appearing in the vertex of gluon emission in the hard part and the momentum p^μ is contracted with the Fierz matrix $\gamma_\mu \gamma^5$ corresponding in the hard part to the meson vertex. First let us note that in the expression (78) one can replace e_T^* by the full polarization vector e^* , i.e.

$$p^\mu \varepsilon^\alpha e_T^* p^n = p^\mu \varepsilon^\alpha e^* p^n. \quad (79)$$

Secondly, the inspection of the quantity (78) or (79) leads to the conclusion that in order to use the Ward identities in a similar way as it was done in the vector part we need to interchange in (78) the indices $\mu \leftrightarrow \alpha$. It is done with the help of the Schouten identity, which for our peculiar case means that

$$p^\mu \varepsilon^\alpha e_T^* p^n = p^\alpha \varepsilon^\mu e_T^* p^n. \quad (80)$$

After that, the momentum p^α acts on the gluon vertex in the hard part, so the consequences of the n -independence of the axial part of the impact factor maybe derived in exactly the same way as we did above in the case of vector correlators, since the vector $\varepsilon^\mu e_T^* p^n$ is completely factorized. One then obtains Eq.(64) from Eq.(63) after the replacements $B \rightarrow D$, $\varphi_3 \rightarrow \varphi_A$, $\varphi_1^T \rightarrow \varphi_A^T$ and $\varphi_1 \rightarrow 0$ since there is no counterpart of the twist 2 DA φ_1 for the axial part.

Since we rely on the n -independence of the amplitude, one may wonder about the effect of the gauge choice, which is fixed by n , on the hard part. The QCD Ward identities require the vanishing of the amplitude in which polarization vector of a gluon is replaced by its momentum provided all other partons are on the mass shell. In the framework of the k_T -factorization (see Sec.III), the t -channel gluons are off the mass-shell. Therefore the replacement of the s -channel gluon polarization vector by its momentum leads to the vanishing of scattering amplitude up to terms proportional to k_{\perp}^2/s where k_{\perp} are transverse momenta of t -channel gluons. From the point of view of the t -channel, the gauge invariance of the impact-factor means that it should vanish when the transverse momentum of any t -channel gluon vanishes. To achieve this property it is necessary to include in a consistent way not only DAs with lowest Fock state containing only quarks but also those involving quarks and gluon, as we will show in detail in Sec.III.

In practice, we here check this invariance by contracting the s -channel emitted gluon vertex in the hard part with the momentum, which in collinear factorization is proportional to the ρ -meson momentum, which leads to simplifications in the use of (collinear) Ward identities.

In order to prove this, one should first project on the various color Casimir structure. In the case of the impact factor (see Sec.III), this means to distinguish N_c and C_F terms. In this case, C_F terms arise from 2-partons diagrams and from 3-partons diagrams where the emitted gluon is attached to a quark line, while N_c terms are obtained from 3-partons diagrams where the emitted gluon is attached to a quark line only between 2 t -channel exchanged gluons or from diagrams involving at least one triple gluon vertex.

The method is almost identical with the one used above when deriving the n -independence equations. Consider first the case of hard 3-partons diagrams entering the vector part of Fierz decomposition. We contract the s -channel emitted gluon vertex with its momentum, which is proportional to p_μ . The next step is to use the same method as the one used in Eq.(76), except that the DA B is not involved here. One thus finally gets two groups of 6 diagrams (which differ by the labeling of outgoing quarks, one being y_1 and \bar{y}_1 for the quark and antiquark, respectively, and the other one being y_2 and \bar{y}_2 for the quark and antiquark respectively). Since we started here from the consideration of the $\gamma_T^* \rightarrow \rho_T$ transition, each of these 6 hard contributions, due to the appearance of the remaining \not{p} from the Fierz structure, thus now encodes the hard part of the transition $\gamma_T^* \rightarrow \rho_L$. This transition vanishes in our kinematics, which leads to the conclusion that this hard part is gauge invariant. The same treatment can be applied to the hard diagrams with derivative insertion displayed in Fig.5, since this insertion corresponds to the peculiar limit of vanishing “gluon” momentum.

The proof for the axial part of the Fierz decomposition goes along the same line. The only difference lays on the appearance of the $\not{p} \gamma^5$ structure, which corresponds to a meson b_1 with quantum numbers $J^{PC} = 1^{+-}$ instead of 1^{--} for ρ , leading finally to the hard part of the transition $\gamma_T^* \rightarrow b_{1L}$ which vanishes in our kinematics.

In the case of contribution proportional to N_c , one can prove that these hard terms are also gauge invariant. This is proven in Appendix A. The reason is the same as the one which led to the conclusion that N_c terms do not lead to additional n -independence condition.

Although our implementation of factorization and n -independence condition is illustrated here on the particular example of the impact factor at twist 3, we expect that this procedure is more general and that the above method can be applied for other exclusive processes, for which the key tool is still the collinear Ward identity. This means in particular that each building block (soft and hard part, for each structure which lead to the introduction of a DA) are separately gauge invariant. This fact simplifies dramatically the use of the n -independence principle.

2. A minimal set of non-perturbative correlators

We now solve the previous equations, namely the two equation of motions (59,60) and the two equations (63,64) coming from the n -independence. This effectively reduces the set of 7 DAs to the set of 3 independent DAs φ_1 , B , D .

To start with we represent the distributions $\varphi_3(y)$, $\varphi_A(y)$, $\varphi_1^T(y)$ and $\varphi_A^T(y)$ generically denoted as $\varphi(y)$ as the sums

$$\varphi(y) = \varphi^{WW}(y) + \varphi^{gen}(y), \quad \varphi(y) = \varphi_3(y), \varphi_A(y), \varphi_1^T(y), \varphi_A^T(y), \quad (81)$$

where $\varphi^{WW}(y)$ and $\varphi^{gen}(y)$ are contributions in the so called Wandzura-Wilczek approximation and the genuine twist-3 contributions, respectively.

The Wandzura-Wilczek contributions are solutions of Eqs. (59, 60, 63, 64) with vanishing 3-parton distributions $B(y_1, y_2)$ and $D(y_1, y_2)$, i.e. which satisfy the equations

$$\bar{y}_1 \varphi_3^{WW}(y_1) + \bar{y}_1 \varphi_A^{WW}(y_1) + \varphi_1^{TWW}(y_1) + \varphi_A^{TWW}(y_1) = 0 \quad (82)$$

$$y_1 \varphi_3^{WW}(y_1) - y_1 \varphi_A^{WW}(y_1) - \varphi_1^{TWW}(y_1) + \varphi_A^{TWW}(y_1) = 0. \quad (83)$$

$$\frac{d}{dy_1} \varphi_1^{TWW}(y_1) = -\varphi_1(y_1) + \varphi_3^{WW}(y_1), \quad \frac{d}{dy_1} \varphi_A^{TWW}(y_1) = \varphi_A^{WW}(y_1). \quad (84)$$

By adding and subtracting Eqs. (82,83) together with the use of Eqs. (84) one obtains equations which involve only φ_3^{WW} and φ_A^{WW}

$$\frac{d}{dy_1} \varphi_3^{WW}(y_1) = -(\bar{y}_1 - y_1) \frac{d}{dy_1} \varphi_A^{WW}(y_1), \quad 2\varphi_1(y_1) = \frac{d}{dy_1} \varphi_A^{WW}(y_1) + (\bar{y}_1 - y_1) \frac{d}{dy_1} \varphi_3^{WW}(y_1) \quad (85)$$

and which solutions, satisfying the normalization conditions

$$\int_0^1 dy \varphi_3^{WW}(y) = 1 \quad \text{and} \quad \int_0^1 dy \varphi_A^{WW}(y) = 1, \quad (86)$$

read

$$\varphi_A^{WW}(y_1) = \frac{1}{2} \left[\int_0^{y_1} \frac{dv}{\bar{v}} \varphi_1(v) - \int_{y_1}^1 \frac{dv}{v} \varphi_1(v) \right], \quad \varphi_3^{WW}(y_1) = \frac{1}{2} \left[\int_0^{y_1} \frac{dv}{\bar{v}} \varphi_1(v) + \int_{y_1}^1 \frac{dv}{v} \varphi_1(v) \right]. \quad (87)$$

These expressions and Eqs. (82, 83) give finally the remaining solutions φ_A^{TWW} and φ_1^{TWW}

$$\varphi_A^{TWW}(y_1) = \frac{1}{2} \left[-\bar{y}_1 \int_0^{y_1} \frac{dv}{\bar{v}} \varphi_1(v) - y_1 \int_{y_1}^1 \frac{dv}{v} \varphi_1(v) \right], \quad \varphi_1^{TWW}(y_1) = \frac{1}{2} \left[-\bar{y}_1 \int_0^{y_1} \frac{dv}{\bar{v}} \varphi_1(v) + y_1 \int_{y_1}^1 \frac{dv}{v} \varphi_1(v) \right]. \quad (88)$$

We note that these two WW results (87) were obtained in Ref. [18] when considering the transition form factor $B \rightarrow \rho \gamma$. The distributions φ^{gen} carrying the genuine twist-3 contributions satisfy the equations

$$\bar{y}_1 \varphi_3^{gen}(y_1) + \bar{y}_1 \varphi_A^{gen}(y_1) + \varphi_1^{Tgen}(y_1) + \varphi_A^{Tgen}(y_1) = - \int_0^1 dy_2 [\zeta_3^V B(y_1, y_2) + \zeta_3^A D(y_1, y_2)], \quad (89)$$

$$y_1 \varphi_3^{gen}(y_1) - y_1 \varphi_A^{gen}(y_1) - \varphi_1^{Tgen}(y_1) + \varphi_A^{Tgen}(y_1) = - \int_0^1 dy_2 [-\zeta_3^V B(y_2, y_1) + \zeta_3^A D(y_2, y_1)], \quad (90)$$

$$\begin{aligned} \frac{d}{dy_1} \varphi_1^{Tgen}(y_1) &= \varphi_3^{gen}(y_1) - \zeta_3^V \int_0^1 \frac{dy_2}{y_2 - y_1} (B(y_1, y_2) + B(y_2, y_1)), \\ \frac{d}{dy_1} \varphi_A^{Tgen}(y_1) &= \varphi_A^{gen}(y_1) - \zeta_3^A \int_0^1 \frac{dy_2}{y_2 - y_1} (D(y_1, y_2) + D(y_2, y_1)). \end{aligned} \quad (91)$$

Similarly as in the WW case, one can obtain equations without distributions φ^{Tgen} by adding and subtracting Eqs. (89, 90) together with the use of (91)

$$\begin{aligned} &\frac{d}{dy_1} \varphi_3^{gen}(y_1) + (\bar{y}_1 - y_1) \frac{d}{dy_1} \varphi_A^{gen}(y_1) \\ &= 4 \zeta_3^A \int_0^1 \frac{dy_2}{y_2 - y_1} D^{(+)}(y_1, y_2) - 2 \zeta_3^V \frac{d}{dy_1} \int_0^1 dy_2 B^{(-)}(y_1, y_2) - 2 \zeta_3^A \frac{d}{dy_1} \int_0^1 dy_2 D^{(+)}(y_1, y_2), \end{aligned} \quad (92)$$

$$\begin{aligned} &\frac{d}{dy_1} \varphi_A^{gen}(y_1) + (\bar{y}_1 - y_1) \frac{d}{dy_1} \varphi_3^{gen}(y_1) \\ &= 4 \zeta_3^V \int_0^1 \frac{dy_2}{y_2 - y_1} B^{(+)}(y_1, y_2) - 2 \zeta_3^V \frac{d}{dy_1} \int_0^1 dy_2 B^{(+)}(y_1, y_2) - 2 \zeta_3^A \frac{d}{dy_1} \int_0^1 dy_2 D^{(-)}(y_1, y_2), \end{aligned} \quad (93)$$

where $O^{(\pm)}(y_1, y_2) = O(y_1, y_2) \pm O(y_2, y_1)$ for $O = B, D$. Let us note that Eq. (93) can be obtained from Eq. (92) and by the interchange $\varphi_A^{gen} \leftrightarrow \varphi_3^{gen}$ and $B \leftrightarrow D$.

From Eqs. (92, 93) supplemented by the boundary conditions $\mathcal{B}(y, y) = 0 = \mathcal{D}(y, y)$ (see later in Section II E)

one gets in a straightforward although somehow tedious way the equation for φ_3^{gen}

$$\begin{aligned} \frac{d}{dy_1} \varphi_3^{gen}(y_1) = & -\frac{1}{2} \left(\frac{1}{y_1} + \frac{1}{\bar{y}_1} \right) \\ & \left\{ \zeta_3^V \left[y_1 \int_{y_1}^1 dy_2 \frac{d}{dy_1} B(y_1, y_2) - \bar{y}_1 \int_0^{y_1} \frac{d}{dy_1} B(y_2, y_1) + (\bar{y}_1 - y_1) \left(\int_{y_1}^1 dy_2 \frac{B(y_1, y_2)}{y_2 - y_1} + \int_0^{y_1} dy_2 \frac{B(y_2, y_1)}{y_2 - y_1} \right) \right] \right. \\ & \left. + \zeta_3^A \left[y_1 \int_{y_1}^1 dy_2 \frac{d}{dy_1} D(y_1, y_2) + \bar{y}_1 \int_0^{y_1} \frac{d}{dy_1} D(y_2, y_1) - \int_{y_1}^1 dy_2 \frac{D(y_1, y_2)}{y_2 - y_1} - \int_0^{y_1} dy_2 \frac{D(y_2, y_1)}{y_2 - y_1} \right] \right\}, \end{aligned} \quad (94)$$

which properly normalized solution can be written in the form

$$\varphi_3^{gen}(y) = \frac{1}{2} \left(- \int_y^1 \frac{dy_1}{y_1} + \int_0^1 \frac{dy_1}{\bar{y}_1} \right) \{ \dots \}, \quad (95)$$

in which both integrals act on the expression inside $\{ \dots \}$ on the r.h.s of Eq.(94). The expression (95) can be simplified after changing the order of the nested integrals. After performing this task we obtain that

$$\begin{aligned} \varphi_3^{gen}(y) = & \frac{1}{2} \int_y^1 \frac{du}{u} \left[\int_0^u dy_2 \frac{d}{du} (\zeta_3^V B - \zeta_3^A D)(y_2, u) - \int_u^1 \frac{dy_2}{y_2 - u} (\zeta_3^V B - \zeta_3^A D)(u, y_2) - \int_0^u \frac{dy_2}{y_2 - u} (\zeta_3^V B - \zeta_3^A D)(y_2, u) \right] \\ & - \frac{1}{2} \int_0^{y_1} \frac{du}{u} \left[\int_u^1 dy_2 \frac{d}{du} (\zeta_3^V B + \zeta_3^A D)(u, y_2) - \int_u^1 \frac{dy_2}{y_2 - u} (\zeta_3^V B + \zeta_3^A D)(u, y_2) - \int_0^u \frac{dy_2}{y_2 - u} (\zeta_3^V B + \zeta_3^A D)(y_2, u) \right]. \end{aligned} \quad (96)$$

Finally, the solution for $\varphi_1^{T\,gen}$ is obtained from the first Eq. (91) and (96)

$$\varphi_1^{T\,gen}(y) = \int_0^y du \varphi_3^{gen}(u) - \zeta_3^V \int_0^y dy_1 \int_y^1 dy_2 \frac{B(y_1, y_2)}{y_2 - y_1}. \quad (97)$$

The corresponding expressions for $\varphi_A^{gen}(y)$ and $\varphi_A^{T\,gen}(y)$ are obtained from Eq.(96) and (97) by the substitutions:

$$\varphi_3^{gen}(y) \xleftrightarrow{\zeta_3^V B \leftrightarrow \zeta_3^A D} \varphi_A^{gen}(y), \quad (98)$$

$$\varphi_1^{T\,gen}(y) \xleftrightarrow{\zeta_3^V B \leftrightarrow \zeta_3^A D} \varphi_A^{T\,gen}(y). \quad (99)$$

In conclusion of this section, we explicitly succeeded in representing our results (87), (88), (96), (97), (98) (99) in terms of 3 independent DAs: the twist 2 DA φ_1 and the twist 3 DAs B, D .

E. Dictionary

For comparison of expressions (19, 20) with the definitions (42, 43) we perform the change of variables $z \rightarrow z_1$, $tz \rightarrow z_2$, $\alpha_d \rightarrow y_1$ and $\alpha_u = 1 - y_2$, i.e. $\alpha_g = y_2 - y_1$. It results in the following identification of the 3-parton DAs in LCCF and CCF approaches

$$B(y_1, y_2) = -\frac{V(y_1, 1 - y_2)}{y_2 - y_1} \quad (100)$$

$$D(y_1, y_2) = -\frac{A(y_1, 1 - y_2)}{y_2 - y_1}. \quad (101)$$

From (100, 101) and Ref.[7] follows the boundary conditions $B(y, y) = 0 = D(y, y)$.

Taking in Eqs.(32, 34) the coordinate z along the light-cone vector n , $z = \lambda n$, permits the identification of the vector DAs in Eq.(10):

$$\varphi_1(y) = \phi_{\parallel}(y), \quad \varphi_3(y) = g_{\perp}^{(v)}(y), \quad (102)$$

and of the axial DA in Eq. (11)

$$\varphi_A(y) = -\frac{1}{4} \frac{\partial g_{\perp}^{(a)}(y)}{\partial y}. \quad (103)$$

We checked also the validity of Eqs.(102, 103) directly by the use of our explicit solutions (87, 96, 98) and expressions for $g_{\perp}^{(v)}$ and $g_{\perp}^{(a)}$ given Ref. [7] in terms of ϕ_{\parallel} , V and A DAs. This non trivial check can be done with the help of methods similar to those used in Appendix B when comparing the results of calculation of the $\gamma^* \rightarrow \rho_T$ impact factor in LCCF and CCF approaches.

III. $\gamma^* \rightarrow \rho_T$ IMPACT FACTOR UP TO TWIST THREE ACCURACY

A. General recall on impact factor representation and kinematics

The $\gamma^* \rightarrow \rho$ impact factor enters the description of high energy reactions in the k_T factorization approach. As an example, one may study the reactions

$$\gamma^*(q) + \gamma^*(q') \rightarrow \rho_T(p_1) + \rho(p_2) \quad (104)$$

or

$$\gamma^*(q) + N \rightarrow \rho_T(p_1) + N \quad (105)$$

where the virtual photons carry large squared momenta $q^2 = -Q^2$ ($q'^2 = -Q'^2$) $\gg \Lambda_{QCD}^2$, and the Mandelstam variable s obeys the condition $s \gg Q^2, Q'^2, -t \simeq \underline{r}^2$. The hard scale which justifies the applicability of perturbative QCD is set by Q^2 and Q'^2 and/or by t . Neglecting meson masses, one considers for reaction (104) the light-cone vectors p_1 and p_2 as the vector meson momenta ($2p_1 \cdot p_2 = s$).

In this Sudakov light-cone basis, transverse Euclidian momenta are denoted with underlined letters. The virtual photon momentum q reads

$$q = p_1 - \frac{Q^2}{s} p_2. \quad (106)$$

The impact representation of the scattering amplitude for the reaction (104) is [19, 20, 21]

$$\mathcal{M} = \frac{is}{(2\pi)^2} \int \frac{d^2 \underline{k}}{\underline{k}^2} \Phi_1^{ab}(\underline{k}, \underline{r} - \underline{k}) \int \frac{d^2 \underline{k}'}{\underline{k}'^2} \Phi_2^{ab}(-\underline{k}', -\underline{r} + \underline{k}') \int_{\delta-i\infty}^{\delta+i\infty} \frac{d\omega}{2\pi i} \left(\frac{s}{s_0} \right)^\omega G_\omega(\underline{k}, \underline{k}', \underline{r}) \quad (107)$$

where G_ω is the 4-gluons Green function which obeys the BFKL equation [22]. G_ω reduces to

$$G_\omega^{Born} = \frac{1}{\omega} \delta^2(\underline{k} - \underline{k}') \frac{\underline{k}^2}{(\underline{r} - \underline{k})^2} \quad (108)$$

within the Born approximation. We focus here on the $\gamma^* \rightarrow \rho$ impact factor Φ of the subprocess

$$g(k_1, \varepsilon_1) + \gamma^*(q) \rightarrow g(k_2, \varepsilon_2) + \rho_T(p_1), \quad (109)$$

illustrated in Fig.9a, in the kinematical region where virtualities of the photon, Q^2 , and t -channel gluons k_{\perp}^2 , are of the same order, $Q^2 \sim k_{\perp}^2$, and much larger than Λ_{QCD} . It is the integral of the S-matrix element $S_\mu^{\gamma^* T g \rightarrow \rho_T g}$ with respect to the Sudakov component of the t-channel k momentum along p_2 . Closing the contour

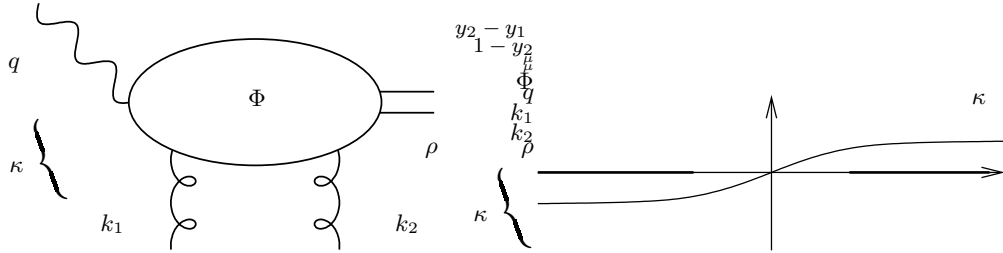


Figure 9: a: $\gamma^* \rightarrow \rho$ impact factor. b: κ integration contour entering the definition of the $\gamma^* \rightarrow \rho$ impact factor.

of integration below shows that the impact factor can be equivalently be written (see Fig.9b) as the integral of the κ -channel discontinuity of the S-matrix element $S_\mu^{\gamma^*_T g \rightarrow \rho_T g}$:

$$\Phi^{\gamma^* \rightarrow \rho}(\underline{k}, \underline{r} - \underline{k}) = e^{\gamma^* \mu} \frac{1}{2s} \int_{-\infty}^{+\infty} \frac{d\kappa}{2\pi} S_\mu^{\gamma^* g \rightarrow \rho g}(\underline{k}, \underline{r} - \underline{k}) = e^{\gamma^* \mu} \frac{1}{2s} \int_0^{+\infty} \frac{d\kappa}{2\pi} \text{Disc}_\kappa S_\mu^{\gamma^* g \rightarrow \rho g}(\underline{k}, \underline{r} - \underline{k}), \quad (110)$$

where $\kappa = (q + k_1)^2$ denotes the Mandelstam variable s for the subprocess (109), as illustrated in Fig.9a.

Note that the two reggeized gluons have so-called non-sense polarizations $\varepsilon_1 = \varepsilon_2^* = p_2 \sqrt{2/s}$.

Considering the forward limit for simplicity, the gluon momenta reduce to

$$k_1 = \frac{\kappa + Q^2 + \underline{k}^2}{s} p_2 + k_\perp, \quad k_2 = \frac{\kappa + \underline{k}^2}{s} p_2 + k_\perp, \quad k_1^2 = k_2^2 = k_\perp^2 = -\underline{k}^2. \quad (111)$$

Finally, let us note that when writing (111) we took an exact kinematics for the fraction of momentum along p_2 . This kinematics naturally extends the usual Regge kinematics in the case where t -channel momentum transfer along p_2 is allowed, which corresponds to the skewed kinematics which is typical of GPD studies. In usual computation of impact factors used in k_T -factorization, one usually makes the approximation that these two fractions are exactly opposite. Here we make such a choice in order to introduce skewness effects in a correct manner since these terms will contribute at the twist 3 order we are interested in. Note that within k_T -factorization, the description of impact factor for produced hadron described within QCD collinear approach requires a modification of twist counting due to the off-shellness of the t -channel partons. Therefore, when here we say "up to twist 3" we only mean twist counting from the point of view of the collinear factorization of the produced ρ -meson, and not of the whole amplitude, e.g. $\gamma^* p \rightarrow \rho p$ or $\gamma^* \gamma^* \rightarrow \rho \rho$.

In order to describe the collinear factorization of ρ -production inside the impact factor (110), we note that the kinematics of the general approach discussed in section II is related to our present kinematics for the impact factor (110) by setting $p = p_1$, while a natural choice for n is obtained by setting $n = n_0 = p_2/(p_1 \cdot p_2)$ (this latter choice for n , though natural, is somehow arbitrary as we discussed above in section II D).

We will now distinguish and make a comparative analysis of two different approaches: LCCF and CCF. We will show that these two results are actually fully equivalent to each other, when using the dictionary II E.

B. Calculation based on the Light-Cone Collinear Factorization approach

1. $\gamma_L^* \rightarrow \rho_L$ transition

Working within the LCCF, we first recall the calculation of the $\gamma_L^* \rightarrow \rho_L$ transition which receives contribution only from the diagrams with quark–antiquark correlators⁶. It is given by contributions from the p_μ term of the correlators (10) of the twist 2. Higher order corrections would start at twist 4, which is below our accuracy. The

⁶ Hereafter, except for final results, we perform the computation for a meson which would be a one flavour quark–antiquark state. Its wave function is then restored at the very end.

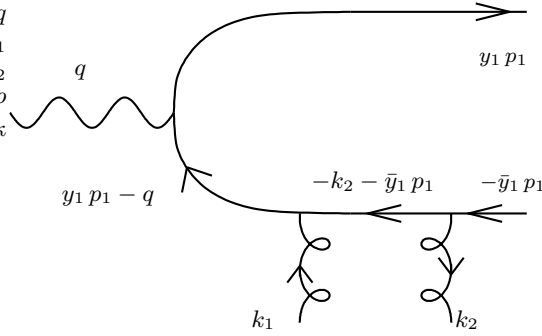


Figure 10: The detailed structure of the diagram (a).

computation of the corresponding impact factor is standard [23]. It involves the computation of the 6 diagrams of Fig.4. The longitudinal polarization of the virtual photon reads, in the Sudakov basis,

$$e_{\gamma L}^\mu = \frac{1}{Q} \left(p_1^\mu + \frac{Q^2}{s} p_2^\mu \right), \quad (112)$$

while the momentum of the ρ reads

$$p_\rho^\mu = p_1^\mu + \frac{m_\rho^2}{s} p_2^\mu, \quad (113)$$

and the longitudinal polarization of the ρ is

$$e_L^\mu \equiv e_{\rho L}^\mu = \frac{1}{m_\rho} \left(p_1^\mu - \frac{m_\rho^2}{s} p_2^\mu \right). \quad (114)$$

Consider for example the diagram (a) of Fig.4, as illustrated in Fig.10. Computing the corresponding S -matrix element, the corresponding contribution to the impact factor reads

$$\Phi_a = -e_q \frac{1}{4} \frac{2}{s} (-i) f_\rho m_\rho g^2 \frac{\delta^{ab}}{2 N_c} \frac{1}{2s} \int_0^1 dy \int \frac{d\kappa}{2\pi} \frac{Tr[\not{e}_{\gamma L}(y \not{p}_1 - \not{q}) \not{p}_2 (\not{k}_2 + \bar{y} \not{p}_1) \not{p}_2 \not{p}_1]}{[(y p_1 - q)^2 + i\eta][(k_2 + \bar{y} p_1)^2 + i\eta]} \varphi_1(y), \quad (115)$$

where the factor $1/4$ is reminiscent from the Fierz identity, the factor $2/s$ comes from the normalization of the non-sense polarizations. Finally, the color factor $\frac{\delta^{ab}}{2 N_c}$ is due to the fact that when summing over the color of the t -channel gluons, the net color coefficient for $\gamma^* \gamma^* \rightarrow \rho \rho$ should be $(N_c^2 - 1)/(4N_c^2)$ (due a Fierz factor $1/N_c$ when factorizing each of the two ρ DAs). Among the two propagators, only the second one, involving $(k_2 + \bar{y} p_1)^2 + i\eta = \kappa \bar{x} - \underline{k}^2 x + i\eta$ has a pole in κ , contributing when closing the contour below (therefore contributing to the discontinuity). The result is then easily obtained after extracting the corresponding residue. Diagram (c) provide the same contribution, since it can be obtained from (a) by the replacement $x \leftrightarrow \bar{x}$. Diagrams (b) and (d) vanishes for this twist 2 transition. Diagrams contributes only when closing the κ contour above. Finally, the net result for the $\gamma_L^* \rightarrow \rho_L$ impact factor is, after taking into account the ρ^0 wave function

$$\Phi^{\gamma_L^* \rightarrow \rho_L}(\underline{k}^2) = \frac{2e g^2 f_\rho}{\sqrt{2} Q} \frac{\delta^{ab}}{2 N_c} \int_0^1 dy \varphi_1(y) \frac{\underline{k}^2}{y \bar{y} Q^2 + \underline{k}^2}. \quad (116)$$

Note that diagrams (a) and (c) of Fig.4 are the only diagrams which contribute when computing the hard part by closing the κ contour below.

2. $\gamma_T^* \rightarrow \rho_T$ transition

We now concentrate on the $\gamma_T^* \rightarrow \rho_T$ transition, which impact factor will be one of the main results of this paper. The 2-parton contribution contains the terms arising from the diagram Fig.4, where the quark–antiquark

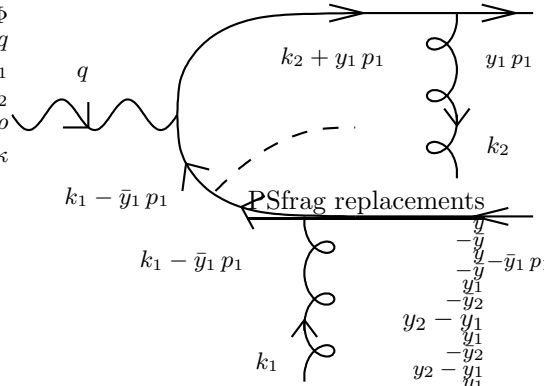


Figure 11: The detailed structure of the diagram (b1).

correlators have no transverse derivative, and from the diagrams Fig.5, where the quark–antiquark correlators stand with a transverse derivatives. The computation of the diagrams of Fig.4 for the $\gamma_T^* \rightarrow \rho_T$ transition goes along the same line as for the twist 2 $\gamma_L^* \rightarrow \rho_L$ transition discussed above. The practical trick used for computing the contributions of Fig.5 is the Ward identity

$$\frac{\partial}{\partial p_\mu} \xrightarrow{p} = \xrightarrow{p} \bullet \xrightarrow{p} \quad \text{where} \quad \xrightarrow{p} = \frac{1}{m - p - i\epsilon}, \quad (117)$$

where lines denotes fermionic propagators. This leads to an additional Feynman rule when inserting a derivative. The corresponding insertions are denoted with dashed lines in Fig.5.

Consider for example the diagram (b1) of Fig.4, illustrated in Fig.11. Computing the corresponding S -matrix element for the vector part, the corresponding contribution to the impact factor reads

$$\Phi_{b1}^V = -e_q \frac{1}{4} \frac{2}{s} (-i) g^2 f_\rho m_\rho \frac{\delta^{ab}}{2 N_c} \frac{1}{2s} \int_0^1 dy \int \frac{d\kappa}{2\pi} \frac{\text{Tr}[\not{\epsilon}_\gamma (\not{k}_1 - \bar{y}\not{p}_1) \not{\epsilon}_T^* (\not{k}_1 - \bar{y}\not{p}_1) \not{p}_2 \not{p}_1 \not{p}_2 (\not{k}_2 + y\not{p}_1)]}{[(k_1 - \bar{y}p_1)^2 + i\eta]^2 [(k_2 + \bar{y}p_1)^2 + i\eta]} \varphi_3^T(y), \quad (118)$$

This part of the impact factor receives (identical) contributions when closing the κ integration contour either from above or from below, which reads

$$\Phi_{b1}^V = -\frac{e_q g^2}{2} f_\rho m_\rho \frac{\delta^{ab}}{2 N_c} \int_0^1 dy y \frac{-e_T^* \cdot e_\gamma (y \bar{y} Q^2 + \underline{k}^2) + 2 e_T^* \cdot k e_T^* \cdot k (1 - 2y)}{(Q^2 y \bar{y} + \underline{k}^2)^2} \varphi_3^T(y). \quad (119)$$

The computation of the axial part is similar (note the $i/4$ factor from Fierz)

$$\Phi_{b1}^A = -e_q \frac{i}{4} \frac{2}{s} (-i) g^2 f_\rho m_\rho \frac{\delta^{ab}}{2 N_c} \frac{1}{2s} \int_0^1 dy \int \frac{d\kappa}{2\pi} \frac{\text{Tr}[\not{\epsilon}_\gamma (\not{k}_1 - \bar{y}\not{p}_1) \gamma_\alpha (\not{k}_1 - \bar{y}\not{p}_1) \not{p}_2 \not{p}_1 \gamma_5 \not{p}_2 (\not{k}_2 + y\not{p}_1)]}{[(k_1 - \bar{y}p_1)^2 + i\eta]^2 [(k_2 + \bar{y}p_1)^2 + i\eta]} \epsilon_{e_T^* p n}^\alpha \varphi_3^T(y), \quad (120)$$

and leads to

$$\Phi_{b1}^A = -\frac{e_q g^2}{2} f_\rho m_\rho \frac{\delta^{ab}}{2 N_c} \int_0^1 dy y \frac{-e_T^* \cdot e_\gamma (y \bar{y} Q^2 - \underline{k}^2) + 2 e_T^* \cdot k e_T^* \cdot k}{(Q^2 y \bar{y} + \underline{k}^2)^2} \varphi_A^T(y). \quad (121)$$

The contributions of 3-parton correlators are of two types, the first one being of "Abelian" type (without triple gluon vertex, see Fig.6) and the second involving non-Abelian coupling with one triple gluon vertex (see Fig.7)

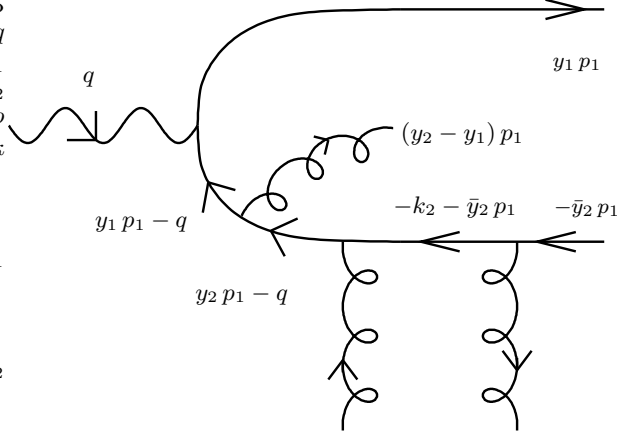


Figure 12: The detailed structure of the diagram (aG1).

or two (see Fig.8). Let us first consider the "Abelian" class. They involve two kind of Casimir invariants:

$$\begin{aligned} \frac{1}{N_c} \text{Tr}(t^c t^a t^b t^c) &= C_F \frac{\delta^{ab}}{2 N_c} \equiv C_a \frac{\delta^{ab}}{2 N_c} : (\text{aG1}), (\text{cG1}), (\text{eG1}), (\text{fG1}) \\ \frac{1}{N_c} \text{Tr}(t^c t^a t^c t^b) &= \left(C_F - \frac{N_c}{2} \right) \frac{\delta^{ab}}{2 N_c} \equiv C_b \frac{\delta^{ab}}{2 N_c} : (\text{bG1}), (\text{dG1}), (\text{aG2}), (\text{cG2}), (\text{bG2}), (\text{dG2}), (\text{eG2}), (\text{fG2}), \end{aligned} \quad (122)$$

where the $1/N_c$ comes from the Fierz coefficient when factorizing the quark-antiquark state in color space. Again, to illustrate the method, we consider the peculiar diagram (aG1) of Fig.6, illustrated in Fig.12. The vector contribution reads

$$\begin{aligned} \Phi_{aG1}^V &= -e_q \frac{1}{4} \frac{2}{s} (i) g^2 f_\rho m_\rho \frac{\delta^{ab}}{2 N_c} \frac{1}{2s} \int_0^1 dy_1 dy_2 \int \frac{d\kappa}{2\pi} \frac{\text{Tr}[\not{\epsilon}_\gamma (y_1 \not{p}_1 - \not{q}) \not{\epsilon}_T^* (y_2 \not{p}_1 - \not{q}) \not{p}_2 (\not{k}_2 + \not{y}_2 \not{p}_1) \not{p}_2 \not{p}_1]}{[(y_1 p_1 - q)^2 + i\eta][(y_2 p_1 - q)^2 + i\eta][(k_2 + \bar{y}_2 p_1)^2 + i\eta]} \\ &\times B(y_1, y_2), \end{aligned} \quad (123)$$

and equals

$$\Phi_{aG1}^V = -\frac{e_q g^2}{2} f_\rho m_\rho \frac{\delta^{ab}}{2 N_c} \int_0^1 dy_1 dy_2 \frac{\not{e}_T^* \cdot \not{e}_\gamma}{\bar{y}_1 Q^2} B(y_1, y_2). \quad (124)$$

The corresponding axial contribution reads

$$\begin{aligned} \Phi_{aG1}^A &= -e_q \frac{i}{4} \frac{2}{s} (i) g^2 f_\rho m_\rho \frac{\delta^{ab}}{2 N_c} \frac{1}{2s} \int_0^1 dy_1 dy_2 \int \frac{d\kappa}{2\pi} \frac{\text{Tr}[\not{\epsilon}_\gamma (y_1 \not{p}_1 - \not{q}) \gamma_\alpha (y_2 \not{p}_1 - \not{q}) \not{p}_2 (\not{k}_2 + \not{y}_2 \not{p}_1) \not{p}_2 \not{p}_1]}{[(y_1 p_1 - q)^2 + i\eta][(y_2 p_1 - q)^2 + i\eta][(k_2 + \bar{y}_2 p_1)^2 + i\eta]} \\ &\times \epsilon_{\not{e}_T^* p n}^\alpha D(y_1, y_2), \end{aligned} \quad (125)$$

and equals

$$\Phi_{aG1}^A = -\frac{e_q g^2}{2} f_\rho m_\rho \frac{\delta^{ab}}{2 N_c} \int_0^1 dy_1 dy_2 \frac{\not{e}_T^* \cdot \not{e}_\gamma}{\bar{y}_1 Q^2} D(y_1, y_2). \quad (126)$$

Consider now the "non-Abelian" diagrams of Fig.7, involving a single triple gluon vertex. They involve two kind of color structure:

$$\frac{2}{N_c^2 - 1} (-i) \text{Tr}(t^c t^b t^d) f^{cad} = \frac{N_c}{2} \frac{1}{C_F} \frac{\delta^{ab}}{2 N_c} : (\text{atG1}), (\text{dtG1}), (\text{etG1}), (\text{btG2}), (\text{ctG2}), (\text{ftG2}) \quad (127)$$

$$\frac{2}{N_c^2 - 1} (-i) \text{Tr}(t^c t^d t^b) f^{cad} = -\frac{N_c}{2} \frac{1}{C_F} \frac{\delta^{ab}}{2 N_c} : (\text{ctG1}), (\text{btG1}), (\text{ftG1}), (\text{atG2}), (\text{dtG2}), (\text{etG2}),$$

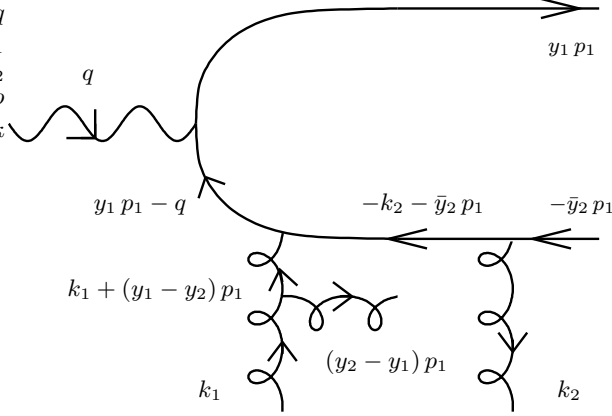


Figure 13: The detailed structure of the "non-Abelian" (with one triple gluon vertex) diagram (atG1).

where the $2/(N_c^2 - 1)$ comes from the Fierz coefficient when factorizing the quark–antiquark gluon state in color space. Let us consider the diagram (atG1) of Fig.7, illustrated in Fig.13. We denote as

$$d^{\nu\rho}(k) = g^{\nu\rho} - \frac{k^\nu n^\rho + k^\rho n^\nu}{k \cdot n} \quad (128)$$

the numerator of the gluon propagator in axial gauge, and

$$V_{\mu_1 \mu_2 \mu_3}(k_1, k_2, k_3) = (k_1 - k_2)_{\mu_1} g_{\mu_1 \mu_2} + \dots \quad (129)$$

the momentum part of the 3-gluon vertex, where k_i are incoming, labeled in the counter-clockwise direction. The contribution of the diagram (atG1) then reads, for the vector DA,

$$\begin{aligned} \Phi_{atG1}^V &= -e_q \frac{1}{4} \frac{2}{s} \frac{(-i)N_c}{2C_F} g^2 m_\rho f_\rho \frac{\delta^{ab}}{2N_c} \frac{1}{2s} \int_0^1 dy_1 dy_2 \int \frac{d\kappa}{2\pi} Tr[\not{\epsilon}_\gamma (y_1 \not{p}_1 - \not{q}) \gamma_\nu (\not{k}_2 + \bar{y}_2 \not{p}_1) \not{p}_2 \not{p}_1] \\ &\times \frac{d^{\nu\rho}(k_1 + (y_1 - y_2)p_1) V_{\rho\lambda\alpha}(-k_1 - (y_1 - y_2)p_1, k_1, (y_1 - y_2)p_1)}{[(y_1 p_1 - q)^2 + i\eta][(k_1 + (y_1 - y_2)p_1)^2 + i\eta][(k_2 + \bar{y}_2 p_1)^2 + i\eta]} p_2^\lambda e_T^{*\alpha} e_\gamma^\mu B(y_1, y_2). \end{aligned} \quad (130)$$

Note that for this diagram, as well as for all "non-Abelian" diagrams, one can easily check that only the $g^{\nu\rho}$ part of (128) contributes.

Closing the κ contour above or below gives for the vector DA part of the diagram (atG1) the result

$$\Phi_{atG1}^V = -\frac{e_q g^2}{2} m_\rho f_\rho \frac{\delta^{ab}}{2N_c} \frac{N_c}{C_F} \int_0^1 dy_1 dy_2 \frac{(y_1 - y_2) \bar{y}_2}{\bar{y}_1 (\bar{y}_1 \underline{k}^2 + \bar{y}_2 (y_2 - y_1) Q^2)} e_T^* \cdot e_\gamma B(y_1, y_2). \quad (131)$$

Similarly, the contribution of the diagram (atG1) reads, for the axial DA,

$$\begin{aligned} \Phi_{atG1}^A &= -e_q \frac{i}{4} \frac{2}{s} \frac{(-i)N_c}{2C_F} g^2 m_\rho f_\rho \frac{\delta^{ab}}{2N_c} \frac{1}{2s} \int_0^1 dy_1 dy_2 \int \frac{d\kappa}{2\pi} Tr[\not{\epsilon}_\gamma (y_1 \not{p}_1 - \not{q}) \gamma_\nu (\not{k}_2 + \bar{y}_2 \not{p}_1) \not{p}_2 \not{p}_1 \gamma_5] \\ &\times \frac{d^{\nu\rho}(k_1 + (y_1 - y_2)p_1) V_{\rho\lambda\alpha}(-k_1 - (y_1 - y_2)p_1, k_1, (y_1 - y_2)p_1)}{[(y_1 p_1 - q)^2 + i\eta][(k_1 + (y_1 - y_2)p_1)^2 + i\eta][(k_2 + \bar{y}_2 p_1)^2 + i\eta]} p_2^\lambda \epsilon_{e_T^{*pn}}^\alpha D(y_1, y_2), \end{aligned} \quad (132)$$

and closing the κ contour above or below gives

$$\Phi_{atG1}^A = -\frac{e_q g^2}{2} m_\rho f_\rho \frac{\delta^{ab}}{2N_c} \frac{N_c}{C_F} \int_0^1 dy_1 dy_2 \frac{(y_1 - y_2) \bar{y}_2}{\bar{y}_1 (\bar{y}_1 \underline{k}^2 + \bar{y}_2 (y_2 - y_1) Q^2)} e_T^* \cdot e_\gamma D(y_1, y_2). \quad (133)$$

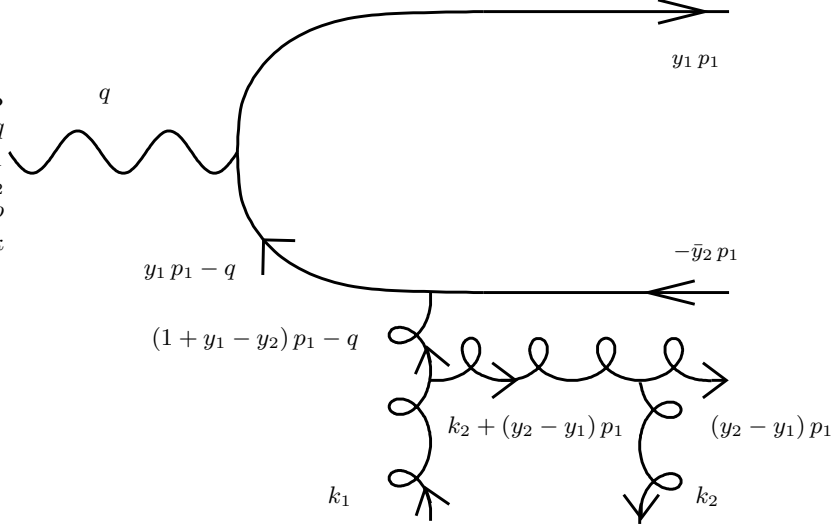


Figure 14: The detailed structure of the diagram (gttG1).

We consider now the "non-Abelian" diagrams of Fig.8, involving two triple gluon vertices. They all involve the color structure

$$-\frac{2}{N_c^2 - 1} \text{Tr}[t^c t^d] f^{cea} f^{edb} = \frac{N_c}{C_F} \frac{\delta^{ab}}{2 N_c}. \quad (134)$$

For illustration, let us consider the diagram (gttG1) of Fig.8, illustrated in Fig.14. It reads, for the vector DA,

$$\begin{aligned} \Phi_{gttG1}^V = & -e_q \frac{1}{4} \frac{2}{s} \frac{(-i)N_c}{C_F} g^2 m_\rho f_\rho \frac{\delta^{ab}}{2 N_c} \frac{1}{2s} \int_0^1 dy_1 dy_2 \int \frac{d\kappa}{2\pi} \text{Tr}[\not{e}_\gamma (y_1 \not{p}_1 - \not{q}) \gamma_\nu \not{p}_1] d^{\nu\rho} (-q + (1 + y_1 - y_2) p_1) \\ & \times \frac{V_{\rho\lambda\alpha}(q - (1 + y_1 - y_2) p_1, k_1, -k_2 + (y_1 - y_2) p_1) d^{\alpha\beta}(k_2 + (y_2 - y_1) p_1)}{[(y_1 p_1 - q)^2 + i\eta][(-q + (1 + y_1 - y_2) p_1)^2 + i\eta][(k_2 + (y_2 - y_1) p_1)^2 + i\eta]} \\ & \times V_{\beta\tau\delta}(k_2 + (y_2 - y_1) p_1, -k_2, (y_1 - y_2) p_1) p_2^\lambda p_2^\tau e_T^{*\delta} B(y_1, y_2). \end{aligned} \quad (135)$$

It equals, when closing the κ contour below on the single pole coming from the third propagator,

$$\Phi_{gttG1}^V = -\frac{e_q g^2}{2} m_\rho f_\rho \frac{\delta^{ab}}{2 N_c} \frac{N_c}{C_F} \frac{1}{Q^2} \int_0^1 dy_1 dy_2 \frac{B(y_1, y_2)}{\bar{y}_1} e_T^* \cdot e_\gamma. \quad (136)$$

The axial DA contribution from the diagram (gttG1) reads

$$\begin{aligned} \Phi_{gttG1}^A = & -e_q \frac{i}{4} \frac{2}{s} \frac{(-i)N_c}{C_F} g^2 m_\rho f_\rho \frac{\delta^{ab}}{2 N_c} \frac{1}{2s} \int_0^1 dy_1 dy_2 \int \frac{d\kappa}{2\pi} \text{Tr}[\not{e}_\gamma (y_1 \not{p}_1 - \not{q}) \gamma_\nu \not{p}_1 \gamma_5] d^{\nu\rho} (-q + (1 + y_1 - y_2) p_1) \\ & \times \frac{V_{\rho\lambda\alpha}(q - (1 + y_1 - y_2) p_1, k_1, -k_2 + (y_1 - y_2) p_1) d^{\alpha\beta}(k_2 + (y_2 - y_1) p_1)}{[(y_1 p_1 - q)^2 + i\eta][(-q + (1 + y_1 - y_2) p_1)^2 + i\eta][(k_2 + (y_2 - y_1) p_1)^2 + i\eta]} \\ & \times V_{\beta\tau\sigma}(k_2 + (y_2 - y_1) p_1, -k_2, (y_1 - y_2) p_1) p_2^\lambda p_2^\tau \epsilon_{e_T^* p n}^\sigma B(y_1, y_2). \end{aligned} \quad (137)$$

It equals, when closing the κ contour below on the single pole coming from the third propagator,

$$\Phi_{gttG1}^A = -\frac{e_q g^2}{2} m_\rho f_\rho \frac{\delta^{ab}}{2 N_c} \frac{N_c}{C_F} \frac{1}{Q^2} \int_0^1 dy_1 dy_2 \frac{D(y_1, y_2)}{\bar{y}_1} e_T^* \cdot e_\gamma. \quad (138)$$

All other diagrams of each class can be computed according to the previous examples.

In order to present now the full result in a compact form, we decompose the result impact factor into spin-non-flip and spin-flip part. The non-flip part is proportional to

$$T_{n.f.} = -(e_\gamma \cdot e_T^*) , \quad (139)$$

whereas the spin-flip part involves

$$T_f. = \frac{(e_\gamma \cdot k_\perp)(e_T^* \cdot k_\perp)}{\underline{k}^2} + \frac{(e_\gamma \cdot e_T^*)}{2} . \quad (140)$$

We label the transverse polarizations as

$$\epsilon^{(+)} \equiv \epsilon^{(R)} = -\frac{i}{\sqrt{2}} [e_1 + i e_2] = -\frac{i}{\sqrt{2}} (0, 1, i, 0) , \quad (141)$$

$$\epsilon^{(-)} \equiv \epsilon^{(L)} = \frac{i}{\sqrt{2}} [e_1 - i e_2] = \frac{i}{\sqrt{2}} (0, 1, -i, 0) . \quad (142)$$

They satisfy

$$\epsilon^{(\lambda)*} = \epsilon^{(-\lambda)} . \quad (143)$$

and

$$\epsilon^{(+)} \epsilon^{(+)*} = \epsilon^{(+)} \epsilon^{(-)} = -1 , \quad \text{and} \quad \epsilon^{(-)} \epsilon^{(-)*} = \epsilon^{(-)} \epsilon^{(+)} = -1 . \quad (144)$$

In this basis,

$$\epsilon_\mu^{(+)} \epsilon_\nu^{(+)*} + \epsilon_\mu^{(-)} \epsilon_\nu^{(-)*} = \epsilon_\mu^{(+)} \epsilon_\nu^{(-)} + \epsilon_\mu^{(-)} \epsilon_\nu^{(+)} = -g_{\perp \mu\nu} . \quad (145)$$

Decomposing the impact factor as the sum of spin-non-flip and spin-flip contributions

$$\Phi^{\gamma_T^* \rightarrow \rho_T}(\underline{k}^2) = \Phi_{n.f.}^{\gamma_T^* \rightarrow \rho_T}(\underline{k}^2) T_{n.f.} + \Phi_f^{\gamma_T^* \rightarrow \rho_T}(\underline{k}^2) T_f , \quad (146)$$

and introducing the notations

$$\alpha = \underline{k}^2/Q^2 \quad \text{and} \quad C^{ab} = -\frac{e g^2 m_\rho f_\rho}{\sqrt{2} Q^2} \frac{\delta^{ab}}{2 N_c} \quad (147)$$

one obtain the following results for the two bodies contribution

$$\begin{aligned} \Phi_{n.f.2}^{\gamma_T^* \rightarrow \rho_T}(\underline{k}^2) &= \frac{C^{ab}}{2} \frac{1}{C_F} C_F \int_0^1 dy_1 \left\{ \frac{(2y_1 - 1) \varphi_1^T(y_1) + 2y_1(1 - y_1) \varphi_3(y_1) + \varphi_A^T(y_1)}{y_1(1 - y_1)} \right. \\ &\quad \left. - \frac{2\alpha(\alpha + 2y_1(1 - y_1))((2y_1 - 1)\varphi_1^T(y_1) + \varphi_A^T(y_1))}{y_1(1 - y_1)(\alpha + y_1(1 - y_1))^2} \right\} \end{aligned} \quad (148)$$

and

$$\Phi_{f.2}^{\gamma_T^* \rightarrow \rho_T}(\underline{k}^2) = \frac{C^{ab}}{2} \frac{1}{C_F} C_F \int_0^1 dy_1 \frac{4\alpha}{(\alpha + (1 - y_1)y_1)^2} [(1 - 2y_1) \varphi_1^T(y_1) + \varphi_A^T(y_1)] . \quad (149)$$

The three bodies contribution reads

$$\begin{aligned} \Phi_{n.f.3}^{\gamma_T^* \rightarrow \rho_T}(\underline{k}^2) &= C^{ab} \frac{1}{C_F} \int_0^1 dy_1 \int_0^1 dy_2 \left\{ \frac{y_1 \zeta_3^A D(y_1, y_2)}{\alpha + (1 - y_1)y_1} \left(\frac{\alpha(N_c - 2C_F)}{(y_1 - y_2 + 1)\alpha + y_1(1 - y_2)} + \frac{\alpha N_c(1 - y_1)}{y_2\alpha + y_1(y_2 - y_1)} \right) \right. \\ &\quad \left. - \frac{y_1 \zeta_3^V B(y_1, y_2)}{\alpha + (1 - y_1)y_1} \left(\frac{\alpha(2C_F - N_c)(2y_1 - 1)}{(y_1 - y_2 + 1)\alpha + y_1(1 - y_2)} + \frac{\alpha N_c(1 - y_1)}{y_2\alpha + y_1(y_2 - y_1)} \right) \right. \\ &\quad \left. + (\zeta_3^V B(y_1, y_2) + \zeta_3^A D(y_1, y_2)) \left(\frac{2C_F y_1}{\alpha + (1 - y_1)y_1} - \frac{1}{1 - y_1} \left[\frac{N_c(1 - y_2)(y_1 - y_2)Q^2}{(1 - y_1)\alpha + (1 - y_2)(y_2 - y_1)} + C_F + N_c \right] \right) \right\} \end{aligned} \quad (150)$$

and

$$\begin{aligned} \Phi_{f,3}^{\gamma_T^* \rightarrow \rho_T}(\underline{k}^2) &= \frac{C^{ab}}{2} \frac{1}{C_F} \frac{4\alpha y_1}{\alpha + y_1(1-y_1)} \left(\frac{2C_F - N_c}{\alpha(1+y_1-y_2) + y_1(1-y_2)} - \frac{N_c}{\alpha y_2 + y_1(-y_1+y_2)} \right) \\ &\times [\zeta_3^A D(y_1, y_2) (1+y_1-y_2) + \zeta_3^V B(y_1, y_2) (1-y_1-y_2)] . \end{aligned} \quad (151)$$

The full result for the impact factor reads, after several simplifications due to the use of the equation of motion and the symmetrical properties of 2 and 3-parton correlators, as

$$\begin{aligned} &\Phi_{n.f.}^{\gamma_T^* \rightarrow \rho_T}(\underline{k}^2) \\ &= \frac{C^{ab}}{2} \left\{ -2 \int dy_1 \frac{(\alpha + 2y_1(1-y_1))\alpha}{y_1(1-y_1)(\alpha + y_1(1-y_1))^2} [(2y_1-1)\varphi_1^T(y_1) + \varphi_A^T(y_1)] \right. \\ &+ 2 \int dy_1 dy_2 [\zeta_3^V B(y_1, y_2) - \zeta_3^A D(y_1, y_2)] \frac{y_1(1-y_1)\alpha}{\alpha + y_1(1-y_1)} \left[\frac{2 - N_c/C_F}{\alpha(y_1-y_2+1) + y_1(1-y_2)} \right. \\ &- \frac{N_c}{C_F} \frac{1}{y_2 \alpha + y_1(y_2-y_1)} \left. \right] - 2 \int dy_1 dy_2 [\zeta_3^V B(y_1, y_2) + \zeta_3^A D(y_1, y_2)] \left[\frac{2 + N_c/C_F}{1-y_1} \right. \\ &+ \frac{y_1}{\alpha + y_1(1-y_1)} \left(\frac{(2 - N_c/C_F)y_1\alpha}{\alpha(y_1-y_2+1) + y_1(1-y_2)} - 2 \right) \\ &+ \left. \left. \frac{N_c}{C_F} \frac{(y_1-y_2)(1-y_2)}{1-y_1} \frac{1}{\alpha(1-y_1) + (y_2-y_1)(1-y_2)} \right] \right\} \end{aligned} \quad (152)$$

and

$$\begin{aligned} \Phi_f^{\gamma_T^* \rightarrow \rho_T}(\underline{k}^2) &= \frac{C^{ab}}{2} \left\{ 4 \int dy_1 \frac{\alpha}{(\alpha + y_1(1-y_1))^2} [\varphi_A^T(y_1) - (2y_1-1)\varphi_1^T(y_1)] \right. \\ &- 4 \int dy_1 dy_2 \frac{y_1\alpha}{\alpha + y_1(1-y_1)} [\zeta_3^A D(y_1, y_2)(-y_1+y_2-1) + \zeta_3^V B(y_1, y_2)(y_1+y_2-1)] \\ &\times \left. \left[\frac{(2 - N_c/C_F)}{\alpha(y_1-y_2+1) + y_1(1-y_2)} - \frac{N_c}{C_F} \frac{1}{y_2 \alpha + y_1(y_2-y_1)} \right] \right\} . \end{aligned} \quad (153)$$

The gauge invariance of the considered impact factor requires a special attention. The $\gamma^* \rightarrow \rho_T$ impact factor is constructed in such a manner that it should vanish when $\underline{k}^2 = 0$. This fact is a consequence of the gauge invariance of the impact factor. From our final formulas (152) and (153), it is obvious to check that Φ_f and $\Phi_{n.f.}$ indeed vanish when $\underline{k}^2 = 0$ since $T_{n.f.}$ is a phase for flip transition, which is regular in the $\underline{k}^2 \rightarrow 0$ limit. The vanishing of the "Abelian", i.e. proportional to C_F part of (152) is particularly subtle since it appears as a consequence of the equations of motions (59, 60). Because of that some comments can be useful. Let us note that the sum of Eq. (59) multiplied by y_1 and of Eq. (60) multiplied by \bar{y}_1 takes the form

$$\begin{aligned} &2y_1\bar{y}_1\varphi_3(y_1) + (y_1 - \bar{y}_1)\varphi_1^T(y_1) + \varphi_A^T(y_1) \\ &= -y_1 \int_0^1 dy_2 [\zeta_3^V B(y_1, y_2) + \zeta_3^A D(y_1, y_2)] - \bar{y}_1 \int_0^1 dy_2 [-\zeta_3^V B(y_2, y_1) + \zeta_3^A D(y_2, y_1)] , \end{aligned} \quad (154)$$

from which, after integration over y_1 of the both sides of (154) multiplied by $\frac{1}{y_1\bar{y}_1}$, we derive the equality

$$\int_0^1 \frac{dy_1}{y_1\bar{y}_1} (2y_1\bar{y}_1\varphi_3(y_1) + (y_1 - \bar{y}_1)\varphi_1^T(y_1) + \varphi_A^T(y_1)) = - \int_0^1 dy_1 \int_0^1 dy_2 \frac{2}{\bar{y}_1} [\zeta_3^V B(y_1, y_2) + \zeta_3^A D(y_1, y_2)] . \quad (155)$$

Now, by inspecting the expression (148) in the limit $\alpha \rightarrow 0$ we see that only the first term in $\{\dots\}$ survives and it has a form of the l.h.s of expression (155). Similarly, by inspecting the expression (150) in the limit $\alpha \rightarrow 0$ we see, that only the last line of this expression survives in the limit $\alpha \rightarrow 0$ and that the resulting expression coincides with the r.h.s of (155). Consequently, the non-vanishing terms cancel out due to the relation (155).

At the same time, the vanishing of non-Abelian ($\sim N_c$) part of (150) is the result of direct cancellation of the non-vanishing contributions of the diagrams (bG1), (dG1), (aG2), (cG2), (bG2), (dG2), (eG2), (fG2) of Fig.6 (see Eq.(122)) with the corresponding ones coming from diagrams of Fig.7 and Fig.8 containing triple-gluon vertices. Thus, the expression for the $\gamma^* \rightarrow \rho_T$ impact factor has finally a gauge-invariant form only provided the genuine twist 3 contributions have been taken into account, hidden in formula (152) when writing $\Phi_{n.f.}$ by the fact that we have used e.o.m., which explicitly relate 2 and 3 particles correlators.

We end up this section with a comment about the problem of end-point singularities. Such singularities does not occur both in WW approximation and in full twist-3 order approximation. First, the flip contribution (153) obviously does not have any end-point singularity. The potential end-point singularity for the non-flip contribution (152) is spurious since $\varphi_A^T(x_1), \varphi_1^T(x_1)$ vanishes at $x_1 = 0, 1$ (this is enough to justify the regularity of the result in the WW approximation), as well as $B(x_1, x_2)$ and $D(x_1, x_2)$.

C. Calculation based on the Covariant Collinear Factorization

We now calculate the impact factor using the CCF parametrization of Ref.[7] for vector meson DAs. Let us outline basic ideas behind our calculation. We need to express the impact factor in terms of hard coefficient functions and soft parts parametrized by light-cone matrix elements. The standard technique here is an operator product expansion on the light cone, $z^2 \rightarrow 0$, which naturally gives the leading term in the power counting and leads to the described above factorized structure. Unfortunately we do not have an operator definition for an impact factor, and therefore, we have to rely in our actual calculation on the perturbation theory. The primary complication here is that $z^2 \rightarrow 0$ limit of any single diagram is given in terms of light-cone matrix elements without any Wilson line insertion between the quark and gluon operators, like

$$\langle V(p_V) | \bar{\psi}(z) \gamma_\mu \psi(0) | 0 \rangle \quad \text{and} \quad \langle V(p_V) | \bar{\psi}(z) \gamma_\mu A_\alpha(t z) \psi(0) | 0 \rangle,$$

we will call conventionally such objects as perturbative correlators. Actually we need to combine together contributions of quark–antiquark and quark–antiquark gluon diagrams in order to obtain a final gauge invariant result.

One should stress that despite working in the axial gauge one can not neglect completely an effect coming from the Wilson lines since the two light-cone vectors z and n are not equal to each other and thus, generically, Wilson lines are not equal to unity. Nevertheless in the axial gauge the contribution of each additional parton costs one extra power of $1/Q$, therefore a calculation can be organized in a simple iterative manner expanding the Wilson line. At twist three level it is enough to consider the first two terms of such expansion

$$[z, 0] = 1 + i g \int_0^1 dt z^\alpha A_\alpha(z t) + \mathcal{O}(A^2). \quad (156)$$

For instance, the quark–antiquark vector correlator can be written, for the general case $z^2 \neq 0$, as

$$\langle V(p_V) | \bar{\psi}(z) \gamma_\mu \psi(0) | 0 \rangle = \langle V(p_V) | \bar{\psi}(z) \gamma_\mu [z, 0] \psi(0) | 0 \rangle - ig \int_0^1 dt \langle V(p_V) | \bar{\psi}(z) \gamma_\mu z^\alpha A_\alpha(z t) \psi(0) | 0 \rangle, \quad (157)$$

where we formally inserted the Wilson line in the r.h.s and performed its approximate subtraction according to (156). Then using relation (41), we express the gluon field operator in the second term of (157) in terms of field strength, which gives us the $\langle V(p_V) | \bar{\psi}(z) \gamma_\mu G_{\alpha\beta}(t z) \psi(0) | 0 \rangle$ correlator. For the later we apply again the procedure of Wilson lines insertion (and its approximate subtraction)

$$\begin{aligned} \langle V(p_V) | \bar{\psi}(z) \gamma_\mu \psi(0) | 0 \rangle &= \langle V(p_V) | \bar{\psi}(z) \gamma_\mu [z, 0] \psi(0) | 0 \rangle \\ &- ig \int_0^1 \int_0^\infty dt d\sigma e^{-\epsilon\sigma} \langle V(p_V) | \bar{\psi}(z) [z, z t + n \sigma] \gamma_\mu z^\alpha n^\beta G_{\alpha\beta}(z t + n \sigma) [z t + n \sigma, 0] \psi(0) | 0 \rangle + \dots, \end{aligned} \quad (158)$$

where \dots stands for the correlators with more than one gluon field.

Such correlator naturally appears (after Fierz decomposition) in the expression for the impact factor generated by the leading order diagrams of perturbation theory. Now we proceed to the extraction of leading $1/Q$

asymptotic. It is achieved, due to the dimensional counting reasons, by the substitution of the off light-cone correlators by their light-cone limit where $z t + n \sigma \propto z$, $z^2 \rightarrow 0$. In this limit, using the CCF parametrization of section II B 2 for the light-cone correlators, one can deduce after some transformations that

$$\langle \rho(p_\rho) | \bar{\psi}(z) \gamma_\mu \psi(0) | 0 \rangle|_{z^2 \rightarrow 0} = f_\rho m_\rho \left[-i p_\mu (e^* \cdot z) \int_0^1 dy e^{iy(p \cdot z)} (h(y) - \tilde{h}(y)) + e_\mu^* \int_0^1 dy e^{iy(p \cdot z)} g_\perp^{(v)}(z) \right] + \dots, \quad (159)$$

where \dots stands for the contributions vanishing at twist 3 level, and

$$\tilde{h}(y) = \zeta_3^V \int_0^y d\alpha_1 \int_0^{\bar{y}} d\alpha_2 \frac{V(\alpha_1, \alpha_2)}{\alpha_g^2}, \quad (160)$$

The physical polarization vector satisfies $e \cdot p_\rho = 0$ (or $e \cdot p = 0$ since $p_\rho = p$ up to twist 3). On the other hand, the polarization vector of transversely polarized meson is chosen to be orthogonal to the light-cone vectors fixed by the external kinematics: $e \cdot n_0 = 0$. But one should take into account that the e_T vector defined by (31) has a non-vanishing scalar product with the vector n_0 ,

$$e_T \cdot n_0 = -\frac{e \cdot z}{p \cdot z}. \quad (161)$$

This relation was used to derive (159).

Note that the $z t + n \sigma \propto z$ condition means actually that the vector z (which is an internal integration variable for the impact factor) is approaching during this limiting procedure the direction of the light-cone vector n , $z \propto n$. One should mention, to avoid any misunderstanding, that it does not mean that we must put, say in Eqs. like (159), the $e \cdot z$ scalar product equal to zero. What we actually do when performing the $1/Q$ power expansion is a Taylor expansion of scalar functions $F(p \cdot z, z^2)$, which depend generically on the two variables $p \cdot z$ and z^2 , with respect to the variable z^2 , whereas any scalar product of z with other vectors should remain intact.

Performing a similar sequence of steps we obtain the following result for the axial-vector correlator at the twist 3 level

$$\langle \rho(p_\rho) | \bar{\psi}(z) \gamma_\mu \gamma_5 \psi(0) | 0 \rangle|_{z^2 \rightarrow 0} = \frac{1}{4} f_\rho m_\rho \left[\epsilon_{\mu\alpha\beta\gamma} e^{*\alpha} p^\beta z^\gamma \int_0^1 dy e^{iy(p \cdot z)} (g_\perp^{(a)}(y) - \tilde{g}_\perp^{(a)}(y)) + \epsilon_{\mu\alpha\beta\gamma} e^{*\alpha} p^\beta n^\gamma p \cdot z \int_0^1 dy e^{iy(p \cdot z)} \tilde{g}_\perp^{(a)}(y) \right], \quad (162)$$

with

$$\tilde{g}_\perp^{(a)}(y) = 4 \zeta_3^A \int_0^y d\alpha_1 \int_0^{\bar{y}} d\alpha_2 \frac{A(\alpha_1, \alpha_2)}{\alpha_g^2}. \quad (163)$$

Comparing the obtained results (159), (162) for the perturbative correlators with initial parametrizations (34), (28) we see that at twist 3-level the net effect of the Wilson line is just some renormalization of the h function in the case of vector correlator, whereas for the axial-vector we obtain in addition to the function $g_\perp^{(a)}$ renormalization a new Lorentz structure, the last term in (162). Nevertheless, we found that the last term in (162) produces at the end a zero contribution to impact factor.

Let us now discuss gluonic diagrams which involves quark-antiquark gluon correlators, like $\langle \rho(p_\rho) | \bar{\psi}(z) \gamma_\mu g A_\alpha(w) \psi(0) | 0 \rangle$. Applying our procedure one can easily show that at twist 3 level

$$\langle \rho(p_\rho) | \bar{\psi}(z) \gamma_\mu g A_\alpha(w) \psi(0) | 0 \rangle|_{w \propto z, z^2 \rightarrow 0} = -m_\rho f_{3\rho}^V p_\mu e_{T\alpha}^* \int D\underline{\alpha} \frac{V(\alpha_1, \alpha_2)}{\alpha_g} e^{i(p \cdot z)\alpha_1 + i(p \cdot w)\alpha_g}, \quad (164)$$

$$\langle \rho(p_\rho) | \bar{\psi}(z) \gamma_\mu \gamma_5 g A_\alpha(w) \psi(0) | 0 \rangle|_{w \propto z, z^2 \rightarrow 0} = -i m_\rho f_{3\rho}^A p_\mu \epsilon_{\alpha\beta\gamma\delta} n^\beta p^\gamma e_T^{*\delta} \int D\underline{\alpha} \frac{A(\alpha_1, \alpha_2)}{\alpha_g} e^{i(p \cdot z)\alpha_1 + i(p \cdot w)\alpha_g},$$

see Eq.(42,43). Note that the first nontrivial effects induced by the Wilson line insertion start for such perturbative correlators at the level of twist 4 only. Therefore taking into account such 3-partons contributions

is quite straightforward: one needs to calculate, projected in accordance with (164), diagrams describing the production of collinear on-shell quark–antiquark gluon state.

One comment is here in order. Perturbative expansion generates, among others, diagrams where the gluon field is attached not to the internal part of the diagrams but to the "external" quark (or antiquark) lines. Such diagrams, in accordance to the logic of collinear factorization, should be factorized in terms of not 3-parton but 2-parton correlators. Quasi-collinear gluon radiation appears at large distances and corresponding subprocess should be factorized not in the hard coefficient but is included in the soft part of the process, described by the 2-parton quark–antiquark correlator.

The internal variable z (and w) integration can be reduced to the Fourier integrals

$$\int d^4 z e^{i(l \cdot z)} = (2\pi)^4 \delta^4(l), \quad \int d^4 z z_\alpha e^{i(l \cdot z)} = -i(2\pi)^4 \frac{\partial}{\partial l^\alpha} \delta^4(l),$$

where l stays here for some combination of the external and internal momenta⁷. The corresponding intermediate calculations do not contain principle difficulties both for the case of 2-partons and 3-partons contributions. Note that the contributions computed here have the same hard part as the one of the section III B, except for 2-partons contributions with derivatives discussed in that section which have no counterpart here. In what follows, we simply give the final results. Then we will discuss in details an important issue related with the restoration of the gauge invariance for the final result.

We use the notations

$$\alpha = \frac{k^2}{Q^2}, \quad c_f = \frac{N^2}{N^2 - 1}$$

For the 3-parton contributions we obtain the result

$$\Phi^3 = -\frac{e g^2 m_\rho f_\rho}{\sqrt{2} Q^2} \frac{\delta^{ab}}{2N_c} \left\{ \Phi^{q\bar{q}g}(\alpha) + \Delta\Phi^3 \right\}, \quad (165)$$

with

$$\Delta\Phi^3 = -\frac{T_{n.f.}}{2} \int \frac{Dz}{\bar{z}_1 \bar{z}_2 z_g} \left\{ \zeta_3^V V(z_1, z_2)(z_1 - z_2) + \zeta_3^A A(z_1, z_2)(\bar{z}_1 + \bar{z}_2) \right\} \quad (166)$$

and

$$\begin{aligned} \Phi^{q\bar{q}g}(\alpha) &= \int Dz \frac{2\alpha}{z_1 z_2 z_g^2} \\ &\times \left\{ (\zeta_3^V V(z_1, z_2) + \zeta_3^A A(z_1, z_2)) T_{n.f.} \left(\frac{(1 - c_f) \bar{z}_g z_1}{\alpha \bar{z}_g + z_1 z_2} - \frac{c_f z_g^2}{\alpha \bar{z}_1 + z_2 z_g} - \frac{(z_2 - \bar{z}_1 c_f) z_1 z_2}{\bar{z}_1 (\alpha + z_1 \bar{z}_1)} - \frac{(z_1 - \bar{z}_2 c_f) \bar{z}_2}{(\alpha + z_2 \bar{z}_2)} \right) \right. \\ &+ (\zeta_3^V V(z_1, z_2) - \zeta_3^A A(z_1, z_2)) 2z_1 T_f \left(\frac{(1 - c_f) \bar{z}_g^2}{\alpha \bar{z}_g + z_1 z_2} - \frac{c_f z_g \bar{z}_1}{\alpha \bar{z}_1 + z_2 z_g} - \frac{c_f z_g \bar{z}_2}{\alpha \bar{z}_2 + z_1 z_g} + \frac{c_f \bar{z}_1 - z_2}{\alpha + z_1 \bar{z}_1} + \frac{c_f \bar{z}_2 - z_1}{\alpha + z_2 \bar{z}_2} \right) \left. \right\}, \end{aligned} \quad (167)$$

where Dz is defined according to (39) and where we have used symmetry properties of gluon distribution amplitudes under the exchange of quark momentum fractions: $V(z_1, z_2) = -V(z_2, z_1)$, $A(z_1, z_2) = A(z_2, z_1)$.

Let us discuss now the 2-parton contributions. We obtain

$$\Phi^2 = -\frac{e g^2 m_\rho f_\rho}{\sqrt{2} Q^2} \frac{\delta^{ab}}{2N_c} \left\{ \Phi^{q\bar{q}}(\alpha) + \Delta\Phi^2 \right\}, \quad (168)$$

with

$$\Phi^{q\bar{q}}(\alpha) = \int_0^1 dz \left\{ T_{n.f.} \Phi^+(z) \frac{\alpha(\alpha + 2z\bar{z})}{z\bar{z}(\alpha + z\bar{z})^2} + T_f \Phi^-(z) \frac{2\alpha}{(\alpha + z\bar{z})^2} \right\} \quad (169)$$

⁷ The subsequent integration over the internal momenta with delta function derivative is done using integration by parts.

where

$$\Phi^\pm(\alpha) = (2z - 1) \left[h(z) - \tilde{h}(z) \right] \pm \frac{g_\perp^{(a)}(z) - \tilde{g}_\perp^{(a)}(z)}{4}, \quad (170)$$

whereas for $\Delta\Phi^2$ term we get

$$\Delta\Phi^2 = T_{n.f.} \int_0^1 dz \left\{ g_\perp^{(v)}(z) - \frac{\Phi^+(z)}{2z\bar{z}} \right\}. \quad (171)$$

Note that $\Phi^{q\bar{q}}(\alpha)$ and $\Phi^{q\bar{q}g}(\alpha)$ vanish in the limit $\alpha \rightarrow 0$, whereas $\Delta\Phi^2$ and $\Delta\Phi^3$ do not depend on α . Now we need to demonstrate that $\Delta\Phi^2$ and $\Delta\Phi^3$ cancel each other. It guarantees the property of the impact factor, $\Phi(\alpha = 0) = 0$, which is directly related to the gauge invariance.

One can now separate from $\Delta\Phi^2$ the contribution $\Delta\Phi_a^2$ that is due to functions $\tilde{h}(z)$ and $\tilde{g}_\perp^{(a)}(z)$, which originates in our method from the Wilson lines insertion procedure,

$$\Delta\Phi^2 = \Delta\Phi_a^2 + \Delta\Phi_b^2, \quad (172)$$

where

$$\Delta\Phi_a^2 = T_{n.f.} \int_0^1 \frac{dz}{2z\bar{z}} \left\{ (2z - 1)\tilde{h}(z) + \frac{\tilde{g}_\perp^{(a)}(z)}{4} \right\}. \quad (173)$$

To calculate $\Delta\Phi_a^2$, it is convenient to present $\tilde{h}(z)$ and $\tilde{g}_\perp^{(a)}(z)$ in the form

$$\tilde{h}(u) = \zeta_3^V \int_0^1 dt \int Dz \delta(u - z_1 - z_g t) \frac{V(z_1, z_2)}{z_g}, \quad \tilde{g}_\perp^{(a)}(z) = 4 \zeta_3^A \int_0^1 dt \int Dz \delta(u - z_1 - z_g t) \frac{A(z_1, z_2)}{z_g}. \quad (174)$$

Using this relation one can easily found that

$$\Delta\Phi_a^2 = \frac{T_{n.f.}}{2} \int Dz \left\{ \zeta_3^V \frac{V(z_1, z_2)}{z_g^2} \ln \frac{z_1\bar{z}_1}{z_2\bar{z}_2} + \zeta_3^A \frac{A(z_1, z_2)}{z_g^2} \ln \frac{\bar{z}_1\bar{z}_2}{z_1z_2} \right\}.$$

The second term in (172) can be reduced to the form

$$\Delta\Phi_b^2 = \frac{T_{n.f.}}{2} \int_0^1 dz \left\{ \ln(z) g^{\uparrow\downarrow}(z) + \ln(\bar{z}) g^{\downarrow\uparrow}(z) \right\}.$$

where [7]

$$g^{\uparrow\downarrow}(z) = g_\perp^{(v)}(z) + \frac{1}{4} \frac{d}{dz} g_\perp^{(a)}(z), \quad g^{\downarrow\uparrow}(z) = g_\perp^{(v)}(z) - \frac{1}{4} \frac{d}{dz} g_\perp^{(a)}(z).$$

Then, we separate the WW and genuine twist 3 contributions to $\Delta\Phi_b^2$,

$$\Delta\Phi_b^2 = \Delta\Phi_b^{2WW} + \Delta\Phi_b^{2gen},$$

in accordance with

$$g^{\uparrow\downarrow}(z) = g^{\uparrow\downarrow WW}(z) + g^{\uparrow\downarrow gen}(z), \quad g^{\downarrow\uparrow}(z) = g^{\downarrow\uparrow WW}(z) + g^{\downarrow\uparrow gen}(z).$$

Using the explicit expressions for these functions in the WW limit

$$g^{\uparrow\downarrow WW}(z) = \int_z^1 \frac{du}{u} \phi_{||}(u), \quad g^{\downarrow\uparrow WW}(z) = \int_0^z \frac{du}{\bar{u}} \phi_{||}(u),$$

one can easily found that the WW contribution to $\Delta\Phi_b^2$ vanishes,

$$\Delta\Phi_b^{2WW} = 0.$$

Then, using results of Ref.[7], which allow to express $g^{\uparrow\downarrow gen}(z)$ and $g^{\downarrow\uparrow gen}(z)$ in terms of 3-partons DAs, we found after some transformations that

$$\Delta\Phi_b^{2gen} = \frac{T_{n.f.}}{2} \int Dz \left\{ \zeta_3^V \frac{V(z_1, z_2)}{z_g} \left(\frac{z_1 - z_2}{\bar{z}_1 \bar{z}_2} - \ln \frac{z_1 \bar{z}_1}{z_2 \bar{z}_2} \frac{1}{z_g} \right) + \zeta_3^A \frac{A(z_1, z_2)}{z_g} \left(\frac{\bar{z}_1 + \bar{z}_2}{\bar{z}_1 \bar{z}_2} - \ln \frac{\bar{z}_1 \bar{z}_2}{z_1 z_2} \frac{1}{z_g} \right) \right\}.$$

These results mean that

$$\Delta\Phi^2 = \frac{T_{n.f.}}{2} \int \frac{Dz}{z_g \bar{z}_1 \bar{z}_2} \left\{ \zeta_3^V V(z_1, z_2)(z_1 - z_2) + \zeta_3^A A(z_1, z_2)(\bar{z}_1 + \bar{z}_2) \right\}, \quad (174)$$

and thus that the constant terms of 2-parton (174) and 3-parton (166) contributions cancel each other

$$\Delta\Phi^2 + \Delta\Phi^3 = 0.$$

Finally, the impact factor is given as a sum of two contributions

$$\Phi(\alpha) = -\frac{e g^2 m_\rho f_\rho}{\sqrt{2} Q^2} \frac{\delta^{ab}}{2N_c} \left\{ \Phi^{q\bar{q}}(\alpha) + \Phi^{q\bar{q}g}(\alpha) \right\} \quad (175)$$

where $\Phi^{q\bar{q}}(\alpha)$ and $\Phi^{q\bar{q}g}(\alpha)$ are given in eqs. (169) and (167).

D. Comparison of the two computations

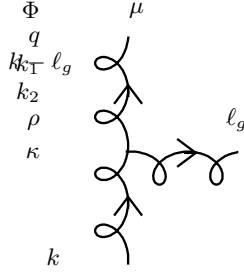
The above results for the $\gamma^* \rightarrow \rho$ impact factor were obtained based on the LCCF and CCF method, and look at first sight very different. As a testing ground of the validity of the dictionary elaborated in section II E, it is interesting to show the exact equivalence between the two results. Since the detailed proof is rather involved and technical, this is done with whole details in Appendix B.

IV. CONCLUSION

In conclusion, we presented a general formalism which allows us to include in a systematic way higher twist effects. The general scheme was exemplified on the study of the *rho*-meson production up to twist 3 accuracy. We did this using two different methods: the LCCF method in the momentum space and the CCF method in the coordinate space. The crucial point in the comparison of these two methods was the use of Lorentz invariance constraints formulated as the n -independence of the scattering amplitude within LCCF method, which leads to the necessity of taking into account the contribution of 3-parton correlators. We derived the dictionary between the DAs appearing in the two methods. Due to different calculational techniques used by the LCCF and CCF methods, we performed the calculation of the $\gamma^* \rho$ impact factor in two different ways; we checked that they lead to the same result. This does not preclude the solution of the well known end-point singularity problem [3, 24] which may still require a separate treatment. The phenomenological application to our result to the HERA data [10] will be discussed in a separate publication [25].

Acknowledgments

We thank V. M. Braun, R. Kirschner, G. Korchemsky and M. Segond for discussions. Special thanks to O. V. Teryaev for many useful comments. This work is partly supported by the ECO-NET program, contract 18853PJ, the French-Polish scientific agreement Polonium, the grant ANR-06-JCJC-0084, the RFBR (grants 09-02-01149, 08-02-00334, 08-02-00896), the NSh-1027.2008.2 grant and the Polish Grant N202 249235. LS acknowledges the support of INT in Seattle during the final stage of this project.

Figure 15: 3-gluon vertex with one open index μ .

APPENDICES

Appendix A: n -INDEPENDENCE CONSTRAINT FOR THE N_c STRUCTURE

In this appendix we show that the n -independence constraint is automatically fulfilled for N_c contributions. According to Eq.(122), one should consider the "Abelian" diagrams (bG1), (dG1), (aG2), (cG2), (bG2), (dG2), (eG2), (fG2), and from Eq.(127) and Eq.(134) all the non-Abelian diagrams.

As a preliminary, let us consider a triple gluon vertex with a t -channel gluon of momentum k (which will stand for k_1 or $-k_2$ in the all cases discussed below), saturated with a non-sense polarization p_2 , and a real gluon of momentum ℓ_g and polarization ϵ_g , leaving the index μ open, as illustrated in Fig.15. It reads

$$V_{\lambda\alpha}^\mu(-k + \ell_g, k, -\ell_g)\epsilon_g^\alpha p_2^\lambda = -(2k - \ell_g)\epsilon_g p_2^\mu + (k + \ell_g)_\mu(p_2\epsilon_g) - (2\ell_g - k)p_2\epsilon_g^\mu \quad (\text{A.1})$$

which reduces, after making the replacement $\epsilon_g \rightarrow \ell_g$ and using the fact that in our kinematics k has no component along p_1 , to

$$V_{\lambda\alpha}^\mu(-k + \ell_g, k, -\ell_g)\cdot\ell_g^\alpha p_2^\lambda = -(2k\cdot\ell_g)p_2^\mu - (\ell_g\cdot p_2)(\ell_g - k)^\mu = -[k^2 - (k - \ell_g)^2]p_2^\mu - (\ell_g\cdot p_2)(\ell_g - k)^\mu \quad (\text{A.2})$$

where in the last line we used the fact that ℓ_g is on mass-shell. Hereafter, we will symbolically denote with the index p_2 the first term in the r.h.s of Eq.(A.2) and with W the second term (having in mind for this second term further use of Ward identities).

We now apply the same method based on the Ward identity which led to Eq.(75), now for graphs (bG1) and

(bG2). This gives⁸

$$\begin{aligned}
 & -(y_2 - y_1) p_\mu \left[\begin{array}{c} \text{Diagram 1} \\ + \\ \text{Diagram 2} \end{array} \right] \\
 = & \text{Diagram 3} - \text{Diagram 4} + \text{Diagram 5} - \text{Diagram 6} \\
 = & \text{Diagram 7} - \text{Diagram 8} \quad (A.3)
 \end{aligned}$$

The p_2 term obtained after applying the identity (A.2) to the diagrams (btG1) and (btG2) gives, respectively

$$\begin{aligned}
 & -(y_2 - y_1) p_\mu \left| \begin{array}{c} \text{Diagram 1} \\ \parallel \\ \text{''}' p_2'' \end{array} \right. \\
 = & - \left[1 - \frac{k_1^2}{(k_1 - \ell_g)^2} \right] \text{Diagram 1} \quad (A.4)
 \end{aligned}$$

and

$$\begin{aligned}
 & (y_2 - y_1) p_\mu \left| \begin{array}{c} \text{Diagram 1} \\ \parallel \\ \text{''}' p_2'' \end{array} \right. \\
 = & \left[1 - \frac{k_2^2}{(k_2 + \ell_g)^2} \right] \text{Diagram 1} \quad (A.5)
 \end{aligned}$$

In the perturbative Regge limit we are considering here, the terms $k^2/(k - \ell_g)^2$ and $k'^2/(k' + \ell_g)^2$ can be neglected, since they are of the order of k^2/s , and therefore Eqs.(A.3, A.4, A.5) exhibit an explicit cancellation.

⁸ The signs in l.h.s of Eqs.(A.3, A.4, A.4) are related to the signs in front of the corresponding N_c coefficients, see Eqs.(122, 127).

Turning now to the case of graphs (dG1) and (dG2) one gets, using again the Ward identity,

$$\begin{aligned}
 -(y_2 - y_1) p_\mu & \left[\begin{array}{c} \text{Diagram (dG1)} \\ \text{Diagram (dG2)} \end{array} \right] \\
 = & \begin{array}{c} \text{Diagram (dtG1)} \\ - \quad \begin{array}{c} \text{Diagram (dtG2)} \end{array} \end{array} \tag{A.6}
 \end{aligned}$$

The p_2 term obtained after applying the identity (A.2) to the diagrams (dtG1) and (dtG2) gives, respectively

$$\begin{aligned}
 (y_2 - y_1) p_\mu & \left[\begin{array}{c} \text{Diagram (dtG1)} \\ \text{Diagram (dtG2)} \end{array} \right] = \left[1 - \frac{k_1^2}{(k_1 - \ell_g)^2} \right] \begin{array}{c} \text{Diagram (dtG1)} \\ - \quad \begin{array}{c} \text{Diagram (dtG2)} \end{array} \end{array} \tag{A.7}
 \end{aligned}$$

and

$$\begin{aligned}
 -(y_2 - y_1) p_\mu & \left[\begin{array}{c} \text{Diagram (dtG1)} \\ \text{Diagram (dtG2)} \end{array} \right] = - \left[1 - \frac{k_2^2}{(k_2 + \ell_g)^2} \right] \begin{array}{c} \text{Diagram (dtG1)} \\ - \quad \begin{array}{c} \text{Diagram (dtG2)} \end{array} \end{array} \tag{A.8}
 \end{aligned}$$

Contributions (A.6), (A.7) and (A.8) add to zero.

The proofs for (aG2) goes along the same line and reads

$$\begin{aligned}
 -(y_2 - y_1) p_\mu & \left[\begin{array}{c} \text{Diagram (aG1)} \\ \text{Diagram (aG2)} \end{array} \right] = \begin{array}{c} \text{Diagram (daG1)} \\ - \quad \begin{array}{c} \text{Diagram (daG2)} \end{array} \end{array} \tag{A.9}
 \end{aligned}$$

The p_2 term obtained after applying the identity (A.2) to the diagrams (atG1) and (atG2) gives, respectively

$$(y_2 - y_1) p_\mu \quad \text{Diagram} \quad \left| \begin{array}{c} \text{Left: } (y_2 - y_1) p_\mu \text{ with loop } y_1 \rightarrow -\bar{y}_1 \text{ and } -\bar{y}_2 \rightarrow y_2 - y_1 \\ \text{Right: } \text{Diagram with loop } y_1 \rightarrow y_1 - y_2 \text{ and } -\bar{y}_2 \rightarrow -\bar{y}_2 \end{array} \right. \quad = \left[1 - \frac{k_1^2}{(k_1 - \ell_g)^2} \right] \quad \text{Diagram} \quad \left| \begin{array}{c} \text{Left: } \text{Diagram with loop } y_1 \rightarrow y_1 - y_2 \text{ and } -\bar{y}_2 \rightarrow -\bar{y}_2 \\ \text{Right: } \text{Diagram with loop } y_1 \rightarrow y_1 - y_2 \text{ and } -\bar{y}_2 \rightarrow -\bar{y}_2 \end{array} \right. \quad (A.10)$$

and

$$-(y_2 - y_1) p_\mu \quad \text{Diagram} \quad \left| \begin{array}{c} \text{Left: } -(y_2 - y_1) p_\mu \text{ with loop } y_1 \rightarrow -\bar{y}_1 \text{ and } -\bar{y}_2 \rightarrow y_2 - y_1 \\ \text{Right: } \text{Diagram with loop } y_1 \rightarrow y_1 - y_2 \text{ and } -\bar{y}_2 \rightarrow -\bar{y}_2 \end{array} \right. \quad = - \left[1 - \frac{k_2^2}{(k_2 + \ell_g)^2} \right] \quad \text{Diagram} \quad \left| \begin{array}{c} \text{Left: } \text{Diagram with loop } y_1 \rightarrow y_1 - y_2 \text{ and } -\bar{y}_2 \rightarrow -\bar{y}_2 \\ \text{Right: } \text{Diagram with loop } y_1 \rightarrow y_1 - y_2 \text{ and } -\bar{y}_2 \rightarrow -\bar{y}_2 \end{array} \right. \quad . \quad (A.11)$$

Contributions (A.9), (A.10) and (A.11) add to zero in the Regge limit.

The proofs for (cG2) goes along the same line and reads

$$-(y_2 - y_1) p_\mu \quad \text{Diagram} \quad \left| \begin{array}{c} \text{Left: } -(y_2 - y_1) p_\mu \text{ with loop } y_1 \rightarrow y_1 - y_2 \text{ and } -\bar{y}_2 \rightarrow y_2 - y_1 \\ \text{Right: } \text{Diagram with loop } y_1 \rightarrow y_1 - y_2 \text{ and } -\bar{y}_2 \rightarrow -\bar{y}_2 \end{array} \right. = \quad \text{Diagram} \quad \left| \begin{array}{c} \text{Left: } \text{Diagram with loop } y_1 \rightarrow y_1 - y_2 \text{ and } -\bar{y}_2 \rightarrow -\bar{y}_2 \\ \text{Right: } \text{Diagram with loop } y_1 \rightarrow y_1 - y_2 \text{ and } -\bar{y}_2 \rightarrow -\bar{y}_2 \end{array} \right. \quad , \quad (A.12)$$

The p_2 term obtained after applying the identity (A.2) to the diagrams (ctG1) and (ctG2) gives, respectively

$$-(y_2 - y_1) p_\mu \quad \text{Diagram} \quad \left| \begin{array}{c} \text{Left: } -(y_2 - y_1) p_\mu \text{ with loop } y_1 \rightarrow y_1 - y_2 \text{ and } -\bar{y}_2 \rightarrow y_2 - y_1 \\ \text{Right: } \text{Diagram with loop } y_1 \rightarrow y_1 - y_2 \text{ and } -\bar{y}_2 \rightarrow -\bar{y}_2 \end{array} \right. \quad = - \left[1 - \frac{k_1^2}{(k_1 - \ell_g)^2} \right] \quad \text{Diagram} \quad \left| \begin{array}{c} \text{Left: } \text{Diagram with loop } y_1 \rightarrow y_1 - y_2 \text{ and } -\bar{y}_2 \rightarrow -\bar{y}_2 \\ \text{Right: } \text{Diagram with loop } y_1 \rightarrow y_1 - y_2 \text{ and } -\bar{y}_2 \rightarrow -\bar{y}_2 \end{array} \right. \quad (A.13)$$

and

$$(y_2 - y_1) p_\mu \quad \text{Diagram} \quad \left| \begin{array}{c} \text{Left: } (y_2 - y_1) p_\mu \text{ with loop } y_1 \rightarrow y_1 - y_2 \text{ and } -\bar{y}_2 \rightarrow y_2 - y_1 \\ \text{Right: } \text{Diagram with loop } y_1 \rightarrow y_1 - y_2 \text{ and } -\bar{y}_2 \rightarrow -\bar{y}_2 \end{array} \right. \quad = \left[1 - \frac{k_2^2}{(k_2 + \ell_g)^2} \right] \quad \text{Diagram} \quad \left| \begin{array}{c} \text{Left: } \text{Diagram with loop } y_1 \rightarrow y_1 - y_2 \text{ and } -\bar{y}_2 \rightarrow -\bar{y}_2 \\ \text{Right: } \text{Diagram with loop } y_1 \rightarrow y_1 - y_2 \text{ and } -\bar{y}_2 \rightarrow -\bar{y}_2 \end{array} \right. \quad . \quad (A.14)$$

Contributions (A.12), (A.13) and (A.14) add to zero in the Regge limit.

The proofs for (eG2) goes along the same line and reads

$$-(y_2 - y_1) p_\mu \quad \text{Diagram} \quad \left| \begin{array}{c} \text{Left: } -(y_2 - y_1) p_\mu \text{ with loop } y_1 \rightarrow y_1 - y_2 \text{ and } -\bar{y}_2 \rightarrow y_2 - y_1 \\ \text{Right: } \text{Diagram with loop } y_1 \rightarrow y_1 - y_2 \text{ and } -\bar{y}_2 \rightarrow -\bar{y}_2 \end{array} \right. = \quad \text{Diagram} \quad \left| \begin{array}{c} \text{Left: } \text{Diagram with loop } y_1 \rightarrow y_1 - y_2 \text{ and } -\bar{y}_2 \rightarrow -\bar{y}_2 \\ \text{Right: } \text{Diagram with loop } y_1 \rightarrow y_1 - y_2 \text{ and } -\bar{y}_2 \rightarrow -\bar{y}_2 \end{array} \right. \quad - \quad \text{Diagram} \quad \left| \begin{array}{c} \text{Left: } \text{Diagram with loop } y_1 \rightarrow y_1 - y_2 \text{ and } -\bar{y}_2 \rightarrow -\bar{y}_2 \\ \text{Right: } \text{Diagram with loop } y_1 \rightarrow y_1 - y_2 \text{ and } -\bar{y}_2 \rightarrow -\bar{y}_2 \end{array} \right. \quad , \quad (A.15)$$

The p_2 term obtained after applying the identity (A.2) to the diagrams (etG1) and (etG2) gives, respectively

$$(y_2 - y_1) p_\mu \quad \text{Diagram} \quad \left| \begin{array}{c} \text{Left: } (y_2 - y_1) p_\mu \\ \text{Right: } = \left[1 - \frac{k_1^2}{(k_1 - \ell_g)^2} \right] \text{ Diagram} \end{array} \right. \quad \text{''} p_2'' \quad (\text{A.16})$$

and

$$-(y_2 - y_1) p_\mu \quad \text{Diagram} \quad \left| \begin{array}{c} \text{Left: } -(y_2 - y_1) p_\mu \\ \text{Right: } = - \left[1 - \frac{k_2^2}{(k_2 + \ell_g)^2} \right] \text{ Diagram} \end{array} \right. \quad \text{''} p_2'' \quad (\text{A.17})$$

Contributions (A.15), (A.16) and (A.17) add to zero in the Regge limit.

Finally, the proofs for (fG2) goes along the same line and reads

$$-(y_2 - y_1) p_\mu \quad \text{Diagram} \quad = \quad \text{Diagram} - \text{Diagram} \quad , \quad (\text{A.18})$$

The p_2 term obtained after applying the identity (A.2) to the diagrams (ftG1) and (ftG2) gives, respectively

$$-(y_2 - y_1) p_\mu \quad \text{Diagram} \quad \left| \begin{array}{c} \text{Left: } -(y_2 - y_1) p_\mu \\ \text{Right: } = - \left[1 - \frac{k_1^2}{(k_1 - \ell_g)^2} \right] \text{ Diagram} \end{array} \right. \quad \text{''} p_2'' \quad (\text{A.19})$$

and

$$(y_2 - y_1) p_\mu \quad \text{Diagram} \quad \left| \begin{array}{c} \text{Left: } (y_2 - y_1) p_\mu \\ \text{Right: } = \left[1 - \frac{k_2^2}{(k_2 + \ell_g)^2} \right] \text{ Diagram} \end{array} \right. \quad \text{''} p_2'' \quad (\text{A.20})$$

Contributions (A.18), (A.19) and (A.20) add to zero in the Regge limit.

We now consider the "Ward" part (second term in the l.h.s of Eq.(A.2)), first for the set (atG1), (dtG1) and

(etG2). The contribution arising from (atG1) reads

$$\begin{aligned}
 & (y_2 - y_1) p_\mu \quad \text{---} \quad \text{Diagram 1} \quad \Bigg| = -\frac{\ell_g \cdot p_2}{(k_1 - \ell_g)^2} (\ell_g - k_1)_\mu \quad \text{---} \quad \text{Diagram 2} \\
 & = \frac{\ell_g \cdot p_2}{(k_1 - \ell_g)^2} \left[\text{Diagram 3} - \text{Diagram 4} \right], \tag{A.21}
 \end{aligned}$$

while the contribution arising from (dtG1) is

$$\begin{aligned}
 & (y_2 - y_1) p_\mu \quad \text{---} \quad \text{Diagram 1} \quad \Bigg| = -\frac{\ell_g \cdot p_2}{(k_1 - \ell_g)^2} (\ell_g - k_1)_\mu \quad \text{---} \quad \text{Diagram 2} \\
 & = \frac{\ell_g \cdot p_2}{(k_1 - \ell_g)^2} \quad \text{Diagram 3}, \tag{A.22}
 \end{aligned}$$

which cancels the last term in r.h.s of Eq.(A.21). The remaining term is thus the first term of the r.h.s of Eq.(A.21), which equals the contribution arising from (etG2) since

$$\begin{aligned}
 & -(y_2 - y_1) p_\mu \quad \text{---} \quad \text{Diagram 1} \quad \Bigg| = \frac{\ell_g \cdot p_2}{(k_1 - \ell_g)^2} (\ell_g - k_1)_\mu \quad \text{---} \quad \text{Diagram 2} \\
 & = \frac{\ell_g \cdot p_2}{(k_1 - \ell_g)^2} \quad \text{Diagram 3}. \tag{A.23}
 \end{aligned}$$

Consider now the set (ctG1), (btG1) and (ftG2). The contribution arising from (ctG1) reads

$$\begin{aligned}
 -(y_2 - y_1) p_\mu & \quad \text{Diagram: } \text{W''} \\
 & = \frac{\ell_g \cdot p_2}{(k_1 - \ell_g)^2} (\ell_g - k_1)_\mu \quad \text{Diagram: } \text{W''} \\
 & = -\frac{\ell_g \cdot p_2}{(k_1 - \ell_g)^2} \left[\text{Diagram: } \text{W''} - \text{Diagram: } \text{W''} \right], \tag{A.24}
 \end{aligned}$$

while the contribution arising from (btG1) is

$$\begin{aligned}
 -(y_2 - y_1) p_\mu & \quad \text{Diagram: } \text{W''} \\
 & = \frac{\ell_g \cdot p_2}{(k_1 - \ell_g)^2} (\ell_g - k_1)_\mu \quad \text{Diagram: } \text{W''} \\
 & = \frac{\ell_g \cdot p_2}{(k_1 - \ell_g)^2} \quad \text{Diagram: } \text{W''}, \tag{A.25}
 \end{aligned}$$

which cancels the first term in r.h.s of Eq.(A.24). The remaining term is thus the last term of the r.h.s of Eq.(A.24), which equals the contribution arising from (ftG2) since

$$\begin{aligned}
 (y_2 - y_1) p_\mu & \quad \text{Diagram: } \text{W''} \\
 & = -\frac{\ell_g \cdot p_2}{(k_1 - \ell_g)^2} (\ell_g - k_1)_\mu \quad \text{Diagram: } \text{W''} \\
 & = \frac{\ell_g \cdot p_2}{(k_1 - \ell_g)^2} \quad \text{Diagram: } \text{W''}. \tag{A.26}
 \end{aligned}$$

Consider now the set (etG1), (btG2) and (atG2). The contribution arising from (etG1) reads

$$\begin{aligned}
 (y_2 - y_1) p_\mu & \quad \text{Diagram: } \text{W''} \\
 & = -\frac{\ell_g \cdot p_2}{(k_2 + \ell_g)^2} (\ell_g + k_2)_\mu \quad \text{Diagram: } \text{W''} \\
 & = \frac{\ell_g \cdot p_2}{(k_2 + \ell_g)^2} \left[\text{Diagram: } \text{W''} - \text{Diagram: } \text{W''} \right], \tag{A.27}
 \end{aligned}$$

while the contribution arising from (btG2) is

$$\begin{aligned}
 & (y_2 - y_1) p_\mu \sim \text{wavy line} \quad \left| \begin{array}{c} \text{loop diagram with } y_1, y_2, \bar{y}_1, \bar{y}_2, \mu \\ \text{and internal lines } y_1 - y_2, -\bar{y}_2 \end{array} \right. \quad \sim \text{wavy line} \\
 & \quad \left. \begin{array}{c} \text{loop diagram with } y_1, y_2, \bar{y}_1, \bar{y}_2, \mu \\ \text{and internal lines } -\bar{y}_1, y_2 - y_1 \end{array} \right. \\
 & = -\frac{\ell_g \cdot p_2}{(k_2 + \ell_g)^2} (\ell_g + k_2)_\mu \sim \text{wavy line} \quad \left| \begin{array}{c} \text{loop diagram with } y_1, y_2, \bar{y}_1, \bar{y}_2, \mu \\ \text{and internal lines } -\bar{y}_1, y_2 - y_1 \end{array} \right. \\
 & = \frac{\ell_g \cdot p_2}{(k_2 + \ell_g)^2} \sim \text{wavy line} \quad , \quad \left. \begin{array}{c} \text{loop diagram with } y_1, y_2, \bar{y}_1, \bar{y}_2, \mu \\ \text{and internal lines } y_1 - y_2, -\bar{y}_2 \end{array} \right. \quad (A.28)
 \end{aligned}$$

which cancels the last term in r.h.s of Eq.(A.27). The remaining term is thus the first term of the r.h.s of Eq.(A.27), which equals the contribution arising from (atG2) since

$$\begin{aligned}
 & -(y_2 - y_1) p_\mu \sim \text{wavy line} \quad \left| \begin{array}{c} \text{loop diagram with } y_1, y_2, \bar{y}_1, \bar{y}_2, \mu \\ \text{and internal lines } -\bar{y}_1, -\bar{y}_2, y_2 - y_1 \end{array} \right. \quad = \frac{\ell_g \cdot p_2}{(k_2 + \ell_g)^2} (\ell_g + k_2)_\mu \sim \text{wavy line} \quad = \frac{\ell_g \cdot p_2}{(k_2 + \ell_g)^2} \sim \text{wavy line} \\
 & \quad \left. \begin{array}{c} \text{loop diagram with } y_1, y_2, \bar{y}_1, \bar{y}_2, \mu \\ \text{and internal lines } y_1 - y_2, -\bar{y}_2 \end{array} \right. \quad (A.29)
 \end{aligned}$$

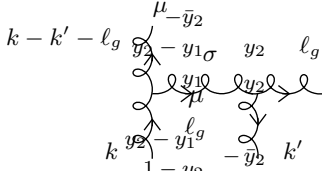
Consider now the set (ftG1), (dtG2) and (ctG2). The contribution arising from (ftG1) reads

$$\begin{aligned}
 & -(y_2 - y_1) p_\mu \sim \text{wavy line} \quad \left| \begin{array}{c} \text{loop diagram with } y_1, y_2, \bar{y}_1, \bar{y}_2, \mu \\ \text{and internal lines } y_1 - y_2, -\bar{y}_2 \end{array} \right. \quad = \frac{\ell_g \cdot p_2}{(k_1 - \ell_g)^2} (\ell_g - k_1)_\mu \sim \text{wavy line} \\
 & \quad \left. \begin{array}{c} \text{loop diagram with } y_2, y_1, \bar{y}_1, \bar{y}_2, \mu \\ \text{and internal lines } y_1 - y_2, -\bar{y}_2 \end{array} \right. \\
 & = -\frac{\ell_g \cdot p_2}{(k_1 - \ell_g)^2} \left[\sim \text{wavy line} \quad - \quad \sim \text{wavy line} \quad \begin{array}{c} \text{loop diagram with } y_1 - y_2 \\ \text{and internal lines } y_2, y_1, \bar{y}_1, \bar{y}_2, \mu \end{array} \right] , \quad (A.30)
 \end{aligned}$$

while the contribution arising from (dtG2) is

$$\begin{aligned}
 & -(y_2 - y_1) p_\mu \sim \text{wavy line} \quad \left| \begin{array}{c} \text{loop diagram with } y_1, y_2, \bar{y}_1, \bar{y}_2, \mu \\ \text{and internal lines } -\bar{y}_1, -\bar{y}_2, y_2 - y_1 \end{array} \right. \quad = \frac{\ell_g \cdot p_2}{(k_1 - \ell_g)^2} (\ell_g - k_1)_\mu \sim \text{wavy line} \quad = \frac{\ell_g \cdot p_2}{(k_1 - \ell_g)^2} \sim \text{wavy line} \\
 & \quad \left. \begin{array}{c} \text{loop diagram with } y_1, y_2, \bar{y}_1, \bar{y}_2, \mu \\ \text{and internal lines } \mu, y_2 - y_1 \end{array} \right. \quad (A.31)
 \end{aligned}$$

which cancels the first term in r.h.s of Eq.(A.30). The remaining term is thus the last term of the r.h.s of

Figure 16: Two 3-gluon vertices connected, with one open index μ .

Eq.(A.30), which equals the contribution arising from (ctG2) since

$$(y_2 - y_1) p_\mu \sim \text{diag} \left| \begin{array}{c} y_2 \\ y_1 \\ \mu \\ y_2 - y_1 \\ -\bar{y}_2 \end{array} \right\rangle = -\frac{\ell_g \cdot p_2}{(k_2 + \ell_g)^2} (\ell_g + k_2)_\mu \sim \text{diag} \left| \begin{array}{c} y_2 \\ y_1 \\ \mu \\ y_2 - y_1 \\ -\bar{y}_2 \end{array} \right\rangle = \frac{\ell_g \cdot p_2}{(k_2 + \ell_g)^2} \sim \text{diag} \left| \begin{array}{c} y_1 - y_2 \\ y_2 \\ \mu \\ y_2 - y_1 \\ -\bar{y}_2 \end{array} \right\rangle. \quad (\text{A.32})$$

Collecting now the 4 remaining contributions (A.23,A.26, A.29, A.32), one gets

$$\text{"Ward terms"} = 2 \left[\frac{p_2 \cdot \ell_g}{(k_1 - \ell_g)^2} + \frac{p_2 \cdot \ell_g}{(k_2 + \ell_g)^2} \right] \left[\sim \text{diag} \left| \begin{array}{c} y_1 \\ -\bar{y}_1 \\ y_2 - y_1 \end{array} \right\rangle + \sim \text{diag} \left| \begin{array}{c} y_2 \\ y_1 \\ y_2 - y_1 \\ -\bar{y}_2 \end{array} \right\rangle \right] \quad (\text{A.33})$$

which vanishes since

$$\text{Tr} \left[\frac{y_1 \not{p}_1 - \not{q}}{(y_1 p_1 - q)^2} \not{p}_2 \not{p}_1 \not{\epsilon}_\gamma \right] + \text{Tr} \left[\not{p}_1 \not{p}_2 \frac{\not{q} - \bar{y}_2 \not{p}_1}{(q - \bar{y}_2 p_1)^2} \not{\epsilon}_\gamma \right] = 0 \quad (\text{A.34})$$

as expected from the fact that a quark–antiquark collinear pair cannot emit a gluon.

We end up by considering the diagrams (gttG1), (httG1), (gttG2) and (httG2). As a preliminary, let us consider two triple gluon vertices connected by a gluon line, with t -channel gluons of momentum k and k' (with $k = k_1$ (resp. $k = -k_2$) and $k' = k_2$ (resp. $k' = -k_1$) for (httG1) and (gttG1) (resp. (httG2) and gttG2)) saturated with non-sense polarizations p_2 and with the gluon momentum ℓ_g , leaving the index μ open, as illustrated in Fig.16. It reads

$$V_{\tau\sigma}^\mu(-k+k'+\ell_g, k, -\ell_g-k') V_{\lambda\alpha}^\sigma(\ell_g+k', -k', -\ell_g) \epsilon_g^\alpha p_2^\lambda p_2^\tau = -(2k-\ell_g) \epsilon_g p_2^\mu + (k+\ell_g)_\mu (p_2 \cdot \epsilon_g) - (2\ell_g-k) \cdot p_2 \epsilon_g^\mu \quad (\text{A.35})$$

which reduces, after making the replacement $\epsilon_g \rightarrow \ell_g$, to

$$\begin{aligned} & V_{\tau\sigma}^\mu(-k+k'+\ell_g, k, -\ell_g-k') V_{\lambda\alpha}^\sigma(\ell_g+k', -k', -\ell_g) \ell_g^\alpha p_2^\lambda p_2^\tau \\ &= (\ell_g \cdot p_2) [p_2^\mu (2k \cdot k' + 2\ell_g \cdot (k-k')) - (k'+\ell_g)^2] + (\ell_g \cdot p_2)(k'+\ell_g-k)^\mu \end{aligned} \quad (\text{A.36})$$

where in the last line we used the fact that ℓ_g is on mass-shell. Hereafter and as for the case of a single gluon vertex, we will symbolically denote with the index p_2 the first term in the r.h.s of Eq.(A.2) and with W the second term (having in mind for this second term further use of Ward identities).

Let us first consider the "Ward" terms. Applying the identity (A.36) to the diagram (gttG1) leads to

$$\begin{aligned} (y_2 - y_1) p_\mu \sim \text{diag} \left| \begin{array}{c} y_1 \\ -\bar{y}_2 \\ \mu \\ y_2 - y_1 \end{array} \right\rangle &= -\frac{(\ell_g \cdot p_2)^2}{(k_1 - k_2 - \ell_g)^2 (k_2 + \ell_g)^2} (-k_1 + k_2 + \ell_g)_\mu \sim \text{diag} \left| \begin{array}{c} y_1 \\ -\bar{y}_1 \\ \mu \\ y_2 - y_1 \end{array} \right\rangle \\ &= \frac{(\ell_g \cdot p_2)^2}{((k_1 - k_2 - \ell_g)^2 (k_2 + \ell_g)^2)} \sim \text{diag} \left| \begin{array}{c} y_1 - y_2 \\ -\bar{y}_2 \end{array} \right\rangle, \end{aligned} \quad (\text{A.37})$$

while the same identity applied to (httG1) gives

$$\begin{aligned}
 \left. \begin{array}{c} \text{Diagram: } (y_2 - y_1) p_\mu \text{ with loop } y_1 \text{ and } y_2 \text{ and internal lines } \mu, -\bar{y}_2, y_2 - y_1. \\ \text{Label: } "W''" \end{array} \right| &= -\frac{(\ell_g \cdot p_2)^2}{(k_1 - k_2 - \ell_g)^2(k_2 + \ell_g)^2} (-k_1 + k_2 + \ell_g)_\mu \sim \sim \text{Diagram: } y_1 \text{ and } y_2 \text{ with internal lines } \mu, y_2 - y_1, -\bar{y}_2. \\
 &= -\frac{(\ell_g \cdot p_2)^2}{((k_1 - k_2 - \ell_g)^2(k_2 + \ell_g)^2)} \sim \sim \text{Diagram: } y_1 \text{ and } y_2 \text{ with internal lines } y_1 - y_2, -\bar{y}_2
 \end{aligned} \tag{A.38}$$

from which we deduce that the sum of the two contributions (A.37) and (A.38) equals zero.

Applying again the identity (A.36) to the diagram (gttG2) leads to

$$\begin{aligned}
 \left. \begin{array}{c} \text{Diagram: } (y_2 - y_1) p_\mu \text{ with loop } y_1 \text{ and } y_2 \text{ and internal lines } \mu, -\bar{y}_2, y_2 - y_1. \\ \text{Label: } "W''" \end{array} \right| &= -\frac{(\ell_g \cdot p_2)^2}{(k_1 - k_2 - \ell_g)^2(k_2 + \ell_g)^2} (-k_1 + k_2 + \ell_g)_\mu \sim \sim \text{Diagram: } y_1 \text{ and } y_2 \text{ with internal lines } -\bar{y}_1, -\bar{y}_2, \mu, y_2 - y_1. \\
 &= \frac{(\ell_g \cdot p_2)^2}{((k_1 - k_2 - \ell_g)^2(k_2 + \ell_g)^2)} \sim \sim \text{Diagram: } y_1 \text{ and } y_2 \text{ with internal lines } y_1 - y_2, -\bar{y}_2,
 \end{aligned} \tag{A.39}$$

while the same identity applied to (httG2) gives

$$\begin{aligned}
 \left. \begin{array}{c} \text{Diagram: } (y_2 - y_1) p_\mu \text{ with loop } y_1 \text{ and } y_2 \text{ and internal lines } \mu, -\bar{y}_2, y_2 - y_1. \\ \text{Label: } "W''" \end{array} \right| &= -\frac{(\ell_g \cdot p_2)^2}{(k_1 - k_2 - \ell_g)^2(k_2 + \ell_g)^2} (-k_1 + k_2 + \ell_g)_\mu \sim \sim \text{Diagram: } y_1 \text{ and } y_2 \text{ with internal lines } \bar{y}_2, \bar{y}_1, \mu, y_2 - y_1. \\
 &= -\frac{(\ell_g \cdot p_2)^2}{((k_1 - k_2 - \ell_g)^2(k_2 + \ell_g)^2)} \sim \sim \text{Diagram: } y_1 \text{ and } y_2 \text{ with internal lines } y_1 - y_2, -\bar{y}_2
 \end{aligned} \tag{A.40}$$

from which we again deduce that the sum of the two contributions (A.39) and (A.40) equals zero.

We now consider the " p_2 " terms. Denoting

$$c_1 = -\frac{(\ell_g \cdot p_2) (2 k_1 \cdot k_2 + 2 \ell_g \cdot (k_1 - k_2) - (k_2 + \ell_g)^2)}{(k_1 - k_2 - \ell_g)^2(k_2 + \ell_g)^2} \tag{A.41}$$

and

$$c_2 = -\frac{(\ell_g \cdot p_2) (2 k_1 \cdot k_2 + 2 \ell_g \cdot (k_1 - k_2) - (-k_1 + \ell_g)^2)}{(k_1 - k_2 - \ell_g)^2(-k_1 + \ell_g)^2} \tag{A.42}$$

and applying the identity (A.36) to the diagram (gttG1), one obtains

$$\begin{aligned}
 \left. \begin{array}{c} \text{Diagram: } (y_2 - y_1) p_\mu \text{ with loop } y_1 \text{ and } y_2 \text{ and internal lines } \mu, -\bar{y}_2, y_2 - y_1. \\ \text{Label: } "p_2''" \end{array} \right| &= c_1 p_{2\mu} \sim \sim \text{Diagram: } y_1 \text{ and } y_2 \text{ with internal lines } -\bar{y}_1, -\bar{y}_2, \mu, y_2 - y_1,
 \end{aligned} \tag{A.43}$$

while the same identity applied to (httG1) gives

$$\begin{aligned}
 \left. \begin{array}{c} \text{Diagram: } (y_2 - y_1) p_\mu \text{ with loop } y_1 \text{ and } y_2 \text{ and internal lines } \mu, -\bar{y}_2, y_2 - y_1. \\ \text{Label: } "p_2''" \end{array} \right| &= c_1 p_{2\mu} \sim \sim \text{Diagram: } y_1 \text{ and } y_2 \text{ with internal lines } \bar{y}_2, \bar{y}_1, \mu, y_2 - y_1,
 \end{aligned} \tag{A.44}$$

from which we deduce that the sum of the two contributions (A.43) and (A.44) equals zero, has was already shown in Eq.(A.34).

Applying again the identity (A.36) to the diagram (ggtG2) leads to

$$\begin{array}{c} \text{Diagram: } (y_2 - y_1) p_\mu \text{ (wavy line)} \text{ enters from left, } y_1 \text{ (solid line)} \text{ enters from bottom-left, } -\bar{y}_2 \text{ (dashed line)} \text{ enters from bottom-right, } \mu \text{ (solid line)} \text{ enters from bottom, } y_2 - y_1 \text{ (solid line)} \text{ exits to right, } ''p''_2 \text{ (solid line)} \text{ exits to bottom-right.} \\ \left| \right. = c_2 p_{2\mu} \text{ (wavy line)} \text{ enters from left, } -\bar{y}_1 \text{ (dashed line)} \text{ enters from bottom-left, } -\bar{y}_2 \text{ (dashed line)} \text{ enters from bottom-right, } \mu \text{ (solid line)} \text{ enters from bottom, } y_2 - y_1 \text{ (solid line)} \text{ exits to right, } ''p''_2 \text{ (solid line)} \text{ exits to bottom-right.} \end{array} \quad (\text{A.45})$$

while the same identity applied to (httG2) gives

$$\begin{array}{c} \text{Diagram: } (y_2 - y_1) p_\mu \text{ (wavy line)} \text{ enters from left, } y_1 \text{ (solid line)} \text{ enters from top, } -\bar{y}_2 \text{ (dashed line)} \text{ enters from bottom, } \mu \text{ (solid line)} \text{ enters from bottom, } y_2 - y_1 \text{ (solid line)} \text{ exits to right, } ''p''_2 \text{ (solid line)} \text{ exits to bottom-right.} \\ \left| \right. = c_2 p_{2\mu} \text{ (wavy line)} \text{ enters from left, } y_2 \text{ (solid line)} \text{ enters from top, } -\bar{y}_2 \text{ (dashed line)} \text{ enters from bottom, } \mu \text{ (solid line)} \text{ enters from bottom, } y_2 - y_1 \text{ (solid line)} \text{ exits to right, } ''p''_2 \text{ (solid line)} \text{ exits to bottom-right.} \end{array} \quad (\text{A.46})$$

from which we again deduce that the sum of the two contributions (A.45) and (A.46) equals zero.

This achieves the proof that the n -independence constraint for the N_c terms is automatically fulfilled and does not lead to any new set of equations.

Appendix B: COMPARISON BETWEEN LCCF AND CCF RESULTS

Let us first consider the 2-parton spin-flip contribution (149). Using the equation of motions (59, 60) we can express φ_1^T and φ_A^T in Eq. (149) in terms of the remaining distributions and we thus obtain from the LCCF approach

$$\begin{aligned} \Phi_{f,2}^{\gamma_T^* \rightarrow \rho_T}(\underline{k}^2) &= \frac{C^{ab}}{2} \\ &\times \int_0^1 \frac{dy_1}{(\alpha + (1 - y_1) y_1)^2} \left[-\frac{1}{2} ((1 - 2y_1)^2 + 1) \varphi_3(y_1) - (1 - 2y_1) \varphi_A(y_1) + 2y_1 \int_0^{y_1} dy_2 (\zeta_3^V B - \zeta_3^A D)(y_2, y_1) \right]. \end{aligned} \quad (\text{B.1})$$

Now our aim is to show that the Eq. (B.1) coincides with the corresponding expression of the CCF approach, i.e. with the flip part of Eq.(169), which reads

$$\begin{aligned} \Phi_f^{q\bar{q}}(\alpha) &= T_f \int_0^1 \frac{dz}{(\alpha + z\bar{z})^2} \left\{ (2z - 1) \left[\int_0^z dv (\phi_{\parallel}(z) - g_{\perp}^v(z)) - \zeta_3^V \int_0^{\bar{z}} d\alpha_1 \int_0^{\bar{z}} d\alpha_2 \frac{V(\alpha_1, \alpha_2)}{\alpha_g^2} \right] \right. \\ &\left. - \frac{1}{4} g_{\perp}^a + \zeta_3^A \int_0^z d\alpha_1 \int_0^{\bar{z}} d\alpha_2 \frac{A(\alpha_1, \alpha_2)}{\alpha_g^2} \right\} \end{aligned} \quad (\text{B.2})$$

We begin with rewriting (B.2) using the results of Ref. [7] in such a way that the form of resulting expression will be similar to one of the Eq. (B.1). For that we reexpress in (B.2) the twist-2 distribution $\phi_{\parallel}(z)$ in terms of other DAs. Let us note that $\phi_{\parallel}(z)$ satisfies equations

$$\phi_{\parallel}(z) = -z \frac{d}{dz} \left(g_{\perp}^{(v)}(z) + \frac{d}{4dz} g_{\perp}^{(a)} - g_{\perp}^{\uparrow\downarrow gen} \right), \quad (\text{B.3})$$

or

$$\phi_{\parallel}(z) = \bar{z} \frac{d}{dz} \left(g_{\perp}^{(v)}(z) - \frac{d}{4dz} g_{\perp}^{(a)} - g_{\perp}^{\uparrow\downarrow gen} \right), \quad (\text{B.4})$$

which follow in an obvious way from the definitions of DAs and their solutions in the WW approximation. Eqs. (B.3, B.4) lead in turn to the consistency condition

$$0 = \frac{d}{dz} g_{\perp}^{(v)}(z) + \frac{1}{4}(z - \bar{z}) \frac{d^2}{dz^2} g_{\perp}^{(a)}(z) - z \frac{d}{dz} g^{\uparrow\downarrow gen} - \bar{z} \frac{d}{dz} g^{\downarrow\uparrow gen}, \quad (\text{B.5})$$

from which it follows that

$$g_{\perp}^{(a)}(z) = 2g_{\perp}^{(v)}(z) + \frac{1}{2}(z - \bar{z}) \frac{d}{dz} g_{\perp}^{(a)}(z) - 2z g^{\uparrow\downarrow gen} - 2\bar{z} g^{\downarrow\uparrow gen} + 2 \int_0^z dv g^{\uparrow\downarrow gen}(v) - 2 \int_0^z dv g^{\downarrow\uparrow gen}(v). \quad (\text{B.6})$$

This relies on the boundary conditions of the different DAs (see [7]), which read

$$g^{\uparrow\downarrow}(1) = g^{\downarrow\uparrow}(0) = g^{\uparrow\downarrow WW}(1) = g^{\downarrow\uparrow WW}(0) = 0, \quad g_{\perp}^{(a)}(0) = g_{\perp}^{(a)}(1) = 0 \quad (\text{B.7})$$

and

$$\int_0^1 du g^{\uparrow\downarrow WW}(u) = \int_0^1 du g^{\uparrow\downarrow}(u) = \int_0^1 du g^{\downarrow\uparrow WW}(u) = \int_0^1 du g^{\downarrow\uparrow}(u) = 1. \quad (\text{B.8})$$

Note that they satisfy the symmetrical properties

$$g^{\uparrow\downarrow}(u) \xleftrightarrow{u \leftrightarrow \bar{u}} g^{\downarrow\uparrow}(u). \quad (\text{B.9})$$

The substitution in Eq. (B.2) of $\phi_{\parallel}(z)$ by the expression (B.3) and then replacing resulting g_{\perp}^a 's by the formula (B.6) leads to the equation

$$\begin{aligned} \Phi_f^{q\bar{q}}(\alpha) &= T_f \int_0^1 \frac{dz}{(\alpha + z\bar{z})^2} \left\{ -\frac{1}{2} ((z - \bar{z})^2 + 1) g_{\perp}^{(v)}(z) + (1 - 2z) \frac{d}{dz} g_{\perp}^{(a)}(z) \right. \\ &\quad \left. + 2z^2 g^{\uparrow\downarrow gen}(z) - 2z \int_0^z dv g^{\uparrow\downarrow gen}(v) - \zeta_3^V (2z - 1) \int_0^z d\alpha_1 \int_0^{\bar{z}} d\alpha_2 \frac{V(\alpha_1, \alpha_2)}{\alpha_g^2} + \zeta_3^A \int_0^z d\alpha_1 \int_0^{\bar{z}} d\alpha_2 \frac{A(\alpha_1, \alpha_2)}{\alpha_g^2} \right\}, \end{aligned} \quad (\text{B.10})$$

in which we observe that the two terms in the first line of (B.10) reproduce -using the vocabulary formulas (102, 103) - the first two terms of expression in [...] of Eq. (B.1).

Now consider the expression in the second line of (B.10), i.e.

$$\begin{aligned} \Phi_f^{q\bar{q}}(\alpha)|_{2nd\ line} &= T_f \int_0^1 \frac{dz}{(\alpha + z\bar{z})^2} \\ &\times \left\{ 2z^2 g^{\uparrow\downarrow gen}(z) - 2z \int_0^z dv g^{\uparrow\downarrow gen}(v) - \zeta_3^V (2z - 1) \int_0^z d\alpha_1 \int_0^{\bar{z}} d\alpha_2 \frac{V(\alpha_1, \alpha_2)}{\alpha_g^2} + \zeta_3^A \int_0^z d\alpha_1 \int_0^{\bar{z}} d\alpha_2 \frac{A(\alpha_1, \alpha_2)}{\alpha_g^2} \right\}. \end{aligned} \quad (\text{B.11})$$

Using results of Ref. [7] the formula for $\Phi_f^{q\bar{q}}(\alpha)|_{2nd\ line}$ reads

$$\begin{aligned} \Phi_f^{q\bar{q}}(\alpha)|_{2nd\ line} &= T_f \int_0^1 \frac{dz}{(\alpha + z\bar{z})^2} \\ &\times \left\{ \zeta_3^V \left[z^2 \left(\int_z^1 \frac{dv}{v} H(v) + M(z) \right) - z \int_0^z dv \left(\int_v^1 \frac{du}{u} H(u) + M(v) \right) - \frac{1}{2}(2z - 1) \int_0^z d\alpha_1 \int_0^{\bar{z}} d\alpha_2 \frac{V(\alpha_1, \alpha_2)}{(1 - \alpha_1 - \alpha_2)^2} \right] \right. \\ &\quad \left. + \zeta_3^A \left[z^2 \left(\int_z^1 \frac{dv}{v} L(v) + N(z) \right) - z \int_0^z dv \left(\int_v^1 \frac{du}{u} L(u) + N(v) \right) + \frac{1}{2} \int_0^z d\alpha_1 \int_0^{\bar{z}} d\alpha_2 \frac{A(\alpha_1, \alpha_2)}{(1 - \alpha_1 - \alpha_2)^2} \right] \right\}, \end{aligned} \quad (\text{B.12})$$

and after interchanging of integration over the variables v and u it can be simplified and takes the form

$$\begin{aligned} \Phi_{f\cdot}^{q\bar{q}}(\alpha)|_{2nd\ line} &= T_f \int_0^1 \frac{dz}{(\alpha + z\bar{z})^2} \\ &\times \left\{ \zeta_3^V \left[z^2 M(z) - z \int_0^z dv (H(v) + M(v)) - \frac{1}{2}(2z-1) \int_0^z d\alpha_1 \int_0^{\bar{z}} d\alpha_2 \frac{V(\alpha_1, \alpha_2)}{(1-\alpha_1-\alpha_2)^2} \right] \right. \\ &\left. + \zeta_3^A \left[z^2 N(z) - z \int_0^z dv (L(v) + N(v)) + \frac{1}{2} \int_0^z d\alpha_1 \int_0^{\bar{z}} d\alpha_2 \frac{A(\alpha_1, \alpha_2)}{(1-\alpha_1-\alpha_2)^2} \right] \right\}. \end{aligned} \quad (\text{B.13})$$

The expressions $M(v)$, $H(v)$, $L(v)$ and $N(v)$ are the integrals over the vector and axial-vector 3-partonic DAs

$$M(v) = \frac{d}{dv} \int_0^v d\alpha_1 \int_0^{\bar{v}} d\alpha_2 \frac{V(\alpha_1, \alpha_2)}{1-\alpha_1-\alpha_2}, \quad (\text{B.14})$$

$$H(v) = \frac{d}{dv} \int_0^v d\alpha_1 \int_0^{\bar{v}} \frac{d\alpha_2}{1-\alpha_1-\alpha_2} \left(\alpha_2 \frac{d}{d\alpha_2} + \alpha_1 \frac{d}{d\alpha_1} \right) V(\alpha_1, \alpha_2), \quad (\text{B.15})$$

$$N(v) = \int_0^v d\alpha_1 \int_0^{\bar{v}} \frac{d\alpha_2}{1-\alpha_1-\alpha_2} \left(\frac{d}{d\alpha_2} + \frac{d}{d\alpha_1} \right) A(\alpha_1, \alpha_2), \quad (\text{B.16})$$

$$L(v) = \frac{d}{dv} \int_0^v d\alpha_1 \int_0^{\bar{v}} \frac{d\alpha_2}{1-\alpha_1-\alpha_2} \left(\alpha_1 \frac{d}{d\alpha_1} - \alpha_2 \frac{d}{d\alpha_2} \right) A(\alpha_1, \alpha_2). \quad (\text{B.17})$$

Using the vocabulary (100, 101) and calculating the derivatives in above definitions we put them into the forms

$$M(u) = - \int_u^1 dv B(u, v) + \int_0^u dv B(v, u), \quad (\text{B.18})$$

$$H(u) = \int_u^1 dv \left(\frac{1}{v-u} - u \frac{d}{du} \right) B(u, v) - \int_0^u dv \left(\frac{1}{u-v} + \bar{u} \frac{d}{du} \right) B(v, u), \quad (\text{B.19})$$

$$N(u) = - \int_u^1 dv D(u, v) - \int_0^u dv D(v, u) + 2 \int_u^1 dy_2 \int_0^u dy_1 \frac{D(y_1, y_2)}{y_2 - y_1}, \quad (\text{B.20})$$

$$L(u) = -u \int_u^1 dv \frac{d}{du} D(u, v) + \bar{u} \int_0^u dv \frac{d}{du} D(v, u) - (\bar{u} - u) \left(\int_u^1 \frac{dv}{v-u} D(u, v) - \int_0^u \frac{dv}{u-v} D(v, u) \right) \quad (\text{B.21})$$

from which we calculate integrals appearing in the formula (B.13)

$$-z \int_0^z du M(u) = z \int_0^z dy_1 \int_z^1 dy_2 B(y_1, y_2) \quad (\text{B.22})$$

$$-z \int_0^z du H(u) = z \left[- \int_z^1 dy_1 \int_0^z dy_2 B(y_2, y_1) \left(\frac{1}{y_1 - y_2} + 1 \right) + z \int_z^1 du B(z, u) + \bar{z} \int_0^z du B(u, z) \right] \quad (\text{B.23})$$

$$-z \int_0^z du N(u) = z \int_z^1 dy_1 \int_0^z dy_2 D(y_2, y_1) \left(1 - \frac{2(z - y_2)}{y_1 - y_2} \right) \quad (\text{B.24})$$

$$-z \int_0^z du L(u) = z \left[z \int_z^1 du D(z, u) - \bar{z} \int_0^z du D(u, z) + \int_z^1 dy_1 \int_0^z dy_2 D(y_2, y_1) \left(-1 + \frac{\bar{y}_2 - y_2}{y_1 - y_2} \right) \right]. \quad (\text{B.25})$$

Finally, after substitution into Eq. (B.13) of the expressions (B.14, ... , B.25) and noting that

$$\int_0^z d\alpha_1 \int_0^{\bar{z}} d\alpha_2 \frac{V(\alpha_1, \alpha_2)}{(1 - \alpha_1 - \alpha_2)^2} = - \int_0^z dy_1 \int_z^1 dy_2 \frac{B(y_1, y_2)}{y_2 - y_1} \quad (\text{B.26})$$

and

$$\int_0^z d\alpha_1 \int_0^{\bar{z}} d\alpha_2 \frac{A(\alpha_1, \alpha_2)}{(1 - \alpha_1 - \alpha_2)^2} = - \int_0^z dy_1 \int_z^1 dy_2 \frac{D(y_1, y_2)}{y_2 - y_1} \quad (\text{B.27})$$

and the simplification resulting on the following properties

$$\int_0^1 dz f_{sym}(z) \int_0^z dy_1 \int_z^1 dy_2 \frac{B(y_1, y_2)}{y_2 - y_1} = 0 \quad (\text{B.28})$$

and

$$\int_0^1 dz f_{antisym}(z) \int_0^z dy_1 \int_z^1 dy_2 \frac{D(y_1, y_2)}{y_2 - y_1} = 0 \quad (\text{B.29})$$

where f_{sym} (resp. $f_{antisym}$) is (anti)symmetric with respect to $z \leftrightarrow \bar{z}$, we obtain that

$$\Phi_f^{q\bar{q}}(\alpha)|_{2nd\ line} = T_f \int_0^1 \frac{dz}{(\alpha + z\bar{z})^2} 2\alpha \left\{ 2z \int_0^{\bar{z}} du (\zeta_3^V B(u, z) - \zeta_3^A D(u, z)) \right\}, \quad (\text{B.30})$$

which reproduces the last term in Eq. (B.1).

We now proceed our comparison by considering the 3-parton flip contribution. We should thus compare the last line of (167), which is the covariant 3-parton flip result, with the corresponding LCCF result (151). This is straightforward after using the dictionary (100, 101) in the last line of (167), in order to express it only in terms of B and D . Then, using the symmetrical properties Eq.(27) ($B(y_1, y_2)$ and $D(y_1, y_2)$ are respectively antisymmetric and symmetric under the transformation $y_1 \leftrightarrow \bar{y}_2$), one should rewrite the prefactors of B in an antisymmetrical form (and correspondingly the prefactor of D in a symmetrical form). Doing this for both expressions leads to identical expressions.

The same method applies to N_c 3-parton non-flip contribution. Indeed, comparing the $N_c/C_F = 2c_f$ term of Eq.(150) with the corresponding c_f contribution for the $T_{n.f.}$ tensor coefficient of (167) after using the dictionary (100, 101) and restoring the symmetry of the integrands, one get identical expressions.

We now focus on the non-trivial proof that the C_F contribution arising from the non-flip contributions are identical in LCCF and CCF approaches. Only this part leads to potential violations of gauge invariance, as we

saw in CCF approach of section III C, where it was needed to combine $\Delta\Phi^2$ and $\Delta\Phi^3$. In LCCF approach, this also requires to combine 2 and 3-parton contributions. We should thus prove that the 2-parton contribution (148) supplemented by the constant term (in color space) of Eq.(150) is identical with the constant term (in color space) of the $T_{n.f.}$ coefficient of (167) supplemented by the $T_{n.f.}$ coefficient of (169).

Consider first the 3-parton non-flip contribution with C_F color structure of the LCCF result (150). It reads

$$\begin{aligned} \Phi_{n.f.3}^{\gamma_T^* \rightarrow \rho_T C_F}(\underline{k}^2) &= C^{ab} \int_0^1 dy_1 \int_0^1 dy_2 \\ &\times \left\{ \zeta_3^V B(y_1, y_2) \left[\frac{-2\alpha y_1(2y_1 - 1)}{\alpha + (1 - y_1)y_1} \frac{1}{(y_1 - y_2 + 1)\alpha + y_1(1 - y_2)} + \frac{2y_1}{\alpha + (1 - y_1)y_1} - \frac{2/\bar{y}_1 + 1/\bar{y}_1}{\bar{y}_1} \right] \right. \\ &\quad \left. + \zeta_3^A D(y_1, y_2) \left[\frac{-2\alpha y_1}{\alpha + (1 - y_1)y_1} \frac{1}{(y_1 - y_2 + 1)\alpha + y_1(1 - y_2)} + \frac{2y_1}{\alpha + (1 - y_1)y_1} - \frac{2}{\bar{y}_1} + \frac{1}{\bar{y}_1} \right] \right\}. \end{aligned} \quad (\text{B.31})$$

In this expression, we have written the last term $-1/\bar{y}_1$ of B and D contributions as $-2/\bar{y}_1 + 1/\bar{y}_1$ in order to prepare the identification with the CCF approach result. Removing for a moment the $1/\bar{y}_1$ contribution from Eq.(B.31) (i.e. last term for both B and D brackets), the obtained expression vanishes in the $\alpha \rightarrow 0$ limit (we therefore denote it with an index *van.*), and, after restoring the appropriate symmetry under $y_1 \leftrightarrow \bar{y}_2$ (antisymmetrized for B and symmetrized for D), it reads

$$\begin{aligned} \Phi_{n.f.3 \text{ van.}}^{\gamma_T^* \rightarrow \rho_T C_F}(\underline{k}^2) &= C^{ab} \alpha \int_0^1 dy_1 \int_0^1 dy_2 \left\{ \zeta_3^V B(y_1, y_2) \left[\frac{y_1 + \bar{y}_2}{(y_1 - y_2)((y_1 + \bar{y}_2)\alpha + y_1 \bar{y}_2)} \left(\frac{1}{\bar{y}_2} - \frac{1}{y_1} \right) \right. \right. \\ &\quad - \frac{1}{y_1 - y_2} \frac{y_1 - \bar{y}_1}{y_1(\alpha + y_1 \bar{y}_1)} + \frac{1}{y_1 - y_2} \frac{\bar{y}_2 - y_2}{\bar{y}_2(\alpha + y_2 \bar{y}_2)} - \frac{1}{\bar{y}_1} \frac{1}{\alpha + y_1 \bar{y}_1} + \frac{1}{y_2} \frac{1}{\alpha + y_2 \bar{y}_2} \\ &\quad \left. + \zeta_3^A D(y_1, y_2) \left[\frac{y_1 + \bar{y}_2}{(y_1 - y_2)((y_1 + \bar{y}_2)\alpha + y_1 \bar{y}_2)} \left(\frac{1}{\bar{y}_2} + \frac{1}{y_1} \right) \right. \right. \\ &\quad \left. \left. - \frac{1}{\alpha + y_1 \bar{y}_1} \left(\frac{1}{y_1(y_1 - y_2)} + \frac{1}{\bar{y}_1} \right) - \frac{1}{\alpha + y_2 \bar{y}_2} \left(\frac{1}{\bar{y}_2(y_1 - y_2)} + \frac{1}{y_2} \right) \right] \right\}. \end{aligned} \quad (\text{B.32})$$

The corresponding expression obtained from the CCF approach reads, according to (167),

$$\Phi_{n.f.}^{q\bar{q}g C_F}(\alpha) = \int Dz \frac{2\alpha}{z_1 z_2 z_g^2} (\zeta_3^V V(z_1, z_2) + \zeta_3^A A(z_1, z_2)) \left(\frac{\bar{z}_g z_1}{\alpha \bar{z}_g + z_1 z_2} - \frac{z_1 z_2^2}{\bar{z}_1(\alpha + z_1 \bar{z}_1)} - \frac{z_1 \bar{z}_2}{\alpha + z_2 \bar{z}_2} \right) \quad (\text{B.33})$$

which after using the dictionary (100, 101) turns into

$$\Phi_{n.f.}^{q\bar{q}g C_F}(\alpha) = - \int_0^1 dz_1 \int_0^1 dz_2 \frac{2\alpha}{z_1 z_2 (1 - z_1 - z_2)} (\zeta_3^V B(z_1, 1 - z_2) + \zeta_3^A D(z_1, 1 - z_2)) \quad (\text{B.34})$$

$$\times \left(\frac{(z_1 + z_2)z_1}{\alpha(z_1 + z_2) + z_1 z_2} - \frac{z_1 z_2^2}{\bar{z}_1(\alpha + z_1 \bar{z}_1)} - \frac{z_1 \bar{z}_2}{\alpha + z_2 \bar{z}_2} \right) \quad (\text{B.35})$$

This reads, after restoring the symmetry properties of the integrands,

$$\begin{aligned} \Phi_{n.f.}^{q\bar{q}g C_F}(\alpha) &= \alpha \int_0^1 dy_1 \int_0^1 dy_2 \frac{1}{y_1 - y_2} \\ &\times \left\{ \zeta_3^V B(y_1, y_2) \left[\frac{y_1 + \bar{y}_2}{(y_1 + \bar{y}_2)\alpha + y_1 \bar{y}_2} \left(\frac{1}{y_1} - \frac{1}{\bar{y}_2} \right) + \frac{\bar{y}_2}{\bar{y}_1} \frac{1}{\alpha + y_1 \bar{y}_1} + \frac{y_2}{\bar{y}_2} \frac{1}{\alpha + y_2 \bar{y}_2} - \frac{y_1}{y_2} \frac{1}{\alpha + y_2 \bar{y}_2} - \frac{\bar{y}_1}{y_1} \frac{1}{\alpha + y_1 \bar{y}_1} \right] \right. \\ &\quad \left. + \zeta_3^A D(y_1, y_2) \left[-\frac{y_1 + \bar{y}_2}{(y_1 + \bar{y}_2)\alpha + y_1 \bar{y}_2} \left(\frac{1}{y_1} + \frac{1}{\bar{y}_2} \right) + \frac{\bar{y}_2}{\bar{y}_1} \frac{1}{\alpha + y_1 \bar{y}_1} + \frac{y_2}{\bar{y}_2} \frac{1}{\alpha + y_2 \bar{y}_2} + \frac{y_1}{y_2} \frac{1}{\alpha + y_2 \bar{y}_2} + \frac{\bar{y}_1}{y_1} \frac{1}{\alpha + y_1 \bar{y}_1} \right] \right\} \end{aligned} \quad (\text{B.36})$$

which agrees with the result (B.32) after elementary algebra.

We now prove that the 2-parton non-flip C_F LCCF result (148) agrees with the non-flip C_F CCF contribution $\Phi_{n.f.}^{q\bar{q}}$, after supplementing the LCCF result with the 3-parton $1/\bar{y}_1$ term of Eq.(B.31).

Starting from the LCCF result (148) and using the equations of motions (59, 60) we can express φ_1^T and φ_A^T in Eq. (149) in terms of the remaining distributions, which leads to

$$\begin{aligned} \Phi_{n.f.2}^{\gamma_T^* \rightarrow \rho_T}(\underline{k}^2) = & \frac{C^{ab}}{2} \int_0^1 \frac{dy_1}{y_1 \bar{y}_1} \left[-\frac{2\alpha(\alpha + 2y_1 \bar{y}_1)}{(\alpha + y_1 \bar{y}_1)^2} \right] \left\{ -2y_1 \bar{y}_1 \varphi_3(y_1) - y_1 \int_{y_1}^1 dy_2 [\zeta_3^V B(y_1, y_2) + \zeta_3^A D(y_1, y_2)] \right. \\ & - \bar{y}_1 \int_0^{y_1} dy_2 [-\zeta_3^V B(y_2, y_1) + \zeta_3^A D(y_2, y_1)] \Big\} - y_1 \int_{y_1}^1 dy_2 [\zeta_3^V B(y_1, y_2) + \zeta_3^A D(y_1, y_2)] \\ & \left. - \bar{y}_1 \int_0^{y_1} dy_2 [-\zeta_3^V B(y_2, y_1) + \zeta_3^A D(y_2, y_1)] \right]. \end{aligned} \quad (\text{B.37})$$

Now let us consider the non-flip CCF result (169, 170), which reads

$$\begin{aligned} \Phi_{n.f.}^{q\bar{q}}(\alpha) = & T_{n.f.} \int_0^1 dz \frac{\alpha(\alpha + 2z \bar{z})}{z \bar{z}(\alpha + z \bar{z})^2} \left\{ (2z - 1) \left[\int_0^z dv (\phi_{\parallel}(z) - g_{\perp}^{(v)}(z)) - \zeta_3^V \int_0^z d\alpha_1 \int_0^{\bar{z}} d\alpha_2 \frac{V(\alpha_1, \alpha_2)}{\alpha_g^2} \right] \right. \\ & \left. + \frac{1}{4} g_{\perp}^{(a)} - \zeta_3^A \int_0^z d\alpha_1 \int_0^{\bar{z}} d\alpha_2 \frac{A(\alpha_1, \alpha_2)}{\alpha_g^2} \right\}. \end{aligned} \quad (\text{B.38})$$

The same series of transformations which led from (B.38) to (B.10) now gives

$$\begin{aligned} \Phi_{n.f.}^{q\bar{q}}(\alpha) = & T_{n.f.} \int_0^1 dz \frac{2\alpha(\alpha + 2z \bar{z})}{z \bar{z}(\alpha + z \bar{z})^2} \left\{ z \bar{z} g_{\perp}^{(v)}(z) - z \bar{z} g^{\uparrow\downarrow gen}(z) + \bar{z} \int_0^z dv g^{\uparrow\downarrow gen}(v) \right. \\ & \left. - \frac{z - \bar{z}}{2} \zeta_3^V \int_0^z d\alpha_1 \int_0^{\bar{z}} d\alpha_2 \frac{V(\alpha_1, \alpha_2)}{\alpha_g^2} - \frac{1}{2} \zeta_3^A \int_0^z d\alpha_1 \int_0^{\bar{z}} d\alpha_2 \frac{A(\alpha_1, \alpha_2)}{\alpha_g^2} \right\}. \end{aligned} \quad (\text{B.39})$$

Using the dictionary (102) one immediately gets agreement between the first term of (B.37) involving φ_3 and the first term of (B.39) involving g_{\perp}^v . We now consider the remaining term of (B.39), involving B and D through $g^{\uparrow\downarrow gen}$, V and A .

Using results of Ref. [7] the formula for $\Phi_{n.f.}^{q\bar{q}}(\alpha)|_{rem.}$ reads, after interchanging the integration over the variables v and u as we did in order to get (B.13),

$$\begin{aligned} \Phi_{n.f.}^{q\bar{q}}(\alpha)|_{rem.} = & T_{n.f.} \int_0^1 dz \frac{2\alpha(\alpha + 2z \bar{z})}{z \bar{z}(\alpha + z \bar{z})^2} \\ & \times \left\{ \zeta_3^V \left[-z \bar{z} M(z) + \bar{z} \int_0^z dv (H(v) + M(v)) - \frac{1}{2}(2z - 1) \int_0^z d\alpha_1 \int_0^{\bar{z}} d\alpha_2 \frac{V(\alpha_1, \alpha_2)}{(1 - \alpha_1 - \alpha_2)^2} \right] \right. \\ & \left. + \zeta_3^A \left[-z \bar{z} N(z) + \bar{z} \int_0^z dv (L(v) + N(v)) - \frac{1}{2} \int_0^z d\alpha_1 \int_0^{\bar{z}} d\alpha_2 \frac{A(\alpha_1, \alpha_2)}{(1 - \alpha_1 - \alpha_2)^2} \right] \right\}. \end{aligned} \quad (\text{B.40})$$

Finally, after substitution into Eq. (B.40) of the expressions (B.14, ..., B.25) and using the properties (B.26) and (B.27), one obtains

$$\Phi_{n.f.}^{q\bar{q}}(\alpha)|_{rem.} = -T_{n.f.} \int_0^1 dz \frac{2\alpha(\alpha + 2z \bar{z})}{z(\alpha + z \bar{z})^2} \int_0^z dy_1 [\zeta_3^V B(y_1, z) - \zeta_3^A D(y_1, z)]. \quad (\text{B.41})$$

Coming back to the LCCF result, the remaining contribution after removing the φ_3 term reads, after using the symmetrical properties (27),

$$\Phi_{n.f.2rem.}^{\gamma_T^* \rightarrow \rho_T}(\underline{k}^2) = \frac{C^{ab}}{2} \int_0^1 \frac{dy_1}{y_1} \left\{ -\frac{4\alpha(\alpha + 2y_1\bar{y}_1)}{(\alpha + y_1\bar{y}_1)^2} \int_0^{y_1} dy_2 [\zeta_3^V B(y_2, y_1) - \zeta_3^A D(y_1, y_2)] \right. \\ \left. - 2 \int_0^{y_1} dy_2 [-\zeta_3^V B(y_2, y_1) + \zeta_3^A D(y_2, y_1)] \right\}. \quad (\text{B.42})$$

Now, the remaining term coming from the LCCF C_F non-flip 3-parton contribution (B.31) which we omitted for the moment is

$$\Phi_{n.f.3rem.}^{\gamma_T^* \rightarrow \rho_T C_F}(\underline{k}^2) = C^{ab} \int_0^1 dy_1 \int_0^1 dy_2 \left\{ \zeta_3^V B(y_1, y_2) \frac{1}{\bar{y}_1} + \zeta_3^A D(y_1, y_2) \frac{1}{\bar{y}_1} \right\}. \quad (\text{B.43})$$

Using the symmetrical properties (27), this contribution is opposite to the contribution from the second line of (B.42) while the first line of (B.42) is identical to the result (B.41). This ends the proof of the exact equivalence between LCCF and CCF results.

- [1] J. C. Collins, L. Frankfurt, M. Strikman, Phys. Rev. D **56**, 2982 (1997).
- [2] M. Diehl, T. Gousset and B. Pire, Phys. Rev. D **59**, 034023 (1999); J. C. Collins and M. Diehl, Phys. Rev. D **61**, 114015 (2000).
- [3] L. Mankiewicz and G. Piller, Phys. Rev. D **61**, 074013 (2000);
- [4] I. V. Anikin and O. V. Teryaev, Phys. Lett. B **554**, 51 (2003), Phys. Lett. B **509**, 95 (2001).
- [5] I. V. Anikin and O. V. Teryaev, Nucl. Phys. A **711**, 199 (2002).
- [6] D. Yu. Ivanov *et al.*, Phys. Lett. B **550**, 65 (2002); R. Enberg, B. Pire and L. Szymanowski, Eur. Phys. J. C **47**, 87 (2006).
- [7] P. Ball, V. M. Braun, Y. Koike and K. Tanaka, Nucl. Phys. B **529**, 323 (1998); P. Ball and V. M. Braun, Phys. Rev. D **54**, 2182 (1996).
- [8] P. Ball and V. M. Braun, Nucl. Phys. B **543** (1999) 201.
- [9] S. A. Morrow *et al.* [CLAS Collaboration], Eur. Phys. J. A **39**, 5 (2009) [arXiv:0807.3834 [hep-ex]].
A. Borissov [HERMES Collaboration], AIP Conf. Proc. **1105** (2009) 19.
V. Y. Alexakhin *et al.* [COMPASS Collaboration], Eur. Phys. J. C **52**, 255 (2007) [arXiv:0704.1863 [hep-ex]].
- [10] A. Levy, arXiv:0711.0737 [hep-ex]. S. Chekanov *et al.* [ZEUS Collaboration], PMC Phys. A **1**, 6 (2007) [arXiv:0708.1478 [hep-ex]].
- [11] D. Yu. Ivanov, M. I. Kotovsky and A. Papa, Eur. Phys. J. C **38**, 195 (2004), D. Yu. Ivanov and A. Papa, Nucl. Phys. B **732**, 183 (2006) and Eur. Phys. J. C **49**, 947 (2007).
- [12] B. Pire, L. Szymanowski and S. Wallon, Eur. Phys. J. C **44**, 545 (2005); B. Pire, M. Segond, L. Szymanowski and S. Wallon, Phys. Lett. B **639**, 642 (2006); R. Enberg, B. Pire, L. Szymanowski and S. Wallon, Eur. Phys. J. C **45**, 759 (2006) [Erratum-ibid. C **51**, 1015 (2007)]; M. Segond, L. Szymanowski and S. Wallon, Eur. Phys. J. C **52**, 93 (2007).
- [13] I. V. Anikin, B. Pire and O. V. Teryaev, Phys. Rev. D **62** (2000) 071501;
- [14] A. V. Efremov and O. V. Teryaev, Sov. J. Nucl. Phys. **36**, 140 (1982) [Yad. Fiz. **36**, 242 (1982)]; E. V. Shuryak and A. I. Vainshtein, Nucl. Phys. B **199**, 451 (1982), Nucl. Phys. B **201**, 141 (1982); R.K. Ellis *et al.*, Nucl. Phys. B **212** (1983) 29; A.V. Efremov and O.V. Teryaev, Sov. J. Nucl. Phys. **39**, 962 (1984); O. V. Teryaev, arXiv:hep-ph/0102296; A. V. Radyushkin and C. Weiss, Phys. Rev. D **64** (2001) 097504.
- [15] I. V. Anikin, D. Yu. Ivanov, B. Pire, L. Szymanowski and S. Wallon, arXiv:0903.4797 [hep-ph].
- [16] I. V. Anikin, D. Yu. Ivanov, B. Pire, L. Szymanowski and S. Wallon, arXiv:0904.1482 [hep-ph]; AIP Conf. Proc. **1105** (2009) 390 [arXiv:0811.2394 [hep-ph]]; arXiv:0909.4038 [hep-ph]; arXiv:0909.4042 [hep-ph].
- [17] Y. L. Dokshitzer, D. Diakonov and S. I. Troian, Phys. Rept. **58** (1980) 269.
- [18] A. Ali, V. M. Braun and H. Simma, Z. Phys. C **63** (1994) 437 [arXiv:hep-ph/9401277].
- [19] S. Catani, M. Ciafaloni and F. Hautmann, Phys. Lett. B **242** (1990) 97; S. Catani, M. Ciafaloni and F. Hautmann, Nucl. Phys. B **366** (1991) 135.
- [20] J. C. Collins and R. K. Ellis, Nucl. Phys. B **360** (1991) 3.
- [21] E. M. Levin, M. G. Ryskin, Yu. M. Shabelski and A. G. Shuvaev, Sov. J. Nucl. Phys. **53** (1991) 657 [Yad. Fiz. **53** (1991) 1059].

- [22] E.A. Kuraev, L.N. Lipatov and V.S. Fadin, Phys. Lett. **B60** (1975) 50-52; Sov. Phys. JETP **44** (1976) 443-451; Sov. Phys. JETP **45** (1977) 199-204; Ya.Ya. Balitskii and L.N. Lipatov, Sov. J. Nucl. Phys. **28** (1978) 822-829.
- [23] I. F. Ginzburg, S. L. Panfil and V. G. Serbo, Nucl. Phys. B **284** (1987) 685.
- [24] S. V. Goloskokov and P. Kroll, Eur. Phys. J. **C 42**, 281 (2005); ibid. **C 50**, 829 (2007); ibid. **C 53**, 367 (2008).
- [25] I. V. Anikin, D. Yu. Ivanov, B. Pire, L. Szymanowski and S. Wallon, in preparation.